University of Central Florida

Orlando FL

The College of Optics and Photonics

Senior Design

8/27/2021

Remotely Controlled Diffused Surface Laser Beam Imaging System

9/9/2021 - 4/22/2021

Members

Name	Major	Graduation date
Madelaine Smith	Optics and Photonics	5/7/2022
Devin Benjamin	Optics and Photonics	5/7/2022
Daniel Oquendo	Computer Engineering	5/7/2022
Miguel Ortiz	Electrical Engineering	5/7/2022

Technical Advisor

Dr. Martin Richardson

Haley Kerrigan

Table Of Contents

Figures Index

1. Executive Summary

Outdoor high energy laser propagation experiments are impacted the inefficient preparation process. Many personnel are required to set up sensitive equipment far from the laser output and that is not intended for outdoor use. The aim of this project is to aid in reducing the amount of personnel required to prepare long range testing and provide weatherproof equipment to do so. The final design aims to create a device that is remotely controlled to find, track and characterize a laser beam off a diffused target board. The user would be able to stay at the laser output and view a live image of the beam. Characteristics like the intensity profile, intensity tracking, and beam tracking will be provided as well.

Investigation into several key components will be conducted. A lens zoom system must be designed to be able to view the 10x10 ft target and then zoom in on the beam, at least 4x magnification. A filtration system needs to be able to filter out ambient sun light. The power source must be designed to be chargeable and if possible, solar powered. The movement of the zoom lenses and the movement of the entire device will be investigated. The data transmission and user interface options will be investigated as well.

Several constraints impede the design, such as economic, environmental, manufacturability and sustainability.

2. Project Description

This section will describe in brief the purpose of the project through discussion of the background, objectives, goals, and approach.

2.1 Project Background

Our team is working with a graduate research group, the Laser Plasma Laboratory at CREOL UCF, to solve a problem that occurs during outdoor high power energy experiments. Currently there are few devices on the market which are built specifically for outdoor high energy laser propagation testing. Without access to such devices, setting up outdoor laser experiments can be both extremely time consuming and inefficient. Current equipment must be aligned by hand and monitored from both the laser output as well as the target. This distance varies but for the purposes of this design the distance is a kilometer. With an automated system that can locate the laser beam and record its characteristics, the amount of personnel on the ground can be reduced. Due to experimenting outdoors, sunlight can make it quite difficult for camera systems to read the laser beam on the surface of the target board. However, a specially designed filter system can control the amount of ambient light entering the system. The equipment being used traditionally is not designed to deal with the outdoor elements. When weather changes sporadically all equipment must be quickly salvaged and covered as to not get damaged. Most optical equipment on the market right now uses a direct power source to power the instruments, which is inefficient for outdoor use. Large batteries or a backup generator are needed to power the equipment. The solution to this is to incorporate a power source which is both chargeable and solar powered. With such a large distance a remotely controlled device will not only cut out the need for additional personnel, saving time and potential costs, but will be able to withstand any weather without the need to be physically covered or removed from its optimal testing location.

2.2 Objective

Design and build a remotely controlled, solar powered and waterproof system that can image and track a laser beam from collected light off of a diffused surface.Goals of building the device are to design and build a zoom system that will be remotely controlled to locate the laser beam on an outdoor diffused surface. Design a filter to control the amount of ambient light introduced to the device. The laser signal captured by the camera system will be sent to a corresponding receiver device and the vital information about beam location and

various characteristics will be displayed on the receiver. Design a battery source which can deliver the appropriate power to each individual system within the device and integrate solar panels for solar charging of the battery. This device will be controlled remotely from the laser's output location (roughly a kilometer away).

2.3 Project Goals

The core goals are to have a battery-operated device that will be able to transmit imaging data 3 meters at one wavelength. Our device will be remotely controlled, at 3 meters, to find and track a beam and its characteristics on a diffused target board.

The advanced goals are to have solar charged battery-operated device that will be able to transmit imaging data 3 meters at multiple wavelengths. Our device will be remotely controlled, further than 3 meters, to find and track a beam and its characteristics on a diffused target board.

The stretch goals are to have a solar powered device that will be able to transmit imaging date more than 3 meters at multiple wavelengths. Our device will automatically find and track a beam and its characteristics on a diffused target board.

2.4 Methodological Approach

Several approaches will be used to optimize the projects outcome. Optical simulation tools such as Zemax will be used to design the zoom system for the camera. CAD software will be used to simulate and design the movement system which will control the tilt and spin of the device. Thorough testing will allow a progressive scale of laser power and wavelengths. Theoretical exploration will help make informed decisions about sensing filters used to filter out ambient lighting. The most efficient way to transfer data is also being discussed and thought out. Ideally our system would transmit data over a medium which does not have to be hardwired. The system will be powered by solar energy. It will have (estimate size) solar panels which will
be connected to a rechargeable battery, providing power to the system. The system will use direct power coming from the solar panels. In the case of low sunlight, i.e. rain or cloudy, the battery will provide its charge to the system. In the case of full sunlight, the system will use the excess power to charge the battery. Between the panels and the battery, a charge controller will regulate the power given to the battery, and supervise the battery charge, avoiding excess charge or discharge, in order to avoid damage. A microcontroller will hold the connections to the components which will allow the camera to move accurately and detect the beam. The components connected to the microcontroller also include an

estimate of two motors adding a precise movement to the system gears. There are two displacement options which are in an angular rotation from left to right, and up and down. The other displacement option is a linear motion vertically and horizontally. Signals to the motors will be controlled through a motor driver that will receive a signal in real time directing the camera platform to follow the beam on the target. Also connected to the controller is the camera, requiring a lower amount of power than the motors. In order to handle the different types of components with varying types of currents and voltages, DC to DC converters will be designed as well as implemented, in order to scale up or down the voltage coming from the solar panels. Since the proposed project will be a weatherproof system, a case will be built in order to keep the components safe. This will increase the heat coming from the components, meaning that a couple of fans will also be powered through solar energy. Heating sensors will be connected inside the housing, which will throw a signal to the controller activating the cooling fans, that way no power is consumed till it's absolutely needed.

3. Project Requirements

This section will cover the restrictions on this project that exist from specifications set by the team internally and by external factors.

3.1 Overall Requirement Specifications

Light Filtration	
Lens Zoom System	
Magnification	At least 4x
Length	Less than 12 in
Camera adjustment system	
Horizontal tilt	90 degrees
Vertical tilt	90 degrees
Remote control system	
Wireless connection	At least 3 m
System delay	Less than 100 ms
Combined Filter/Lens/Camera systems	
Weight	Less than 25 lbs
Size	Less than 4 cubic feet
Power discharge time	At least 30 min between charges
Housing	Water/weatherproof

Table 1: Design requirements

3.2 Constraints

Several constraints impede the design, the main concerns being, economic, environmental, manufacturability and sustainability. The economic constrain is that due to worldwide shortages certain devices and materials are either unavailable or outside of design budget. The environmental constrain involves the weather for outdoor testing. The design of this device needs to be weatherproof, and temperature controlled. Health and Safety constraints are a main factor when testing this device. The testing laser diode is a class 3B laser, and the proper safety eyewear is needed when in its proximity. Additionally, any indoor facility needs to be approved for such devices. However, the devices for any demonstration are safe for everyone
in proximity. Materials used must be commercially available, easily accessible, and do not require customization. This device needs to be sustainable in that the

designed battery is chargeable, can be used for at least 30 minutes, and charged with a solar power.

3.3 Standards

This section covers any social, political, environmental, and economic standards that have been found that this project will be under the purview of and must be followed.

3.3.1 Radio Frequency Spectrum Standards

The Federal Communications Commission (FCC) sets the allocations of the radio frequency spectrum as used in the jurisdiction of the United States. The allocations are set for various uses ranging from radio/television broadcasts, radionavigation, satellite communications, and for scientific research using radio waves in things like radio telescopes (i.e. not telling a camera control mechanism what to do). As demonstrated on the United States Frequency Allocation Chart released by the United States Department of Commerce National Telecommunications and Information Administration, amateur/public use is allowed in various bands across the spectrum, the ones below being the most relevant: 2.39-2.4835 GHz (referred to as the 2.45 GHz band) and 5.65-5.925 GHz (referred to as the 5.8 GHz band).

3.4 House of Quality

			Engineering Requirements								
			Cost	Weight	Delay	Signal Strength	Magnification	Power Efficiency	Filtration	Sensor	Size
			-	-	-	+	+	+	+	+	-
Marketing Requirements	Compact	+	↓	↑↑			↓	↓↓			↑↑
	Ease of Set up	+	↓	↓	↓	↑	↑	↑			↓
	Weatherproof	+	↓	↓↓		↓					↓
	Ease of Use	+	↓	↓	↓	↑	↑				↓
	Engineering Requirement Targets		<$2500	< 25 lbs	<100 ms	> 3ms	x3	> 30 Minutes	TBD	TBD	< 3ft^3

Table 2: House of Quality

Legend:

- \+ Positive Polarity
- – Negative Polarity
- ↑ Positive Correlation
- ↓ Negative Correlation
- ↑↑ Strong Positive Correlation
- ↓↓ Strong Negative Correlation

4. Research and Investigation

The following is the technical research the means by which this project may come together and develop into a functioning system. This covers our investigations of the optical, electrical, and computational components of the project and our decisions made based on those investigations.

4.1 Surfaces

When a laser beam is incident upon a smooth surface the propagation characteristics are easily quantified. The material used will dictate the amount of absorption, transmission, and specular reflection that takes place on the incident signal. The material will also have differed effects on the beam depending on the wavelength transmitted. Some surfaces are sensitive to wavelengths and may alter the polarization, amplitude, or even wavelength of the incident signal. Typically, with a smooth surface the incident light will strike the surface at some angle and the reflected light will travel at the same angle transversely to the incident beam. This type of reflection is specular reflection. Specular reflection most commonly occurs when light is incident upon smooth surfaces. Specular reflection typically will give the surface a glossy appearance. Most specular reflection occurs when light is incident upon glass or a glossy coated smooth material. Coatings can be used on the smooth surface as well to design the propagation response. Certain coating will have a higher reflectance percentage of the light thus can be designed to reflect whatever percentage of the beam desired. Certain coatings can reflect close to 100% of the original beam if required, since there will always be a small loss due to the medium the signal is traveling through.

In contrast a diffused surface is not as predictable to calculate the propagation behavior of the laser beam after striking the materials surface. Diffused surfaces consist of a structure which is not of equal crystalline construct throughout like a smooth surface. This inconsistency in lattice structure causes a unique propagation response from the laser beam depending on the material. The wavelength of the incident beam can be altered depending on the spacing of the diffused surface and how close the distance between the imperfect lattices atomic structure. When the laser beam is incident upon the diffused surface the wave fronts will experience absorption, transmission, diffused reflection, and specular reflection. Both reflections will be in many directions. When a laser signal propagates and is incident upon a diffused surface the light beam experiences transmission, diffused reflection, specular reflection, and absorption. The degree to which each response of the beam occurs and what percentage of light signal experiences the effects depends on the properties of the diffused surface. Diffused surfaces typically have a matte appearance which is due to the

nonhomogeneous construct of the material. For this experiment the light which will be collected by the device will be reflected light from the diffused surface.
Diffused reflection occurs due to the randomness of the materials lattice structure on the surface as well as in the lattice structure. The surface is considered non-uniform and will reflect the different rays of the light source uniquely. Each ray traveling within the wave packet of the laser beam will strike the surface at differing orientations of the surface. The surface is ridged and will have random peaks and troughs of differing angular orientation. Each individual photon will strike the diffused surface at differing location and angles and will reflect accordingly. The randomness of this surfaces construct makes predicting the behavior of the light signal challenging. Some of the incident light will also transmit through the body of the diffused surface. The construct of the material will dictate the refractive index and how the light will travel inside of the material. Due to the lattice also being of random alignment the light will internally reflect randomly and the photons that are not absorbed will transmit back out of the surface as scattered light. The scattered light reflection is what will be observed by the camera of the device. Due to the randomness and differing directions of which the light will scatter, a percentage of the intensity of the original signal will be lost when collecting data. Along with the surface being non-uniform and causing random reflected beams some of the light which reaches the surface will transmit through into the structure and have internal refection which will cause body reflection and randomly scatter light.

The diffused surface for this experiment will be coated so that it has Lambertian characteristics. Lambertian refers to Lambert's cosine law which states "*the measure of radiant energy from a surface that exhibits Lambertian reflection is directly proportional to the cosine of the angle formed by the measurement point and the surface normal".* This law is depicted in the following equation:

For example, considering a light source as a point source, this point source will have a luminous intensity in all directions. This can be states as the luminous flux divided by four pi. At a calculated distance from the point source a screen is placed. The illuminance at a point directly in front of the source at an angle of zero degrees will be the maximum intensity and can be calculated by dividing the luminance intensity of the point source by the distance away from the screen squared. Now for a point on the screen at an angle theta the illuminance at his point will be the luminous intensity multiplied by cosine of theta than divided by the distance of the points source from the screen squared. This point at an angle can also be written as the maximum intensity multiplied by the cosine of the angle theta, which is Lamberts cosine law which is depicted in the equation below.

$$I = I_0 Cos(\theta)$$

The Lambertian surface when viewed form any angle will appear equally as bright from all directions. This phenomenon is directly correlated to the

Lambertian BRDF. The measure of diffused reflection is notated as the albedo or symbolized as ρ. The albedo is measured from a range of zero to one. Zero being a completely black surface and one being a completely white surface. The completely lower the albedo (closer to black) the more absorption will take place versus reflectance and vice versa for the white surface which will experience a much higher reflectance as albedo increases. The Lambertian BRDF is the albedo divided by pi. This is proportional to brightness of a surface when incident light is reflected from the surface. The geometry of the surface is a factor which will change how to calculate the diffused reflection variable. Albedo is considered the hemispherical-directional reflectance. This is the measurement of how much light is reflected from any direction for the incident light around the surface normal of the object. Albedo is calculated using the following integration where f_r is the BRDF at the position x for any incident radiance traveling along w_i and w_o integrated along the full hemisphere:

$$\rho = \int_{\Omega} f_r(x, \omega_i, \omega_o)(\omega_i . n) d\omega_i$$

Through experimentation it will be observed at what particular angles the device is placed in front of the diffused surface which will aid in collecting the most reflected light rays to have the most accurate intensity profile data. The lab experimentation with the 532 nm laser light source will be used to gauge how the light beam reflects at differing positions of incidence on the diffused surface. The diffused surface will be marked at differing locations and distances along the surface. These marked surfaces will than be shone up with the laser at an incidence angle of zero degrees. Data will be collected at each of the different locations to compare the amount of light intensity collected by the devices at each of the points on the surface. Next the previous procedure will be repeated by at differing angles of incident light. The laser source will be placed upon a rotation stage which will aid in accurate angular measurements. The laser will again be shone upon the marked regions at differing angles and the intensity of the light will be recorded. The piece of material used in experimentation will have to be the same as the one used in the demonstration since it is a diffused surface, and a different piece would not have the same build and results. Once the data is recorded with multiple angles at differing locations along the diffused surface, the angle of the actual device will be altered. This data will help aid in understanding how the differing angles of both the incident light and orientation of the device affect the ability for the lens system to collect the most reflected light rays as possible. The optimal position will be found through this experimentation.

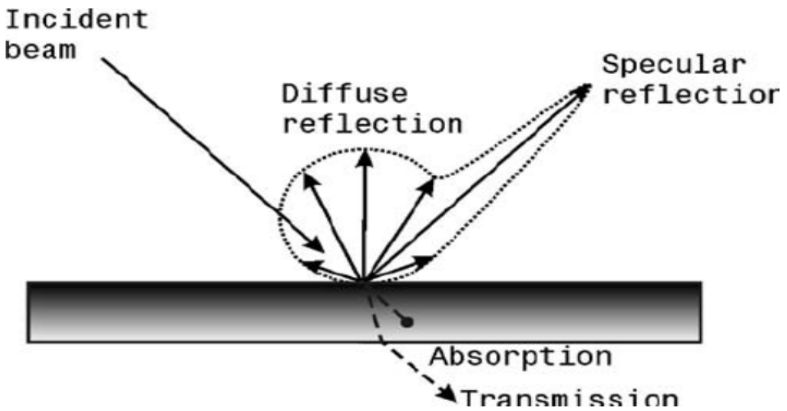

Figure 1: Light Interaction When Striking a Diffused Surface
Photo taken from (The influence of incident angle, object colour and distance on CNC laser scanning)

4.2 Camera Working Properties

ADC stands for analog to digital converter and represents the ability to convert the captured image into a digital file. ADC is given in units of bits, which corresponds to the amount of color values each pixel has access to. A higher ADC allows for the camera to capture more values and create an image with smoother gradients and better shadows. The minimum ADC determines the dynamic range which is the range of darkest value to brightest value. 8 bit has 256 possible values per pixel while 12 bit has 4,096. Because we are going to be developing an intensity profile based on the image captured, a higher ADC is a high priority. The slight variations of pixel value will give a more accurate profile of the beam (Plumridge, 2020).

Dynamic range is the ratio of the largest signal and the smallest possible signal that a sensor can generate. A large dynamic range increases the detail and contrast in a captured image. Brighter pixels capture photons faster than darker pixels so oversaturation can lead to blooming and image distortion. High contrast images typically have the most issues with dynamic range because high intensity light can blow out highlights and reduce the overall detail in the image (Plumridge, 2019).

Back focus is the distance from the sensor to the front of the camera. Shorter back focuses give you more flexibility with what you can include in your system. It's also useful if you're looking to use smaller filters with larger sensors as the close distance can reduce vignetting." However, several issues can arise from short back focus systems. Condensation can become an issue with cooled sensors being close to optical windows. Reflections from the optical window can produce artifacts in the image (Plumridge, 2018).

Frame rate is the speed in which images are shown in a video. 24 fps is a similar frame rate that our eyes see. 30 fps is usually the frame rate used for television, while 60 fps is used in slow motion video or sports recordings,

because high motion recording typically require higher frame rates (Brunner, 2017).

The higher the frame rate the more detail will be collected in the context of this project. However, it is not determined how much the beam moves on the target at this time. If the beam traves around the frame a lot, we may need to consider a higher frame rate to keep up with the detail needed to be collected. 60 fps or more will probably be unnecessary for data collection (Brunner, 2017).

Full well is the amount of charge that can be stored within an individual pixel without the pixel becoming saturated. There is a linear relationship between the light intensity and the signal degradation as the pixel approaches the saturation limit. A higher full well is needed for the application of this project because intensity profiles are likely to have highly saturated pixels. If pixels become oversaturated, then the intensity profile will be inaccurate (Instruments).

Blooming is an image artifact that results from over saturated pixels. When a pixel reaches saturation, they are unable to contain any additional charge, so the charge begins to spread into adjacent pixels. This will cause rings or a saturated blob around the high intensity pixel along with a long vertical streak down the image. The streak is due to the direction the signal travels in the sensor during the CCD readout (Instruments).

Mega pixels refer to the resolution of the image, and one megapixel is one million pixels. A higher megapixel spec allows for zooming or cropping of a photo without an optical zoom system. This does not seem to be a defining specification for our purposes.

Peak quantum efficiency, sometimes called spectral sensitivity, describes the ability for the sensor to absorb photons at a particular frequency. The peak quantum efficiency would be the maximum efficiency the sensor can guarantee, often found between 500 and 600 nm, corresponding to green (495-570 nm) to orange (590-620 nm) colors.

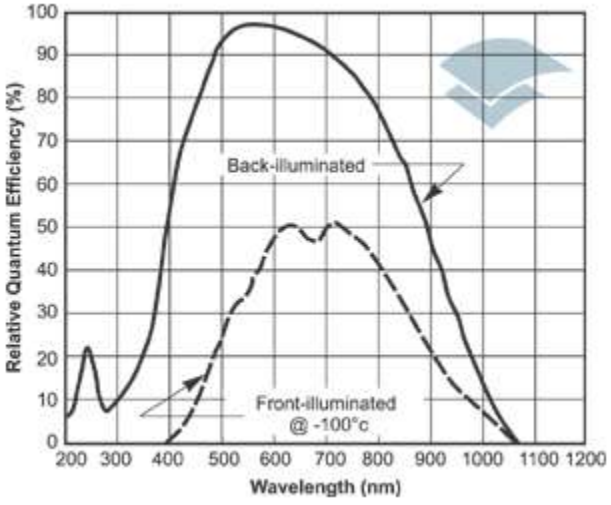

Figure 2: Quantum efficiency in cameras. The peak quantum efficiency lays between 500 and 600 nm. Taken from (Andor, 2018)

Read noise is the main source of noise in a short exposure image. The specification is given in a median value in units of e-. the lowest read noise is the most desirable because this permits high dynamic range and detection of low-level signals. Read noise is affected by the user settings and applications the camera is used for. Typically, settings that increase the frame rate will increase the read noise

4.2.1 CCD vs CMOS Sensors

CCD (charge coupled device) and CMOS (complementary metal-oxide semiconductor) are camera sensors whose main function is to convert photons into electrons. CCDs physically transport the charge across the sensor to a corner of the pixel matrix when it is read out while CMOS sensors transport the charge using wire. The CCD is not as flexible in design because each pixel cannot be read individually (Karim Nice, 2020). Both sensors have their place within camera design, but each have advantages and need to be looked at in order to choose which is best for a given application.

The CCD sensor is arranged at a pixel array composed of photodiodes specifically designed to process and create distortion-less images, in the way they transport electrons. The sensor can create low noise images with high quality light sensitivity. Historically the CCD sensor has a longer production run, and the technology is more mature, giving users more pixels and higher quality images. CCD sensors, though, consume more power, nearly 100 times that of the CMOS sensor and can often be more expensive (Karim Nice, 2020).

CMOS sensors have a pixel array that is composed of transistors situated directly next to one another. Because of this arrangement, light sensitivity can be an issue and the images are susceptible to blooming and other saturation problems. The read noise is typically not as low as that of the CCD sensor. CMOS sensors consume little power, have a long battery life, and are easily manufactured, making them an inexpensive alternative to CCDs.

While the image quality is better in a CCD sensor, the battery life and power consumption is appealing for this project. Additionally, the price of the CMOS sensor cameras is in budget while the CCD cameras are far more expensive. Though knowing the difference and the pros and cons related to both help make educated decisions based on the capabilities.

4.3 Zoom System

This section covers investigation into the properties of the zoom system to be used in the project and the considerations that are to be made in this area.

4.3.1 Zoom Lens System Properties

Zoom lens systems are a collection of lens groups, where each group has their own function within the system. The entire system creates an image with a magnification that is equal to the product of the magnifications of the individual groups. One or more group moves along the optical axis, changing the magnification of the individual group and therefore the entire system.

$$magnification = m'_1 m'_2 m'_3 \dots m'_n$$

When designing the zoom lens system, the first group's magnification is always considered zero, so the focal length is used instead. The image plane remains the same in a zoom system, but as the groups move, the focal length of the system varies continuously. The effective focal length of the system is then the product of the first group's focal length and the remaining group's magnification, at any position in the zoom.

$$effective\ focal\ length = f'_1 m'_2 m'_3 \dots m'_n$$

The zoom ratio, γ, also known as the zoom range, is the ratio of the max focal length to the min focal length attained by the zoom of the system. Small zoom range corresponds to γ range between 1-2, medium zoom is γ between 3-12, and large zoom is where γ>12. The larger the zoom ratio, the more complex the lens system must be for significant performance.

The groups of the lens system are named for their function. There are two consistent groups spanning a wide range of design types. These groups are the variator and the compensator. The variator typically moves linearly, while the compensator generally moves nonlinearly. The nonlinear path that the compensator move in is called the cam curve. The variator controls the zoom magnification of the system, while the compensator keeps the image plane stationary. Careful attention must be given to the internal magnification of the design, otherwise situations can easily arise where multiple groups devolve into variators which increase the possibility of discontinuity. Other lens groups include fixed, moving, focusing, and field correcting groups, all of which provide unique function within the system.

Optically compensated zoom was one of the first developed zoom system types. In this configuration, both the compensator and the variator moved in the same way, preventing clear images at all positions through the zoom range. Also, there are fewer elements which cannot sufficiently minimize aberrations. Though seldom used today, optically compensated zoom is an important historical concept that led to mechanically compensated zoom, commonly used today. Mechanically compensated zoom allows the compensator and variator to move autonomously with different and optimized motion paths.

Assuming a thin lens design, the conjugate changes when any of the lens groups move.

$$object\ to\ image\ distance = f'(2 - \frac{1}{m'} - m')$$

A main concern when designing a lens system is the aberrations of the image caused by the series of lenses. Distortions in the image emerge from rays not converging to one focal point due to the limitations of the lenses and the system. Accuracy in image after passing through the zoom system is crucial for correct intensity profiles and collected data.

4.3.2 Afocal vs. Focal Systems

Afocal systems involve two or more lenses where the input light and the front focal point are located at infinity. This type of configuration is common in beam expanders, telescopes, and binoculars. In a two-lens configuration, where zoom is not factored and the magnification is unchanging, the rear focal point of the first lens and the front focal point of the second lens coincide. The incoming rays are parallel to the optical axis in the object space, and the output rays in the image space are parallel to the axis but conjugate to the incoming rays. The transverse and longitudinal magnification do not change in this type of set up. Afocal zoom systems do not focus the light, rather, simply changes the size of the incoming beam.

Focal systems are optical systems where all incoming rays are focused to a particular focal point. Even rays originating at infinity are focused to the focal point in this type of system. Focal systems have a consistent magnification, though are able to resolve high quality images.

Afocal systems are consistently used in zoom systems, though require a focusing lens behind the system to create a clear image.

4.3.3 Two–Group Zoom

The most basic, conceptually, configuration and the best starting point when designing a zoom lens system is the Two-group zoom. A two-group lens system refers to a zoom design only containing two groups. These two groups are the compensator and the variator. By changing the spacing between the two components, t, the optical power, Φ, of a system in air is given as:

$$\Phi = \Phi_A + \Phi_B + t\Phi_A\Phi_B$$

There are four possible configurations of lens groups, where N is negative optical power and P is positive optical power. These configurations are PP, NN, PN, and NP. The NN configuration cannot work, as it is unable to focus collimated light. The three remaining configurations, the PP, PN and NP arrangements, are conducive to the zoom lens system design. In these arrangements the first group is considered the compensator and the second group, the variator.

Though PP configurations can provide zoom, they are undesirable due to the systems length. The zoom ratio is small, while the barrel length is large, making it impractical for most applications.

The PN configuration, usually called a telephoto lens, is compact with a minimal barrel length. However, PN type constructions have a limited field of view and limited zoom ratio, and it does not correct for aberrations sufficiently. Small zoom range is ideal for this configuration. This type of design is often employed in photography applications.

When designing zoom systems, wide angle positions (semi- angle coverage >20°) need large front group diameter. The NP arrangement forces the entrance pupil to be located nearest the front group, overcoming this difficulty. The NP configuration allows for a large field of view, large zoom ratio, and favorable aberration compensation. Still, the NP design is not compact as the back focal length is far larger than that of the PN arrangement. In addition, the second positive group typically result in diameters that are at least as thick as the first negative group, which is not ideal. Rather, it is better to consider PNxx arrangements, with lens groups that decrease in diameter, as it is more advantageous in mass and movement. Common in compact PNxx type systems, added aperture stops near the front group allow wide angle issues to be overcome, however, it requires that the stop also move during zoom.

Two-group zoom designs are limited in design freedoms because the choice of optical power for both the compensator and variator are constrained. For the two-group system with an object at an infinity, the light must be collimated, and the system must provide focused light. Adding additional lens group(s) so that there are lens groups on both sides of the image kernel, the light is no longer required to be collimated, and the variator and compensator can then receive and deliver convergent or divergent light.

While two-group zoom is not as robust or complex as larger group systems, sharp images can be attained, and first order aberration requirements can be achieved. Higher order aberrations are a concern however in this type of lens arrangement.

4.3.4 Three–Group Zoom

Three-group zoom lens systems offer more design freedom and flexibility than its two-group counterpart because of the added complexity in lens groups. The three-group system allows for a larger zoom ratio than two-group zoom. Typically, arrangements are that of NPN and PNP Donders telescopes. A Donders telescope is an afocal three-group system where there is one fixed prime lens in addition to the variator and compensator groups. The prime lens holds the location of the image plane stable and is usually located in the rear of the system.

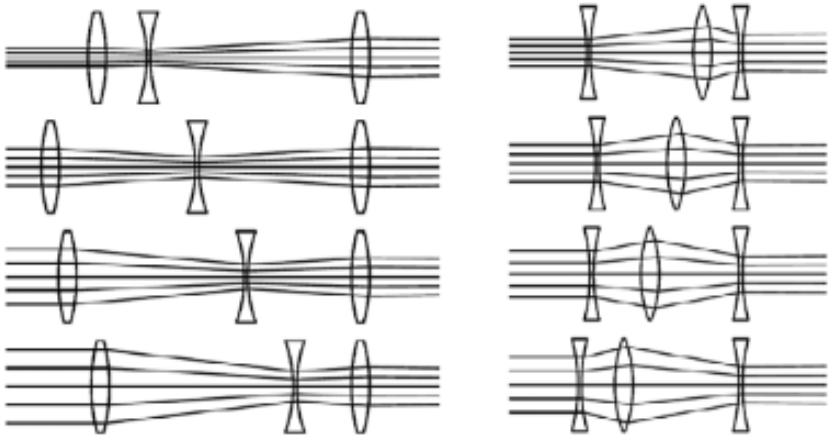

Figure 3: lens systems where incoming light is from the left, and outgoing light to the right. The camera in this type of system would lay behind the third lens to the right of these set ups. PNP lens configuration, left and NPN lens configuration, right Donders type telescope. Both these lens configurations are afocal. Taken from (Sasian 2019)

Fourth order aberrations can be corrected in this configuration, as three-group zoom systems have more complex lens groups and group design, than the two-group arrangement. Spherical aberration, astigmatism and coma can be corrected at the limits of the zoom by adding complexity to the lens groups. Aberrations can be overcome simply by splitting the singlets into multiple optical elements, commonly doublets or triplet, but some designs utilize more. More control of the aberrations comes at the expense of the system's simplicity.

Several considerations affect designs of three-group zoom systems. As complexity increases in each group, they then become thicker. In this case, overlapping lenses must be avoided. Additionally, the position of the compensator and its cam curve require careful attention, as the zooming mechanism cannot overcome steep changes quickly.

4.3.5 Four–Group Zoom

Four-group zoom lens systems increase the design flexibility because of the increase in complexity of the groups in addition to adding a focusing group. The focusing group is the first lens group in this type of configuration. This group maintains the conjugate distance to the following kernel groups.

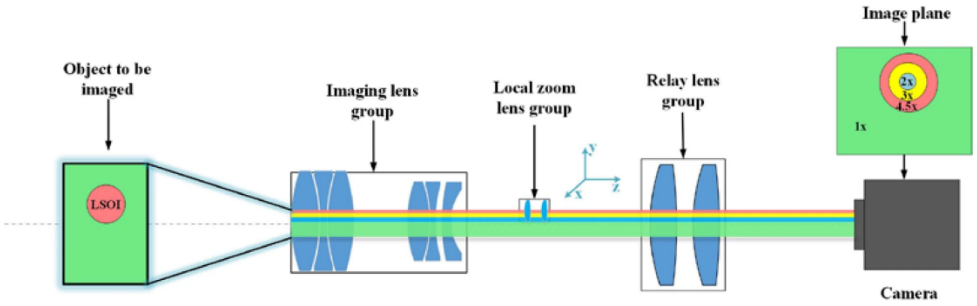

Figure 4: Four-group zoom lens configuration with camera and image plane design

The four-group zoom system increases the zoom ranges as well as improves the resulting image quality. Four-group systems are the best when the design is used to meet specific focusing requirements.

An interesting effect that can arise from the addition of the focusing group is called breathing. It occurs because this group inherently changes the field of view of the following lenses. This can create unnatural movements of bodies within the object plane and can be unacceptable in applications of high movement or detail-oriented imaging.

4.4 Light Collecting Plano Convex Lens

A large concern of the design is the ability to collect as much of the diffused light of the laser reflected from the diffused surface into the optical system. The initial approach was to have the front lens of the zoom system to act as the collecting lens but due to budgetary restrictions the optics for the zoom system will be too small to act as a collecting lens. A collecting lens is typically a large diameter plano convex lens which will be able to collect a large array of the light rays and focus them to its focal length. There are some restrictions and trade offs which must be considered when selecting the proper lens for the design. Since all real lenses have some thickness and are not the ideal thin lens the focal point is calculated using the following equation where R is the radius of curvature and n is the index of refraction. The material for the lenses being

looked at is N-BK7 which has a refractive index of 1.5195 at a wavelength of 532 nm.

$$f = \frac{R}{n-1}$$

The F-Number, lens diameter, and numerical aperture of the lens are the main properties which are taken into account when choosing the best light collecting lens. The diameter of the lens and its corresponding focal length are the first variables which are examined with a collecting lens. A larger diameter lens will be able to collect more light versus a smaller diameter lens. The relationship between focal length (f) of the lens and its diameter (D) are what dictate the F-Number of the lens. This relationship between diameter and focal length is shown below.

$$F\# = \frac{f}{D}$$

An increase in diameter of the lens will in turn lower the F-number. Essentially this means that the lens will be able to collect more radiant flux (ϕ_c), but there is a tradeoff. The amount of radiant flux collected by the lens is the inverse of the F-number squared as seen below.

$$\phi_c = \frac{1}{(F\#)^2}$$

Although more radiant flux is collected when the F-number low, the radiant flux information collected may introduce undesired effects into the system including aberrations. The aberrations introduced will negatively impact the quality and coherence of the light rays entering the system. Any undesired effects of the light rays entering the system from the collecting lens will only be compounded as it travels through the zoom system to the CMOS sensor. It is crucial to have the proper collecting lens that will be able to collect enough radiant flux from the diffused reflected light while in turn not adding negative qualities to the wave fronts of the light traveling through the lens. In reality the convex lens will have some thickness to it which will refract the light, the thinnest possible thickness is being sought for the lens. The lenses that are being looked at are from Thorlabs and are uncoated N-BK& Plano convex lenses. Uncoated lenses do have the potential to cause reflection interference which can affect the propagation of the light through the system. A coated lens would be more suitable but are out of budget for the design. The undesired effects of the uncoated lens will be analyzed through zemax first to determine the appropriate Plano convex lens to purchase. This is still in the works and will be decided before the submission of the final paper.

4.5 Laser Source

The laser source for this design was compared between two lasers advertised as having a central wavelength of 532 nm. Both laser's powers were measured in the laboratory using a power meter. The scope laser reading resulted in 2.5 mW. The handheld laser source was measured using a power meter and a neutral density filter of optical density 2 and was roughly 100 mW. Both spectrums were measured using a spectrometer and the scope laser bandwidth was centered with a far right shift of the desired 532 nm as seen in **Figure 5**. The handheld laser spectrum included a high output of 532 nm frequency just shy of being central. The handheld laser and the materials it is composed of do cause it to have some infrared leakage which can be seen in the spectrometer reading in **Figure 6**. The leakage is not an issue because the bandpass filter will block out those undesired wavelengths which is confirmed by measuring the laser spectrum through the bandpass filter into the spectrometer with the results shown in **Figure 7** confirming that the laser is 532 nm with a narrow linewidth. The 100 mW handheld laser was chosen for it has a higher power output allowing more light intensity to travel through the system, it lases close to peak 532 nm wavelength, and the bandpass filter will aid in filtering out the leaking radiation from the laser. 100 mW is more than enough power for the device's camera to capture images of the reflected wave fronts from the diffused surface. The lens system and filter deplete a percentage of the light intensity as the reflected light propagates through the system. The diameter of the beam aperture is 3 mm. The intensity of the laser with a coherent beam is 1.4147 W/mm^2 which was calculated using the equation below. .

A. Equations

$$I = \frac{P}{\pi * d^2}$$

B. Lab Results

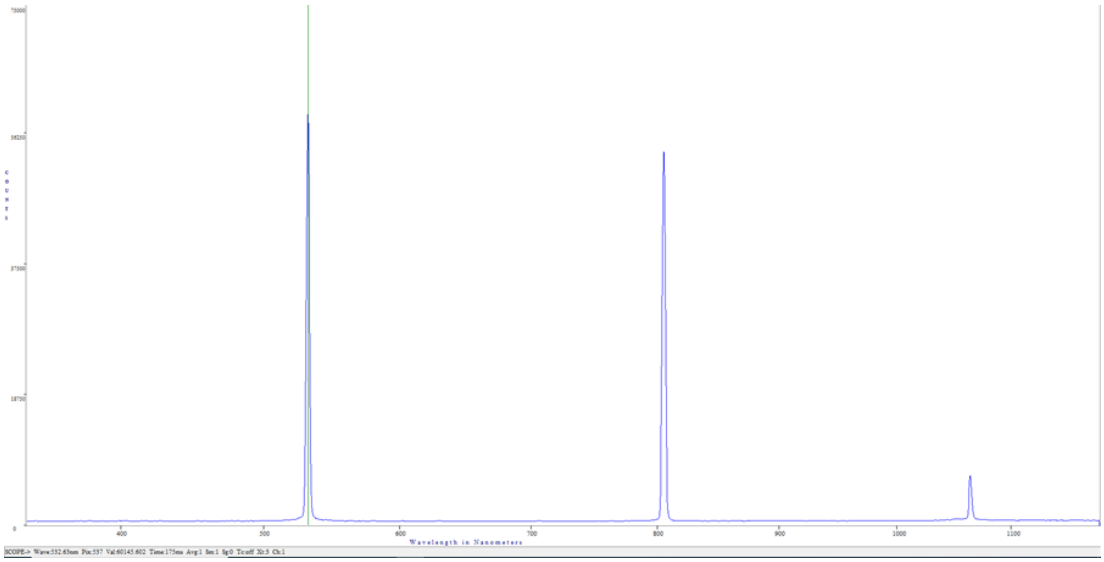

Figure 5: Spectrum of 100 mW handheld laser on spectrometer

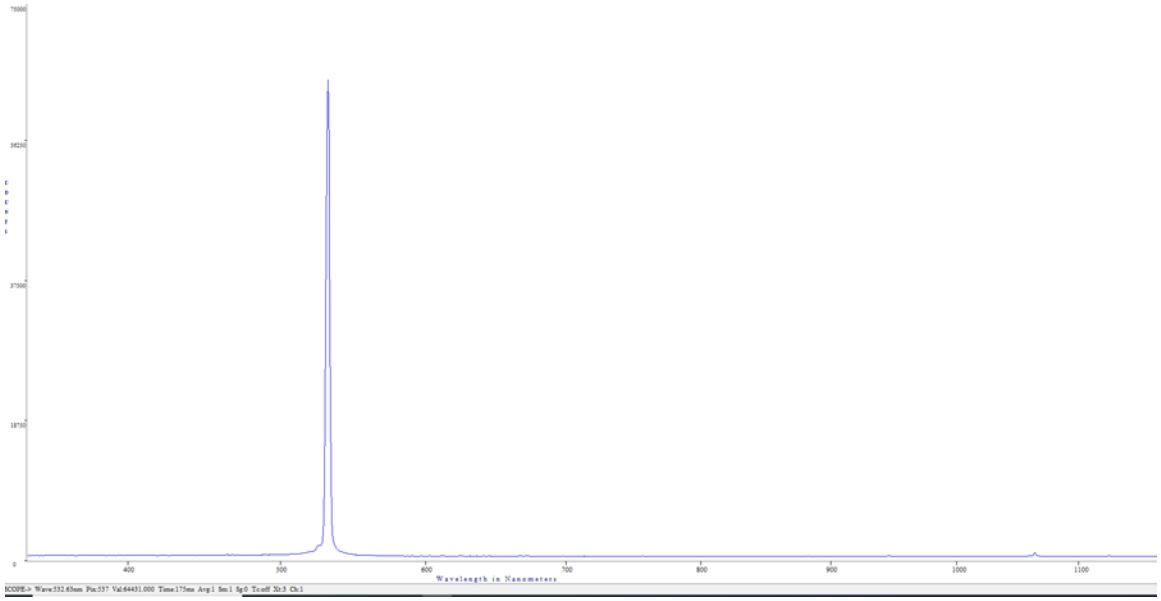

Figure 6: Spectrum of 100 mW handheld laser on spectrometer with Bandpass Filter

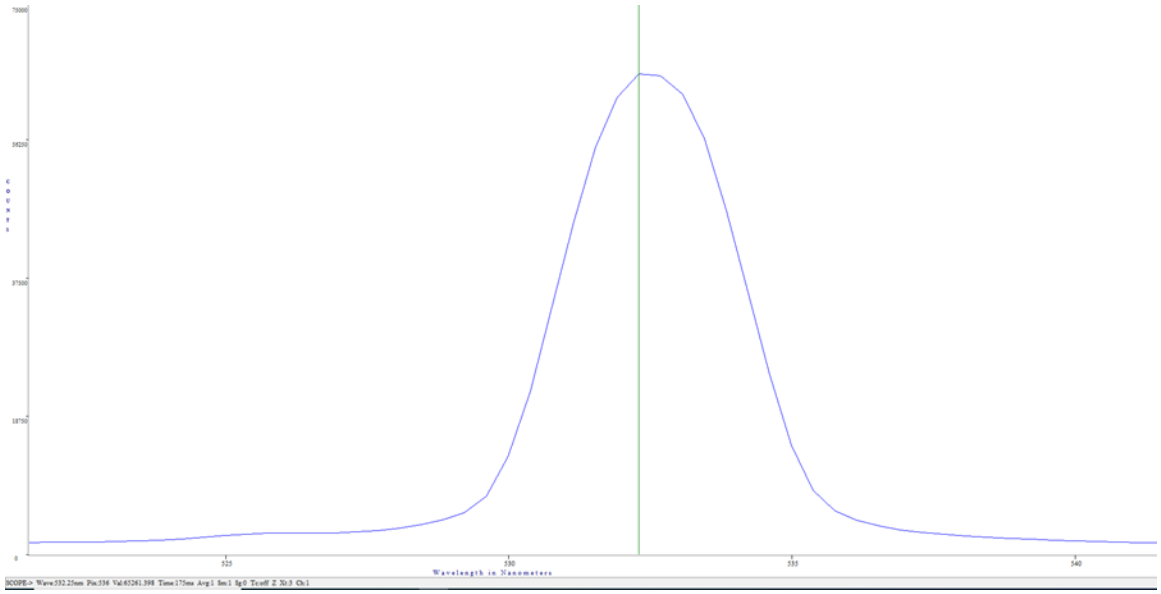

Figure 7: Spectrum of 100 mW handheld laser on spectrometer with Bandpass Filter and green line central wavelength of 532.25 nm

4.6 Optical Filters

An optical filter is typically made up of film materials which may be stacked with a specific thickness which have unique properties allowing a selected band of frequencies of a traveling optical signal to pass through. The outer band or bands of frequencies outside of the desired band are a blocked by absorption, interference, or reflected. Whether certain frequencies of the propagating wavefronts are absorbed, reflected, or interfered with depends on the type of optical filter and the materials it is made from. Optical filters also are used to split up an optical frequency into its many differing wavelength components for thorough analysis of a single wavelength of an optical signal. Optical filters which are angle sensitive act similarly to a prism or grating. These types of filters can be used in applications which require spectroscopic analysis or the splitting of frequencies throughout an optical system. An optical signal propagating through an optical cavity, sent over some predetermined distance without being directly coupled will experience some type of noise or interference throughout the length of travel. This extra noise and interference can completely destructively interfere with the signal or alter it to the point that the receiver on the other end cannot decipher the original signal sent. A way to repair the altered signal back to its original form is to place optical filters within the path of the optical signal as it travels through the optical system. What type of optical filter used depends on the application and the type of light source being emitted at the input of the optical system. Optical filters are used in a variety of applications including but not limited to machine vision, spectroscopy, microscopy, chemical analysis, and

imaging. The optical filters working properties that are most important in deciding the appropriate filter for a design project include the optical filter's central wavelength, bandwidth, full width half maximum, blocking range (optical density), slope, cut on wavelength, cut off wavelength, edge steepness, and ripple. Optical filters also have certain physical properties as well which determines the propagation of the light signal traveling through. These physical properties are related to both the thickness of the filter and the materials which are used to create the optical filter. There are many types of filters available on the market including long pass filters, short pass filters, bandpass filters, notch filters, neutral density filters, and interference (dichroic) filters. Each type of filter functions with unique properties to block undesired frequencies along specified bands of the electromagnetic spectrum. Before choosing a particular type of optical filter for a design the working properties and physical properties of the optical filter must be understood. With this knowledge one can confidently decide the proper type of optical filter that will best suit the design or experiment being conducted. There are many ways to approach using optical filters in an experiment. Optical filters can also be stacked in a parallel construct to selectively choose a particular bandwidth region of wavelengths to pass through the optical system. Both a short pass and long pass filters stacked will create a unique bandpass filter which will be designed to have a particular bandwidth region of selected frequencies which can propagate through. Filters can be placed anywhere along an optical system. Optical filters may be placed at the input of an optical system for filtering out certain frequencies of light from an input source with either a narrow bandwidth (laser light) or broader bandwidth (lamp source or L.E.D). Optical filters may be placed within the system in front of certain optical equipment to filter out generated frequencies that are created through excitation within the system (this is where the optical filters for this design are placed). Optical filters may also be placed near the end of the optical system. This is generally to filter out any unwanted frequencies at the output, so the signal at the receiver has can reconstruct the original signal sent or decipher the newly created filtered signal

4.6.1 Optical Filter Working Properties

Optical filters have many unique properties which make them crucial to be used within many design experiments. The cut on wavelength of an optical filter determines where the wavelength transmission will begin to increase significantly from an area of attenuated frequency transmission to a frequency area of very high transmission. At this threshold the transmission will increase to about 50% transmission. Typically, $\lambda_{Cut\text{-}On}$ is used to denote the cut on wavelength. The cut on wavelength is also referred to as the 5% absolute transmission line of the optical filter transmission spectral band. The cut on wavelength is the edge parameter of a long pass optical filter. The cut off wavelength of an optical filter essentially is the opposite spectrum from the cut on. The cut off wavelength determines where the wavelength transmission will begin to decrease

significantly. At the cut off threshold the transmission will begin to decrease by about 50%. $\lambda_{Cut\text{-}Off}$ is used to denote the cut off wavelength. The cut off wavelength similar to the cut on wavelength is also referred to as the 5% absolute transmission line of the optical filter transmission spectral band. The cut off wavelength is the edge parameter of a short pass optical filter. The cut on and cut off wavelengths of a bandpass optical filter will determine the central wavelength. The central wavelength is the center passband or notch of the optical filter. A notch is the band reject region of an optical filter. It is the opposite of the passband, where only the notch region will be rejected or absorbed. The central wavelength is used to describe both a passband filter or a notch filter. The central wavelength can be determined by using the following equation:

$$\frac{2(\lambda Cut-On)(\lambda Cut-Off)}{\lambda Cut-Off+\lambda Cut-Off} = \text{Central Wavelength } (\lambda_{CW})$$

The bandwidth of the bandpass filter is the allotted band of wavelengths which are able to travel through the optical filters. The bandwidth of the bandpass filter will be between the two edges of the cut on and cut off wavelengths. This region of the spectrum is determined by the absolute points on the spectrum that the optical signal will be able to achieve > 50% transmission. The width of the bandpass filter divided by the central wavelength and multiplied by 100 will give the band width as a percentage. The width is crucial for design and determines how many wavelengths will travel through. A broader bandwidth will allow more frequencies to travel into the system whereas a narrower bandwidth will only allow a very precise range of wavelengths into the system. A laser has a much narrower bandwidth than that of an L.E.D or lamp source. The full width half maximum is the region half power is transmitted through the system. This parameter is used to describe a band pass filter and relates to the two edges of the pass band. The blocking range of an optical filter is the spectral area of frequencies which are attenuated out by the filter. The blocking range is also directly related to the optical density of the optical filter. For a bandpass optical filter, the blocking range region would be the spectral area outside of the pass band, whereas for a notch optical filter this region would be the spectral area inside of the band. The blocking range of the optical filter is denoted as the optical density and can be calculated using the following equation:

$$Optical\ Density\ (OD) = \quad -log_{10}(Transmission)$$

Optical density is traditionally notated as a number falling from one to eight. One being the least optically dense and eight being the most optically dense. The higher the optical density the less light that will be able to travel through the optical filter in the block band regions. For example, an optical

density of one will allow ten percent of the light to travel through the optical filter. Whereas an optical density of two will allow one percent of the light through an optical filter. This scale is logarithmic with each increase in optical density value, will have one tenth the amount of light able to travel through. When stacking optical filters with their own optical densities it is easy to assume that the overall density would just be the addition of the two optical densities. Optical density is not linear in that way and will only slightly increase the optical density. For example, creating a bandpass filter with a short pass filter and long pass filter of optical density 2. The overall optical density will only be slightly over 2. Selectively placing the optical filters a calculated distance from each other can increase the optical density and is required for interference filters. The optical density parameter is crucial to design and can affect how much of the signal is attenuated. If the original signal is quite low in intensity, a high optical density may cause little to none of the signal to be able to be propagated to the receiver. Optical filters can either absorb undesired spectral frequencies, reflect undesired spectral frequencies, or use interference through multiple layers within a single optical filter of desired thickness. Slope is a variable related to the specifications of an edge filter (long pass and short pass optical filters). The slope is indicative of when the transition takes place from peak blocking of frequencies to peak transmission of frequencies as the signal travels through the optical filter. The edge steepness of an optical filter is the calculated distance between the region where the optical density is greater than six (essentially the non-transmittable region blocked by the short pass, long pass, or band pass filter) and the point at which 50% transmission occurs on the spectrum. Edge steepness is pertinent to edge filters such as short pass, long pass, and band pass optical filters. The edge steepness is related to how quickly a transition between the transmission region of the filter occurs and its complementary optical density region. Edge steepness can be calculated using the following equation:

$$100 * \frac{|\lambda(50\%transmission) - \lambda(Optical\ Density)|}{\lambda(50\%transmission)}$$

Ripple relates to the fluctuations within the frequency band of the optical filter. This band can either be a pass band or a stop band. Ripple directly affects the performance of an optical filter system. Ripple is measured in dB and is ideal to be as low as possible for the best performance.

4.6.2 Optical Filters Physical Properties

Optical filters physical properties are both the thickness of the optical filter itself and the material used to make the filter. The thickness of the optical filter is directly related to the transmission percentage of the optical signal which travels

through. A filter can be one of either extreme, too thick or not thick enough for the experiment. The thickness parameter is important to take into consideration when dealing with an optical system with many optical devices where the light signal will be traveling through. The materials refractive index along with the thickness will control the behavior of the optical signal propagating through. The more optical devices introduced into the optical system such as lenses, gratings, beam splitters, etc. the more the optical signals intensity will be attenuated. It is important to know what power of the light signal is required at the output when deciding which types of optical devices to use within the system. If there are so many optics that the final light signal at the output is too weak to get any pertinent reading, then the experiment will not result in accurate experimental data to be analyzed. The filter can also be too thin with a low optical density and not block out the undesired frequencies sufficiently. When this occurs there will be bleed of frequencies at the output signal which in turn can cause the inability to decipher an original optical signal from both noise and undesired frequency interference. Thickness of the filter is also considered when stacking optical filters. Stacking optical filters will allow for more control over which spectral frequencies are allotted to travel through the system. Stacking of the optical filters will result in a thicker optical filter and a higher optical density. Each optical filter have their own transmission percentage. When these optical filters are stacked the transmission percentage will also stack and inevitably determine the total transmission of the pass band for the optical filter system. The optical filter system as a whole unit, when there are no non-linear optics involved is a linear system, resulting in a linear transformation and transmission percentage calculation. For the following example two optical filters will be denoted as optical filter one H_1 and optical filter two H_2. Since the system is linear it does not matter which order the optical filters are stacked in because the end result of transmission will be the same. This also applies to differing types of filters which do not have non-linear behaviors.

$$H_1 * H_2 = H_2 * H_1.$$

It is necessary to take this into account when stacking optical filters for if the transmission of one is much lower than that of the other it will lower the transmission of the optical signal significantly. The following equation can be used to calculate the total optical transmission through the system:

$$H_{1(\text{transmission})} * H_{2(\text{transmission})} = H_{\text{Total(transmission)}}.$$

For example, if optical filter one (H_1) has a transmission rate of 65% and optical filter two (H_2) has a transmission rate of 85%. The total transmission rate of the two stacked optical filters in this optical system would be equal to 55.25%. That is almost half of the original signal being transmitted through. This again is why it is necessary to be aware of the transmission rates of all optical devices within the system. Whether the filters are starting at the input, in between, or at the output of the optical system, the amount of optical signal traveling through is attenuated

50% before traveling through any other optical devices within the optical path length. The material used in creating the filter will dictate the propagation characteristics of the optical signal as it travels through the filter. Filters can also change the polarization of the wavefronts traveling through it. Optical filters thickness selectively controls the transmission of the optical signal through the optical system, and the material controls the refractive nature of the optical signal. Most filters are typically composed of either a glass or a polymer. The material used is important and will directly affect the design aspect of creating an optical filter. Optical filters are passive devices and will not consume any power from the battery source of the design.

4.6.3 Types of Filters

There are many different types of optical filters on the market today which can be designed to match any necessary requirements for experimentation. These types of optical filters include long pass filters, short pass filters, bandpass filters, notch filters, neutral density filters, absorptive filters, interference (dichroic) filters, and refractive optical filters. Each type of filter may be used for differing applications or within the same system with multiple differing optical filters. Different types of optical filters may also be stacked to design a particular desired output spectrum. Each type of optical filter has different working properties and are composed of different materials. The material used will dictate how the propagating light will be refracted as it travels through the optical filter. Long pass filters are edge filters which

Reflection of spectral frequencies typically takes place when a signal will be directed on another path within the optical system. This typically happens when an optical beam is split within the optical system by the optical filter itself. The wavelengths can be split and sent into differing directions for experimentation that is needed to separate wavelengths. When the signal is split there are angles of incidence that must be considered which adds another component to the equation of characterizing the behavior of the optical system. Absorption is typically used when reflectance is not necessary for the optical system (most commonly used for applications). Absorptive filters typically are colored filters which absorb particularly spectra by design ranging from far U-V to far infrared. The thicker the absorptive filter the more effective it becomes by being able to absorb more of the undesired wavelengths within the optical signal.

Absorptive filters traditionally are composed of glass which is tinted using both organic and inorganic dyes which aid in capturing the undesired optical signal frequencies and allow the desired optical signal frequencies to transmit. The absorption of the undesired wavelengths is converted into heat within the optical filter. These types of optical filters do not depend on angle of incidence. Absorptive filters are ideal to use for experimentation when a particular band of frequencies that is sought or when a reflective filter will introduce unwanted noise into the system. Absorptive filters are typically less expensive to fabricate. While being more cost efficient, they are limited to particular spectrums which can

cause designing to be difficult if the desired filtered region is not compatible with absorptive spectrum that is available.

Interference (dichroic) filters are optical filters which are designed to have several layers within the filter of a particular thickness. These layers are traditionally thin films which are stacked on top of each other and are angle sensitive. Every layered component of an interference pattern must be precise to get the desired spectrum on the output of the optical filter. The thickness of each sub layer must be the exact dimension required for the desired spectrum to be produced. As the optical signal travels through the filter the edge of each sublayer will reflect some of the incoming light just perfectly to constructively interfere and filter out the undesired wavelengths. This process continues to happen through each sublayer until the final output is the desired optimal optical spectrum. Any slight mis calculation of thickness will undoubtedly cause the optical signal on the output to be slightly off the required spectrums central wavelength. These types of filters are more expensive and are typically used in specialized experimentation.

Neutral density filters are optical filters which suppress all wavelengths of light evenly by a certain optical density degree. These types of filters are used when the intensity of the light signal needs to be decreased by a certain percentage. Neutral density filters are also used to block out ambient light from a detector during experimentation.

Long pass optical filters are edge filters which by design will attenuate shorter wavelengths while allowing longer wavelengths to transmit through. Longer wavelengths lie on the lower energy region of the electromagnetic spectrum. These optical filters have a cut on wavelength and a rejection wavelength range. Long pass optical filters are typically not sensitive to angle of incidence which makes them ideal in experimentation that is not sensitive to the angle of which the light signal propagates through the optical system. Long pass optical filters are ideal for applications when higher energy shorter wavelengths must be attenuated out of the optical system.

Short pass optical filters are also edge filters that attenuate longer wavelengths. Short pass optical filters allow transmission of wavelengths which are shorter or toward the higher energy region of the electromagnetic spectrum. Short pass optical filters have a cut off wavelength and a rejection wavelength. Similar to the long pass filters, short pass optical filters are also not sensitive to the angle of incidence making them ideal for experimentation that is not sensitive to the angle of which the light signal propagates through the optical system. Short pass optical filters are ideal for applications when lower energy longer wavelengths must be attenuated out of the optical system.

Bandpass optical filters are a combination of both an optical short pass filter and optical long pass filter stacked together. These optical filters have a bandwidth of wavelengths which are able to be transmitted through. Outside of the edges of the band pass region the optical density begins to increase and the outer spectrum will be rejected. Bandpass optical filters have a center wavelength where transmission is the highest. Depending on how the bandpass filter is designed the transmission percentage will begin to lower on both edges

until it reaches the cut on and cut off regions of the pass band. Bandpass optical filters also have a full width have maximum cut on and cut off wavelengths. Bandpass optical filters are not sensitive to the angle of incidence of the incoming light signal. Bandpass optical filters are ideal for applications that need a specific bandwidth of transmission such as fluorescence applications, spectral radiometry, machine vision and laser line separation. The bandpass filter is what will be designed for this project and ideally will have a narrow bandwidth of a few nm width and filter out all other frequencies with an optical density of at least 2.

4.6.4 Optical Filter Design

A filter is necessary for the design of this project for the sole reason of blocking out the highest percentage of ambient light that would propagate through the system to the camera and optical sensor. One main objective of this design is to gauge how much light intensity measured in lux is being collected by the system's camera and is penetrating the surface of the CdS light resistant diode. The filter is placed between the converging lens which is closest to the camera and the middle diverging lens. This position allows for the filtering of the undesired light frequencies reaching both the camera and light resistant diode, to only measure wavelengths of a very narrow bandwidth. The ideal bandpass filter will have five desirable traits. The first being a. central wavelength of 532 nm The central wavelength of 532 nm is crucial for the bandpass filter. The central wavelength will allow the highest percentage of light to pass through. There will be wavelengths on each shoulder of the curve which will also pass but in lower quantities until it reaches the cut off and cut on frequencies. As soon as the cut off frequencies are reached the light transmitting through at those frequencies will be exponentially less. The second train is a narrow bandpass filter.The narrower the bandpass bandwidth the better. The closer the cut off and cut on frequencies are to the desired central wavelength the smaller number of undesired wavelengths will be able to travel through the filter at higher transmittance percentages. This narrow bandpass bandwidth is key in getting accurate measurements from the light dependent resistor and measuring the actual amount of lux reaching the camera's surface. The third trait is a filter with a high optical density. A high optical density is necessary for making sure that the least number of undesired frequencies are leaking through the bandpass filter. No filter is perfect at completely blocking out all frequencies outside of the desired bandwidth but the higher the optical density the smaller the transmittance percentage of those frequencies to pass through. The fourth trai is a high transmission percentage of desired frequencies. The minimum transmission rate should be at least 40%. The higher the transmission rate the larger the quantity of light intensity reaches the camera. In an ideal world all of the light at the desired wavelength would reach the camera. There is always a tradeoff which effects this transmission percentage. Dependent upon how many optical devices the light propagates through as well as the material the filter is made up will

suppress a percentage of the light that reaches the camera and sensor. The fifth trait is a square footage of the active region of the filter to be able to cover both the camera and LDR sensor. The size of the filter is an important factor for making sure that no ambient light will pass around the edges of the filters area and reach the camera or light dependent resistor sensor. The price of the filter exponentially rises as the area of the filter increases. The minimum size of the filter to fit both the light dependent sensor filter and camera fully behind is at the minimum 25 mm.

4.7 Light Source

The light source used in experimentation will be a full visual spectrum light source. These types of light sources emit light similar to the spectrum of the sun and will aid in testing outdoor application of the device within a laboratory setting. The full spectrum lights are rated based off of their color rendering index. Color rendering index of a light source refers to how closely the emitted light spectrum is to sun light or commonly referred to “natural light”. Quality full spectrum light bulbs typically have a color rendering index ranging from 90% to 96%. Full spectrum lights use filters of wavelengths that range including the full spectrum from ultraviolet to infrared, mimicking natural light. There are also similar spectrum lights which only produce the visual spectrum for testing devices where the eye may be used. Another important factor is the number of lumens that the light bulb emits. The higher the lumens the higher the quality of the light bulb and its emission spectrum. As a reference the sun gives off roughly 16.24 quintillion lumens that reach Earth. To scale that in a lab setting is nearly impossible, but a full spectrum light with at least 800 lumens will be the starting point for experimental testing. With this type of light bulb artificial natural light will be introduced to the system within a lab setting and then it can be compared to outdoor settings at a later time. This approach will guide how to the properly differentiate the frequencies that are entering the device from the wave fronts reflecting off of the diffused surface versus the full spectrum emission from the light bulb. The optical filter system will filter out the majority of wavelengths outside the cut on and cut off regions of the narrow bandpass of 532 nm. For the stretch goal the device will be outdoors and exposed to the blackbody radiation of the sun which emits all frequencies from ultraviolet to the far infrared. Due to the Earth’s natural barriers, portions the majority of ultraviolet frequencies do not reach the earth. The frequencies that mostly penetrate the earth are the visible spectrum to far infrared. Both the 632 nm wavelength and 800 nm wavelength of the sun’s spectral irradiance will propagate and mix with the diffused laser light into the system. The aperture size at the input will be tested to find the optimal window of allowed light irradiance into the device for best results. There are many full spectrum light sources on the market for laboratory simulation of outdoor testing. The full spectrum light bulb will be attached to a portable lamp that can be used in differing settings. Analysis of the experiment will also take

place using the incandescent lab lights to see how differing light sources affect the light collection by the device and the corresponding data collected by the camera. When the lab space is not in use by other students the full spectrum light will be used and the lab incandescent light will be turned off. After looking around online at the many options for a full spectrum light source, the best option found with a sufficient number of lumens is sold on amazon. The light bulb is an eleven-watt bulb which produces 800 lumens of light. It is a NorbSMILE full spectrum light bulb and costs 19.99$. This bulb will be used initially for testing and if a brighter light is required than it will be purchased.

4.8 Battery

Different specs of a battery are measured and compared along this paper, where it will show the steps taken to choose a battery efficient, and powerful enough to energize our system and all its components. Next, we will show the engineering investigation done, which guided us towards understanding the important values to calculate and compare for a smooth product search.

Along with calculating the overall consumption of power by our system, our group made an effort to understand what type of battery chemistry would match well with the area where the system will be utilized. Understanding how to calculate a battery's capacity, in order to forecast a battery life cycle, as well as the amount of time a device can be run without any interruptions. Some extra key factors which affect a battery and its efficiency are important to list and to also mention how these factors can be related to our system.

4.8.1 Battery Chemical Composition

Choosing a battery is a heavy task, because it’s giving life to our entire system which is looking for reliability and accuracy. Batteries are manufactured in many ways, two of the most common batteries in the market right now are Lead-Acid batteries and Lithium-ion batteries, the names being the chemical approach for each. A Lead-Acid battery brings a couple more variables to the design. The way this specific style of battery is implemented, it could bring some more physical adjustments to the system. It’s always important that there are specifications that cannot be surpassed. Knowing this, there still a great amount of Lead-Acid batteries in the market which could still be implemented into our system. On the other hand, Lithium-ion batteries are increasingly popular in the electronics circle. By using lithium salt to increase the efficiency of energy. This efficiency and other useful characteristics of this battery makes implementation with this battery favorable during the research process. Another important point

(besides the values in the datasheet), Lithium-ion batteries are in the high price range. Careful research is going to be conducted in order to calculate a stable system with power supply that will not hinder the system. As a tip seen by professors and professionals, always overshoot the values.

4.8.2 Battery Capacitance

As we select batteries for our system, the battery's capacity is a key measurement for the system to have adequate power. Knowing the capacity for a battery for a fixed amount of time is key, to understand when the battery needs to recharge. The equation below allows us to calculate for the capacity when the current drawn and the time running are known.

$$C = x*T$$

Where C is for capacity, x is for current drawn and T is the time running. There are strategies that will allow us to perhaps get a longer life cycle than what the batteries promote. One of the strategies is to run the battery normally till its capacity hits 80%. The equation below extends the equation above for finding the battery capacity needed for some specific variables, and calculates the capacity needed for a battery to run efficiently till 80%.

$$C' = C/0.8$$

Where C' is the new capacity needed for the batter to run till it hits 80%.

4.8.3 Key Factors of a Battery

As mentioned in the previous section, there are a variety of factors that could affect the efficiency and the life cycle of the battery. First factor is the temperature surrounding the battery when in use. As the temperature increases there's a possibility for the batter to lose long term capacity. Keeping an eye on the temperature of the battery by adding a few temperature sensors will help us control the temperature and get a longer life cycle. Another promising feature of a Lithium-ion battery is that they require low maintenance and are not as delicate to temperature as Lead-Acid batteries.

A second factor is the rate at which a battery is discharged or charged. For high charge or discharge values, the battery life cycle and capacity rates will be affected. This happens because as you increase the discharge/charge rate it increases the temperature inside the battery damaging it inside. A third factor is

the limit of the voltage as you charge it, typically a battery should not be charged to its 100% capacity, since it will decrease its charge cycles. One recommendation that was found during our engineering investigation was that it might be ideal to charge the battery to 85% of its capabilities.

4.9 Motor

One of the key features of our system is the freedom of movement of our camera. This is able to happen because of the motors. We've been investigating different types of motors, the top two in our list are a stepper motor and a servo motor. Two movements are going to be provided by whichever motor is chosen, both are going to be rotational movements. One motor will provide the force for the camera to rotate 180 degrees from left to right, the other motor will provide the camera to rotate 180 degrees up and down. Each motor will have a shaft diameter of around 5 mm, where a timing belt pulley will be attached. A timing belt will be connected to the pulley attached to the motor, and a bigger pulley (around 80 tooth). This will provide a slower speed for each rotation and will also help control this rotation with more precision, since our camera will move small angles when searching for the laser. For our system we need our motor to move clockwise and counterclockwise, that way we can find the right position for the laser refraction. Depending on the chosen motor (stepper or servo), a different design will be used in order to make the back-and-forth movement possible, since each of these motors use extra components which allow the motors to function correctly. One key topic when investigating a motor is its power, we are shooting for an average of 36 Watts per motor, which will result in a total of 72 Watts for our system's motors. Along with power, holding torque is important, our system requires between 51 oz. in - 63 oz. in. These torque values will allow the system to maneuver smoothly without any stalls, when holding the camera. The camera will be size, power, accuracy, torque, and cost are some of the few key components when choosing a motor that will be right for our system.

4.9.1 Motor Sizing

In order to find the right size for each motor that will allow the system to move in each desired direction without any error, three main areas out of the system must be calculated. These are the load torque, load inertia and speed. Our system contains two different types of motions, along with different weights. For example, our overall system is going to be weighing an estimated 4.5 kg, which will be handled by the two large motors (M1 & M2). Our system will be designed to be a rectangular body of lengths of around 50 cm, with a width of around 17 cm. In order to create movement to the body of the system when it is stationary, it's important to be able to calculate the load inertia in order to take

into account the amount of resistance against movement. investigating the amount of torque needed from the motor, we calculate the two components that will be present in the time of use. Frictional load will be observed at the point of contact and rotation, which is located at one end of the system. Both M1 and M2 will be placed along some gears which increase the torque. Friction can be measured at the axis, where all the weight of the system sits, adding some pressure to the contact point creating fractional load. As for anybody of mass, gravity plays a big role in systems where a load is lifted up, while also maintaining its position. As mentioned before, M1 and M2 are the larger motors out of the four, because it's holding the overall system. Not only the overall weight of the system will affect the gravitational load, but the distance where the axis of rotation is located, and the force given by the motors.

The following sections will go over each component that composite the system. As mentioned through this paper, the overall system will have the capabilities of rotating around two different axes. It will also contain a sub system, which will move two bodies of mass linearly, and independently. Our group is using a range between 11 Ncm to 45 Ncm torque size motors, each individual motor will be sized ideally to hold, start motion from a stationary position, and stop from a motion to a stationary position, at a fairly low speed. Using knowledge from previous sections, we calculate the moment of inertia of each load, along with each external force that will act on each individual motor. The motor must be selected specifically to sustain all these forces with a large enough torque, including a safety factor. Setting the right speed for each individual motor is a value which can reduce the required torque for our motors to reach, also reducing the cost for components. The following sections will calculate each motor's speeds, compare it with torque, and display numerically and visually the effects that both values have on each other.

4.9.2 Motor Speed

Speed is the third key element for the sizing of each motor. For our system, the speed at which the 'arm' rotates vertically or horizontally is not critical. For the 'arm' of the system, a reasonable angular speed is required for the load to move more smoothly. Our group understands that the rectangular casing protecting our entire system will not need movies at high speeds. Having this in mind, calculations for an estimated velocity will be conducted by using the previously mentioned equation which calculator the speed of an object;

$$\text{Speed} = \text{Distance} / (\text{time} - \text{acceleration time})$$

Where, the distance the object covers is divided by the time it takes the object to get from point A to point B, subtracting this time by the time it takes for the load to reach a constant acceleration, or the acceleration time. Using the formula above, and by selecting the rectangular casing to rotate a distance of 2π

radians. Also reaching this distance in a time of 60 seconds and an acceleration time of 2 seconds, to reach a constant speed. This results in an angular velocity 0.1083 rad/s for the rectangular casing. This means that ideally our system will move 0.1083 radians every second.

Now inside the filtering subsystem, we calculate the linear velocity that our motors M3 and M4 will need, in order to reach a specific constant velocity for the filters. Solving for the speed using the previous formula, with a target distance of 0.3048 m, to be covered by the load in 40 seconds, with an acceleration time of 2 seconds. This results in a speed of 0.008 m/s, having the load moving 0.008 m every second. Our system is does not have an urgency for high speeds rotation or translation, a reliable low velocity for each of these bodies of mass is acceptable, since the application where the system will be used, does not require quick acting movements The speed versus time motion profile, where the velocity and the speed to reach that velocity will be labeled.

4.9.3 Servo Motors

Servo motors are very popular for their precision and reliability, that is the reason our team had to look into this option, in order to open our options and compare prices with other motors. Servo motors are implemented as a closed loop connection, making them very efficient and reactive to feedback from the load being controlled. Servos can be divided into two different types, one being standard servos whose angle or rotation ranges from 0 degrees to 90 degrees. This type of servo can be useful for our system and can be implemented to create motion for the filter system. As it will be discussed in further sections, the filters will cover a very small distance compared to the other two motors which will give motion to the entire system itself. The second type of servo is continuous, this type will rotate their shaft in the range of 0 degrees to 360 degrees. As it can be assumed, having the versatility of rotating 360 degrees will give our system the freedom of rotating with no limit. Following our system idea, for the filter system, a continuous servo would not be as essential, as it is from the motors that add horizontal and vertical motion. One of the downsides of the Servo motors is the weight of the servo, meaning that in the case our system needs more torque, the weight of servo will increase more than the steppers. Also, servo motors can claim the price later relatively rapidly since the component itself is more complex than a stepper.

4.9.4 Nema 17 Stepper Motor

There are two options when it comes to a stepper motor, unipolar or bipolar. Both are promising for our system, since our system does not hold much weight. At this point, there is more interest in bipolar having a higher torque than

unipolar. There is much interest in a stepper motor that averages a current of 3 amps, along with voltage of 12 Volts. This will result in a reasonable wattage, which can be powered with a 12 volt battery. We're also interested in the step angle of the motor, for our system we're looking for a 1.8 degrees step angle. This is important to know, since a stepper motor has to be implemented with a motor driver. By knowing that 1.8 degrees is equivalent to 200 pulses per revolution, we can program our driver to send signals to our motor appropriately. Nema 17 is an example of a stepper motor that provides a compact design, averaging 42 mm all around (frame size and body length).

4.10 Gears

In order to aid the motor with the task to hold and move the weight which this system is composed of, technology investigation towards gears was conducted. There are many types of gears combinations which the group filtered through, in order to find the most efficient gear-motor combination. Understanding the values that physically affect a gear, will be key for when it's time to utilize two gears, where they will transfer energy to one another. Each time power is transferred from one gear to another, one of three stages is happening; it increases speed, increases force, or changes direction. An important fact about gears is transferring power from a bigger to a small gear will increase speed, as well as decrease force. Vice versa, if power is transferred from a small to a bigger gear speed decreases, but force increases. As mentioned earlier, there are adjustable values or variables which affect the physical specifications for a gear. We will be describing the purpose of these specifications and how they affect the performance of gear combination. This information helps our group to set an understanding and combine it with our project requirements to set a doable goal.

4.10.1 Torque

Our project will be utilizing three different motors, which will be holding and moving different amounts of payloads. As we begin our investigation, we can approximate using three different types of motor sizes, because as we will show along this presentation, our system will hold and move different types of weights, which is a main priority for a motor decision. Torque is the force which will allow the motor in a joint of the system, to be able to hold the link which includes the payload. Torque can be calculated by using the following equation;

$$t = r * F \qquad \text{(Eq.4.10.1)}$$

Where, r is the radial distance from the axis of rotation and the force vector, and F is the force applied at that distance. This shows torque being a crucial value to have in consideration when picking a motor. Our system needs to hold a certain amount of weight when receiving the laser beam, and also be able to hold the position for around 20 minutes without any errors. With that being said, our system also needs to be able to move and carry the payload weight without any “stalls”, which is when a motor misses a step when in rotation carrying payload. Having this in mind, careful calculations of the torque have to be taken, as the system can fail to hold the right weight and damage the equipment. The gravitational force, and the angular acceleration are two important values for our needed torque value of our system’s motors. By understanding what each of these values affected, we will be able to make an informed decision about what motors to buy for the prototype stages, and final design.

4.10.2 Gravitational Force

Force as shown in equation 4.10.1, can be described also as;

$$F = m * g \qquad \text{(Eq.4.10.2)}$$

Where, m is the mass of the payload and g is the gravitational acceleration. When talking about our system, the force is coming from the casing that is sounding the camera, filter subsystem (including a motor), and any connections needed. Meaning, we need to size the motor to contradict this gravitational with some room for errors. The sketch below shows a simple example of a force on a rectangular body with its axis of symmetry in the middle of the body. This simple sketch is very useful, because this movement is one of the three that our system will showcase. In order to hold the rectangular body (our camera connected to our filter subsystem) in an angle, the motor’s torque will need to work against the gravitational force.

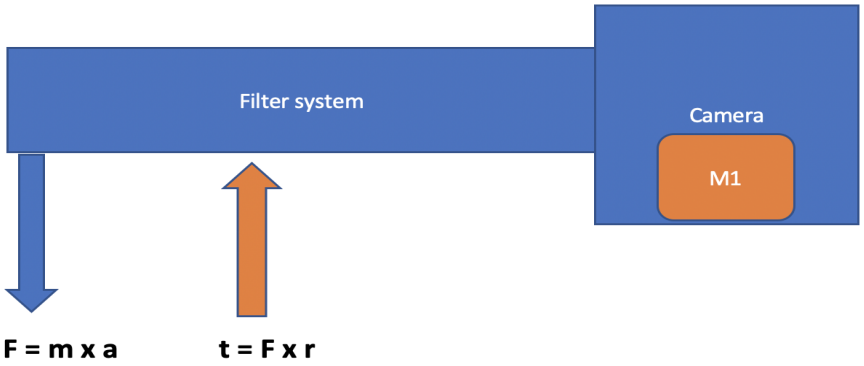

Figure 8: Force on a rectangular body with symmetry in middle of body

4.10.3 Angular Acceleration

Along with gravitational force, angular acceleration is one of the components that will show the required torque for our system's motors. Angular acceleration gives the system the ability to add movement to a link, and payload. Torque can be calculated from the following equation.

$$t = I \times \alpha \qquad \text{(Eq. 4.10.3)}$$

Where, I is the rotational inertia and α is the angular acceleration. Rotational inertia is the force that works against the body slowing the increase of velocity. In our system it is important to have angular acceleration in mind, since this acceleration is correlated directly to the motor's resistance to a change of velocity. The group will find the right torque that will overcome the rotational inertia that our system's filter components will create. A side view of our system demonstrating the torque working against the rotational inertia is shown in **Figure 9**. M2(motor creating the horizontal motion), produces an angular acceleration (seen in blue), which will work against the force (seen in red) preventing the body of the system to start accelerating. Having this knowledge, along with the understanding that our system will not need to be implemented with high speed is key to creating a lightweight system, for our motor, battery, and efficiency.

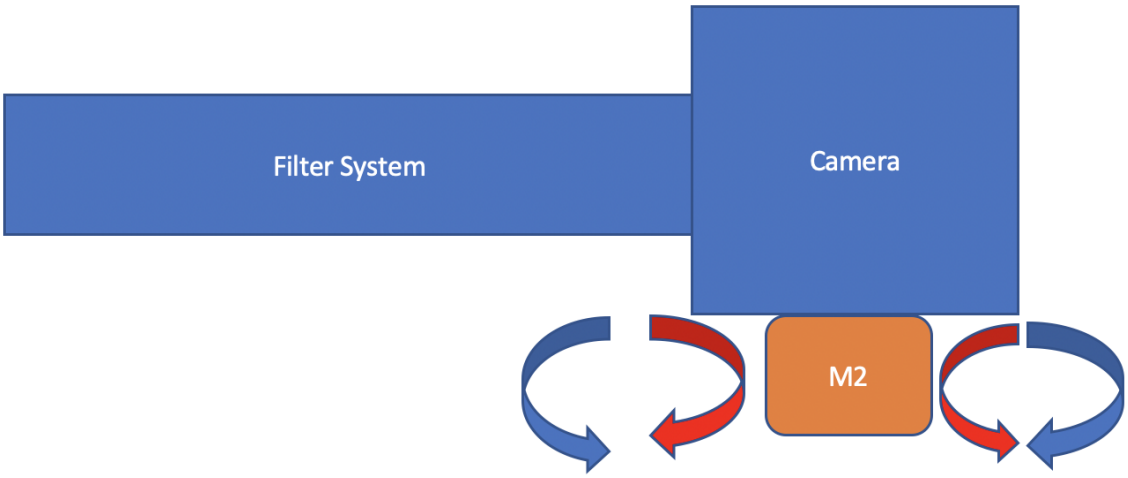

Figure 9: Torque vs rotational inertia

4.10.4 Moments of Inertia

First, our group focused on vertical motion, our system will be around 50 cm long and 16 cm of width. By estimating the body of the system to be around 4.5 kg, the moment of inertia will be calculated by the following inertia formula for an off-center axis, as mentioned in the previous sections:

$$J = (1/12) \times m \times (w^2 + B^2 + 12L^2),$$

where m is the mass of the body, w is the width of the body, B is the length of the body and L is the distance between the axis of rotation and center of mass of the body. After calculations, the system's moment of inertia results at 0.03317 kg-m^2. This inertia was concerning at first, since it can be difficult to find a motor with a rotor inertia large enough to handle the load. As we build a prototype, it is important to design and experiment with a few body frames with different specifications. Our group understands that in order to find the right size of a motor, adjustments to the dimensions of the body might need to be done. As seen in the formula above, the width, length or even the distance between the center of the body and the axis of rotation, can make a significant result on the moment of inertia.

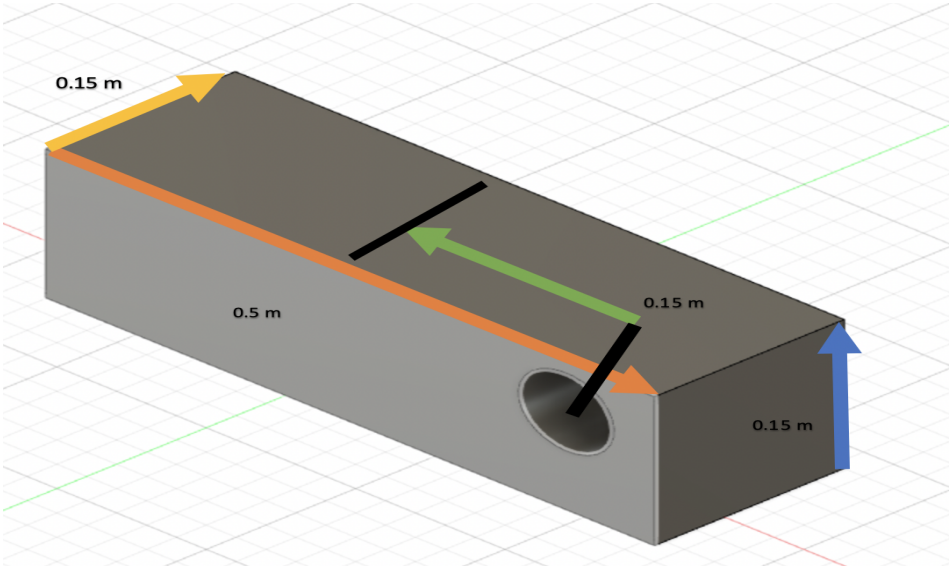

Figure 10: System's arm, with an of center axis

In a similar situation, motor two (M2) will be located on the same side as M1, which will be on the right side of the system's body. **Figure 11** illustrates both a side and front view of the system, in the left side, the side view shows where the motor is planned to be located and on the right image, the rotation given to the system's body is illustrated from a front view. As seen in these images, M2 will be connected to the rotary surface, where the motor will rotate the driver gear, which rotates the driven gear in order to obtain more torque. Comparing M2 to M1, which is in charge of the vertical motion, M1 does not have a large amount of gravitational force, since M1 will be the motor that will have enough holding torque to hold the load without any assistance from other motors. The key functionality of M2 is to add vertical motion to the system's body when needed to locate the refracted laser beam. In order to get this done, change acceleration must be done by M2, where the system body's moment of inertia will create a resistance to this attempt to motion. Having in mind that M2 is also creating movement for the entire system's body, the moment of inertia against M2 will be equal to the moment of inertia against M1, which is 0.03327 kg-m^2. As mentioned earlier, this moment of inertia is quite high, so our group will use the strategy of using gear reduction in order to increase the torque given by the motors alone. Further down this report, we will explain our approach to this issue.

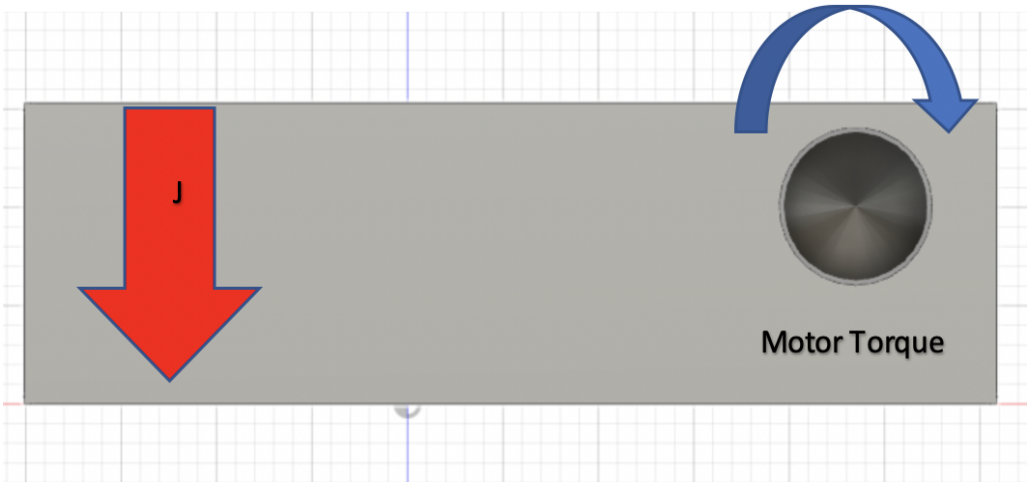

Figure 11: Side view of system's arm. Moment of inertia against the motor's torque

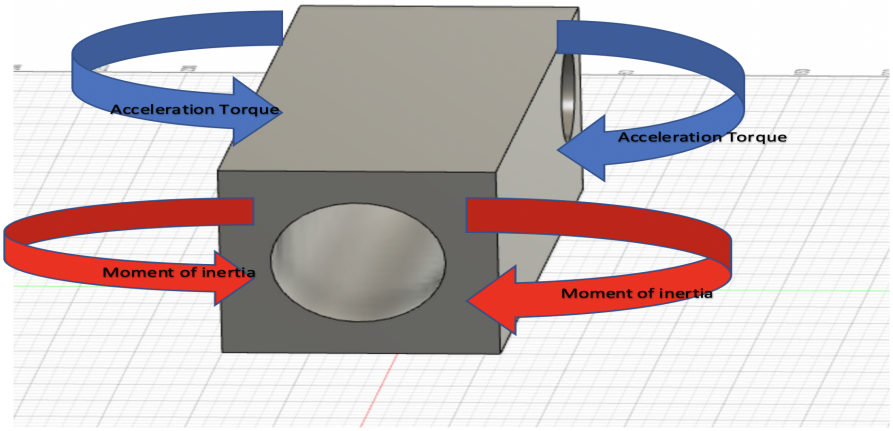

Figure 12: Front side of system, with moment of inertia and acceleration torque

Now, we take a look into our system which is a composite of two independent linear motions. Our system consists of a rectangular body, where at one end will encase all the electrical components, along with the camera. As the rectangular body of our system extends, along the 'arm' will encase a filter system which is composed of four laser filters. Each filter's job is different and was explained in earlier sections. As explained earlier, we know that two of these filters will be in motion independently and will also carry a load linearly back and forth inside the 'arm' of our system. Fortunately, the filters being used for our filtering system will be light, at around 5 grams each filter. Utilizing the formula for the moment of inertia of a linear moving body, as explained in earlier sections, we calculate inertia as.

$$J = m \times (A/2pi)^2 ,$$

Where m is the mass of the load, and A is the unit of movement. Having in mind that the overall mass includes the filter and the platform which the filter is sitting on. Plugin in the overall mass to the previous equation, the moment of inertia results in 0.0007958 kg-m^2. With this result, we understand that the resistance created from the filter's motion will not be as significant as the resistance seen by M1 and M2. For this subsystem, Moment of Inertia will be manageable, and it will allow us to select smaller motors, which will add less weight to the system's overall weight. It's important to our group to find the lightest components when it comes to the 'arm' of the system. This is because we want to find the best ways to add the least moment of inertia that affects both M1 and M2.

We have calculated the moment of inertia of each moving body in our system. The overall weight of the system, where it's mechanics would imitate an 'arm', with the motors attached to one side of the rectangular casing which surrounds the electronics, will be held by the motors. The moment of inertia of our system will allow the group to choose the right motors to give the body of the system enough acceleration and deceleration to move and to stop, when moving around positions looking for the laser beam. From the calculations obtain in this section, both motors M1 and M2 have to be able sustain a minimum moment of inertia of 0.03317 kg-m^2, and M3 and M4 will have to be able to sustain a minimum moment of inertia of 0.0007958 kg-m^2 when motion is required. It's important to remember that moment of inertia is only a factor when the 'arm' of our system is in motion, where load torque, which will be discussed next, maintains the system stationary. Table 4 illustrates the effects of the moment of inertia, from the dimensions of the rectangular casing, as well as the distance between the center of mass and the center of rotation. The table helps shine a light on having in mind the dimensions of the system could help lower the cost of the system overall, without lowering efficiency.

Mass (kg)	Width (m)	Length (m)	Offset for axis(m)	Moment of inertia (kg -m^2)
2.27	0.152	0.254	0.1016	0.04
4.54	0.127	0.254	0.1016	0.06
4.54	0.152	0.254	0.0508	0.04

Table 3: Moment of inertia resulted from different dimensions

4.11 Light Sensor

Multiple ideas have been examined about how to approach the light sensor for the design. The intensity of the light being introduced into the system

will be recorded using the CMOS camera. As the light travels through the optical system there will be a conflict with ambient light due to the suns blackbody radiation spanning from the ultraviolet into the infrared (blackbody radiation). For accurate measurement of the only the lasers intensity, the sun's intensity must be subtracted from the total intensity profile captured by the device. The initial idea for this approach was to have a spectrometer within the system along with a spectral camera. The diffused light from the laser along with the ambient light from the outdoors/lab full spectrum lighting will both enter the optical system. As the light travels through the designed lens zoom system it will eventually be focused onto the optical filters. As the light signal travels through the optical filters the majority of the undesired ambient light will be absorbed by the optical filters. What will transmit through is a narrow bandwidth of light including the desired laser wavelength. Within that narrow bandwidth will also include the intensity of the undesired ambient light which will give an inaccurate reading to the true intensity of the laser.

The initial approach was to have a beam splitter in the path of the optical lenses. The beam splitter specifications required would only split about 10% of the light perpendicular to the light signal path and allow the other 90% to travel into the optical filters into the camera. That small percentage of light would be focused onto a spectrometer or similar spectral reading instrument to give a basis of the intensity spectrum of light entering the optical system prior to being filtered. The other portion of the optical signal would travel through the optical filters and a spectral camera would measure and display the actual intensity reaching the camera. By having the base measurement from the spectrometer and the reading from the spectral camera, the two sets of data can be analyzed and subtracted to result in the true intensity. This idea does not work because both the split signal and the filtered signal would still be a superimposed signal of the sun light at 532 nm and the laser light at 532 nm. The signal that reaches the camera although filtering out the undesired frequencies on the outside edges of the band pass filter, would still be a similar superimposed signal of the two mixed light signals. The signal reaching the camera would be much more attenuated than that of the one reaching the spectrometer so subtracting the signals will not work. Also, spectrometers tend to be quite expensive in the range of thousands of dollars so this would but the design way over budget.

The second approach was to use a hyperspectral sensor or a multichannel spectral sensor. There are many different types of these light sensors on the market which can be easily designed. The multichannel sensor would have been a two-channel sensor one being sensitive to the 532 nm green laser light and the other being sensitive to the 800 nm laser light for the stretch goal. The sensor will need to be both sensitive to the visual spectrum as well as the infrared spectrum. The hyperspectral sensor After further research, this approach is not going to result in the desired response for the system.

Instead of the aforementioned approaches, an ambient light sensor. Ambient light sensors are broken down into three different categories. These sensors are photodiodes, photoconductive cells, or phototransistors (photodetector and amplifier). The ambient light sensor collects the lux intensity

of the light which is shone upon it and then will transmit a voltage of proportional intensity to the ambient light. This sensor will be able to detect the differences between laser light, sunlight, and the full spectrum light bulb introduced into the design of the system. Important characteristics of the ambient light sensor are the operating temperature, the required voltage, The ambient light sensor will be used to control the amount of light entering the camera as well as detect the luminous intensity of the light signal traveling through the device. The device will have a housing and will be absent of light other than what is allowed in by the aperture. A full visual spectrum light will be used as the ambient light source which will mimic the visual spectrum of a day outdoors while in a laboratory setting. The ambient light sensor will adjust the camera to the incoming light. The camera will be able to be adjusted to a brightness of optimal reading of the incoming signal. There are many different types of light sensor that will be able to measure the appropriate intensity of the incoming light signal and relay that data to be compared with the recorded spectral reading from the camera. The sensor being sought for experimentation is sensitive to the red, blue, green visible spectrum. The sensor will attenuate infrared light which will help keep the band integral of data to only the visible spectrum. The stretch goal is to be able to block out the undesired wavelengths of light through the optical system and then sense, how much of the wavelength is actually being measured from the 800 nm laser versus the full spectrum visible light source. The full spectrum light source will introduce 532 nm wavelength into the system superimposed with that of the diffused wavefronts from the laser pointer source. The color sensor will be able to detect the differences in the laser wavefronts from the full spectrum ambient lights source. This will aid in being able to deduct the additional 532 nm light introduced by the full spectrum ambient light source and get an accurate reading on the intensity of the diffused wavefronts of the laser signal reaching the camera. This approach is to be tested to find the appropriate way to differentiate the additional 532 nm wavelength entering the device from the laser. Initially a baseline will be recorded by testing the device in the dark with only the laser light on. This information will be used as the baseline before the full spectrum ambient light source is turned on. Another reading with the ambient light source only on will be recorded to analyze how much of the 532 nm light is coming into the device from the device. The ambient light source can be both an active or passive device depending on the specific type. A photoconductive cell does not require a direct power source. The photoconductive properties will change when directly exposed to electromagnetic radiation. Photoconductive cells are considered passive devices. Similar to the photoconductive cell is the light dependent resistor which is a piece of semiconductor material that’s resistance will change when light is exposed upon the surface. The resistor will create electron hole pairs as more light is shone upon it and the resistance will decrease as the illumination increases. These types of sensors tend to have a longer response time, so they are not ideal for this specific project. A photodiode light sensor is a P-N junction which has a much better response and sensitivity to lower energy light near the red and infrared regions. When electromagnetic radiation falls upon the surface of a photodiode electron hole pairs are created

and a current is given off. This current is proportional to the light intensity on the photodiode. These sensors have typically a much faster response time than the photoconductive cell. This type of sensor may be good for the stretch goal but not for the main objective of the design. The phototransistor on the other hand is similar to the photodiode but is amplified and much more sensitive. and will require power from the battery source. Ideally the size of the device will weigh heavily on both the optical design as well as the size of the power source. A sensor with the lowest power consumption is ideal in this design. The sensor must have a strong spectral response on the order of the photopic response of the light coming in. The sensor will neglect additional infrared wavelengths and aid in proper lighting for the camera. The ideal choice for spectral and intensity measurements of the ambient light for this device will be a photodiode. There are vast variety of different types of photodiodes on the market which can be designed and specialized with specifications. The photodiode necessary for this experimentation will need to be very sensitive to 532 nm wavelengths and ideally will require a low voltage for operation. There are many photodiodes on the market currently which meet these specifications.

4.11.1 PIN Photodiode Transimpedance Op Amp (Initial Design)

To properly detect how much ambient light from the full spectrum light source and blackbody radiation of the sun, a PIN photodiode is the best choice. PIN photodiodes operate with a reverse bias voltage applied which is also known as the photoconductive mode. The photoconductive mode increases the depletion region's depth as well as the strength of the electric field. A larger depletion region means that the sensor will be much more sensitive. Also along with a larger depletion region the junction capacitance is also significantly decreased. A lower junction capacitance in turn allows for the PIN photodiode to have a larger cut off frequency. A large cut off frequency in turn means a larger bandwidth region of detection. The advantage of the PIN photodiode compared to other types of photodetectors is its higher speed, a more linear measurement of current, a lower capacitance, and higher quantum efficiency. A disadvantage of a photodiode versus other types of sensors is that it lacks an amplifier. The main constraint on accurate measurement that is introduced to the photodiode is a larger dark current which must be taken into consideration when analyzing the data obtained. The dark current refers to the flow of current through the photodiode even when there is no illuminance on the surface. The dark current can lead to inaccurate measurements if not taken into account. The dark current can be measured prior to experimentation to have a baseline and be subtracted from the overall intensity measurement to get an accurate reading. The PIN photodiode is the right choice for this design because of its high sensitivity in the visible to near infrared regions. This type of photodiode is suitable for both the showcase 532 nm sensitive device and stretch goal of the near infrared 800 nm experimentation. The cutoff region of the broadband is dependent upon the thickness of the intrinsic region of the PIN photodiode. The rise time of

electron-hole pairs to get from the intrinsic region to the doped region limits the bandwidth of the device. Some important characteristics and equations for selecting the proper PIN photodiode are listed below.

Responsivity (R_D): Current produced (I_P) / Input optical power (P_{in})

$$\frac{I_p}{P_{in}} = R_D$$

Quantum Efficiency (η) : α are the losses and L is the length of the intrinsic region.

$$\eta = 1 - e^{-\alpha L}$$

Rise Time (T_r): τ_{tr} is the electron transit time and τ_{RC} is the time constant of the circuit.

$$T_r = ln\,9\,(\tau_{tr} + \tau_{RC})$$

Bandwidth (Δf):

$$\Delta f = \frac{1}{2\pi(\tau_{tr}+\tau_{RC}}$$

Dark current also introduces noise to the system known as shot noise or dark noise. It is ideal to have a high sound to noise ratio (SNR). The lower the SNR the more corrupted the signal will be at the receiver sometimes to the point its not even decipherable. The noise of the photodiode and the SNR are calculated using the equations below.

RMS value of Shot noise (I_{sn}): I_d is dark current and I_p is average current.

$$I_{sn} = \sqrt{2q\left(I_P + I_D\right)\ f}$$

RMS value of Thermal noise (I_{jn}): R_L is load resistance

$$I_{jn} = \sqrt{\frac{4k_B T\ f}{R_{SH}}}$$

Sound Noise Ratio (SNR):

$$SNR = \frac{I_p^2}{(I_{sn}^2 + I_{jn}^2)}$$

4.11.2 LDR Optical Sensor (Final Design)

The ideal sensor for this application will have a high sensitivity to wavelengths in a bandwidth region containing 532 nm. There are many different types of measurements which can be achieved using an optical sensor and for this design illuminance was chosen. For this design, two different approaches were compared to see which would be the best option for measuring the illuminance of the incoming reflected light waves. These two options were measuring the voltage of a PIN photodiode transimpedance optical amplifier circuit or measuring the output voltage of a voltage divider light dependent resistor circuit. After testing both circuits in the lab the light dependent resistor circuit was the most viable. The transimpedance PIN photodiode circuit had a quicker response time than the light dependent resistor. The light dependent resistor is much more sensitive to the 532 nm light being measured, about 3 times as sensitive. The PIN photodiode had a spectral sensitivity to 532 nm of about 0.3 where the light dependent resistor's sensitivity is about 0.95. The variable most important to the design is the sensitivity due to low light conditions within the cavity of the device itself so speed is sacrificed for sensitivity. The LDR will be designed in a voltage divider circuit with a 10 kilo-ohm resistor. The LDR node will be biased with 5 volts and the voltage across the divider will be connected to an arduino.The arduino will be able to convert the voltage measured from the light intensity hitting the surface of the LDR into a lux intensity reading. The reading will then be displayed on an LCD on the rear of the box to give a real time reading of the luminous flux of the lasers diffused light entering the optical system.

4.11.3 Lux Meter

A lux meter was designed using the 5506 LDR in a voltage divider circuit. The lux of the light intensity reaching the surface area of the LDR was viable information in it allowed for an accurate perspective of how much diffused light is actually traveling through the optical system to the camera.feed. Lux is typically used to measure ambient light. The room when lit will have ambient light of the spectrum 532 nm. By using a filter only allowing through a narrow bandpass the amount of ambient light hitting the surface of the LDR can be calculated. This is a challenging problem to solve and differentiates depending on the ambient light source whether it be sunlight, a home light bulb, or any point source of light. This

project did not solve that problem but the light intensity when the lights were off only from the laser was able to be read quite efficiently. A factory shipped lux meter was used to help calibrate the lux meter to most ambient room light settings. This calibration was than converted to one from lab experimentation using the bandpass filter along with a fiber light of varying intensities. This lab experimentation data was used to code the arduino to calculate the lux from the voltage divider voltage as well as display it on the LCD. An open source code free to use was used as the base for the final coding which resulted in the lux meter calibration. In the end the lux meter worked, but did not give as viable of information as originally thought for the goal of the device. **Figure 13** is a photo of the LDR, arduino, and LCD display connected and ready to use.

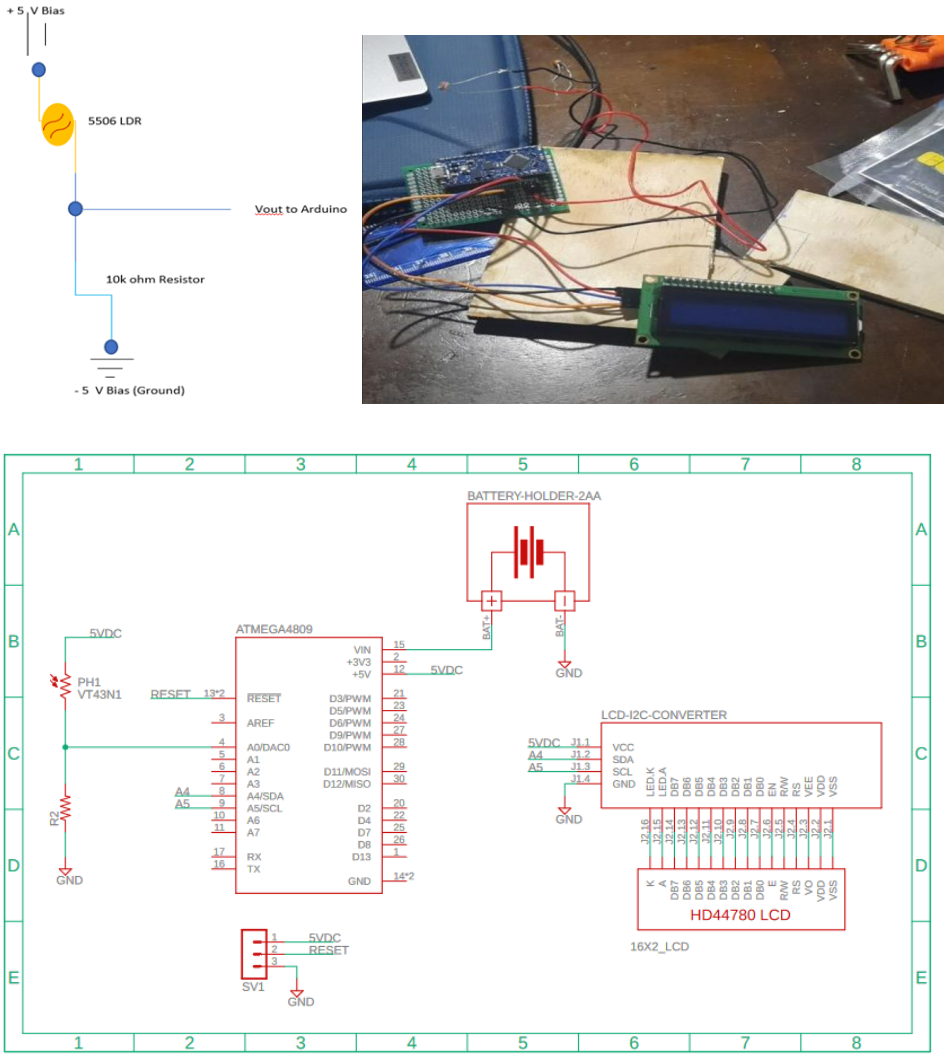

Figure 13: Top Left image (Schematic of voltage divider circuit used for 5506 LDR) Top Right Image (Lux meter all connected. LDR soldered onto red and black wires connected to the arduino through a voltage divider circuit. LCD is connected to output of the Arduino). Bottom image is the schematic of the LDR circuit

4.11.4 Motion Update

As mentioned in previous sections, one of the goals for the system was not only to have a filtering system with motion inside the case, but also to create motion to the overall box enclosing the system. The project is implemented to 10 lbs which created a problem to design a mount tall and strong enough to hold the weight. In addition, the purchase of the motors which would have the job of carrying and holding this load were out of the group's budget. For this reason, our group focused on the primary goal, which was the filtering and tracking system.

4.12 Wireless Communication

For the purposes of this project wireless communications will be utilized, as these means provide adequate convenience regarding set up and making this solution more practical. For the distances the components for this project are to be designed to operate in wired means of communications between components would be unwieldly for set up unless the setup is to be more permanent which is not desired from this design. A wired setup would also have additional issues depending on implementation, as this project is oriented towards outdoor use and as such the cables used would need to meet certain requirements for such conditions. As such utilizing wireless communications would be the preferred option.

4.12.1 Private Wi-Fi Network

A common technology for wireless communications in most consumer electronics and in come commercial applications is the use of Wi-Fi. Wi-Fi has plenty of draws, including a base range of 300 meters in outdoor environments with the ability to utilize devices such as repeaters to extend the range further. This would also be a good solution regarding video transmission as this would allow the images from the camera to be transmitted to the user without sacrificing image resolution. The drawbacks however are the limitations that would be faced in either setting up the LAN every time or in implementing a permanent solution. The limitations for both implementations being the issue of how long it would take to set up the network and configure the devices into the network and troubleshooting any issues with the network as they may arise. This would also be one of the more expensive solutions with the added cost of a router and whatever means for achieving the desired range, as well as the additional cost due to the recent increase in demand in such devices as a result of the COVID-19 pandemic.

4.12.2 Bluetooth

Bluetooth is the standard regarding short-range wireless communications, generally having an optimal operating range within 10 meters. Bluetooth is used in various applications in devices used in healthcare, security, and consumer electronics amongst other areas. Bluetooth operates along the 2.4 GHz band of frequencies (2.402 - 2.480 GHz). Although Bluetooth was standardized by the IEEE under IEEE 802.15.1 back in 2002, that standard has since become defunct, and the standard is now governed by the Bluetooth Special Interest Group (henceforth referred to as SIG) which notably handles the developed specifications of Bluetooth and manages the qualification program. In order to maintain signal quality between devices Bluetooth utilizes Frequency-Hopping spread spectrum (FHSS) which “hops” between the frequencies in the 2.4 GHz band. FHSS has the added benefit of security from eavesdropping as a result of the rapid shifting of frequencies.

While Bluetooth would be adequate for transmitting the control signals from the control device to the camera control setup at the range used in the demonstration at the conclusion of Senior Design 2 (3 meters), but for the more extensive range of 1 kilometer that this project is to be designed for Bluetooth is simply not suitable. Bluetooth utilization would also hamper the use of video in this project, as the technology doesn’t have the required bandwidth in order to adequately transmit the video data, at least not as anything other than a few images per second.

4.12.3 Radio Frequency (RF)

RF is a commonly used solution for communication between devices over various distance ranges due in part to its versatility in design and simple implementation. RF can achieve distances much longer than the other means evaluated, with lower frequencies having the longer ranges. The constraints that exist Regarding the hardware necessary for implementation for the controls, modules can be used for transmitting and receiving signals between the devices. These modules can be obtained for prices that are much more friendly for the allocated budget for the transmission portion of this project, especially when compared to the necessary expenses to implement solutions such as the private Wi-Fi network.

4.12.4 Video Transmission Considerations

For video transmission Bluetooth is not an optimal option Bluetooth does not have enough of the necessary bandwidth for adequate video transmission and is only optimal for short range communications within 10 meters. As the device is intended to work at an extended distance from the device and the target the device is to be aimed at in the stretch goals of this project, a means of long-distance video transmission should be considered for this project. Unfortunately, most commercial solutions for wireless video transmission are either cost prohibitive for this project, notably those utilizing wireless HDMI video transmitters, or are impractical for the intended use of this project, such as Wi-Fi video transmitters that would require the two devices to be on the same short-range Wi-Fi network. Luckily there is a solution to implement wireless video transmission, which is to utilize the same analog First-Person Video (FPV) transmission tools used in devices such as those used in remote controlled planes and quadcopter drones. These FPV video transmitters generally utilize the 5.8 GHz frequency band that is legal for amateur use which has a wider bandwidth and many channels for use that are not as commonly occupied like the 2.4 GHz band is. In the United States the allowed frequencies are between 5.685 GHz and 5.905 GHz. There are various considerations to make regarding analog video transmitters including the power requirements for transmitting the signal, the frequency band of the transmitter, and the maximum range of the transmitter.

4.13 Microcontroller

For this project we needed three microcontrollers, one to operate the motors in the camera adjustment system and receive instructions for said adjustments, one to accept operator inputs corresponding to adjustments needing to be made by the camera adjustment system, and one to handle the calculations from the LDR and display the results for the operator. The considerations that needed to be made regarding which controller is used came down to the following factors:

- low power draw,
- development support,
- cost,
- availability,
- output.

The need for low power draw from the MCU comes from the assumption that the system will need to be operating on battery power given its application. Given the camera doesn't need to be continuously adjusted the entire time it is in operation for experiments, the MCU does not need to be sapping power while the motors are on standby. Some form of low power or standby modes for the MCU would be highly desired for this application. For development support how the microcontroller is programmed to and the existing knowledge of those who will be

developing the software needed to operate the microcontroller are important considerations to consider. A microcontroller that has plenty of accessible documentation and can be programmed using a language that is known or at least very simple to adapt to for the developer is along the lines of what is desired in the microcontroller that is to be used. The cost of the microcontroller and the availability of the board are also important considerations, especially as this project is being done during a time of major shortages for electronic components where it is unlikely vendors will know when they will have a given component back in stock after it is out, and the prices of components may increase given those shortages.

4.13.1 Arduino Nano Every

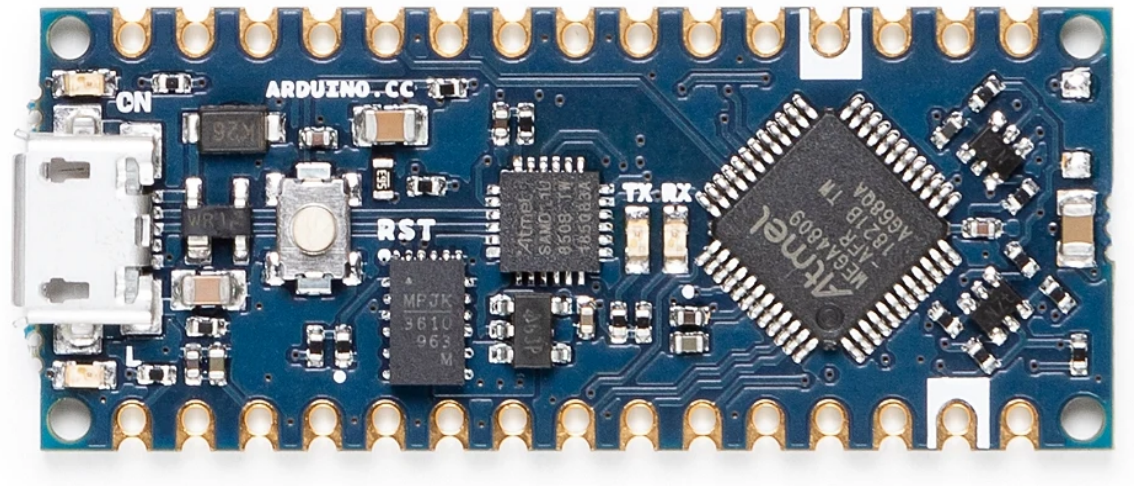

Figure 14: Arduino Nano Every Board (Arduino AG, 2021)

The Arduino Nano Every is an incredibly small single board microcontroller that is popular in DIY electronics and educational projects that require the use of small and easy to use controllers. A major factor in the board's popularity comes from the extensive support for the board, with plenty of extensive libraries that are user-friendly, with this board being one of the more novice friendly options available, and the fact that due to Arduino's Creative Commons licensing for hardware the boards can be made by various suppliers using the same specifications as the official Arduino boards. Regarding specifications the board utilizes the ATMega4809, an 8-bit RISC microcontroller running on a 20MHz clock and utilizes 41 GPIO pins. In active mode the board has an absolute maximum power consumption of 425 µA/MHz at peak operating temperature and highest clock speed, with the maximum power consumption at the board's low power mode being 15 µA/MHz. Regarding temperature tolerances the board can operate in temperatures between -40°C and 125°C, making this one of the more flexible and resilient boards available in that aspect.

The operating voltage is between 1.8V and 5.5V, again making this one of the more flexible boards for voltage tolerance. For memory the board has 6KB of SRAM available and has 48KB of onboard flash memory. The board does allow for UART, I2C, and SPI.

The Arduino Nano Every utilizes the Arduino Integrated Development Environment, or Arduino Software (IDE) is an IDE written in Java and utilizes the C/C++ language alongside simplified functions in the IDE. Arduino boards are known for not requiring high level knowledge of programming languages, adding to the accessibility of the boards.

Overall, this board was a strong choice for this portion of the project, as the low power draw combined with the strong development support around this board very much indicate why this board is a popular choice overall in various projects. The low cost of the board as well as its current availability are additional pluses for the board. There are some features that will need to be added to the board to implement necessary functions of the board, specifically a wireless communication module.

4.13.2 MSP430FR6989

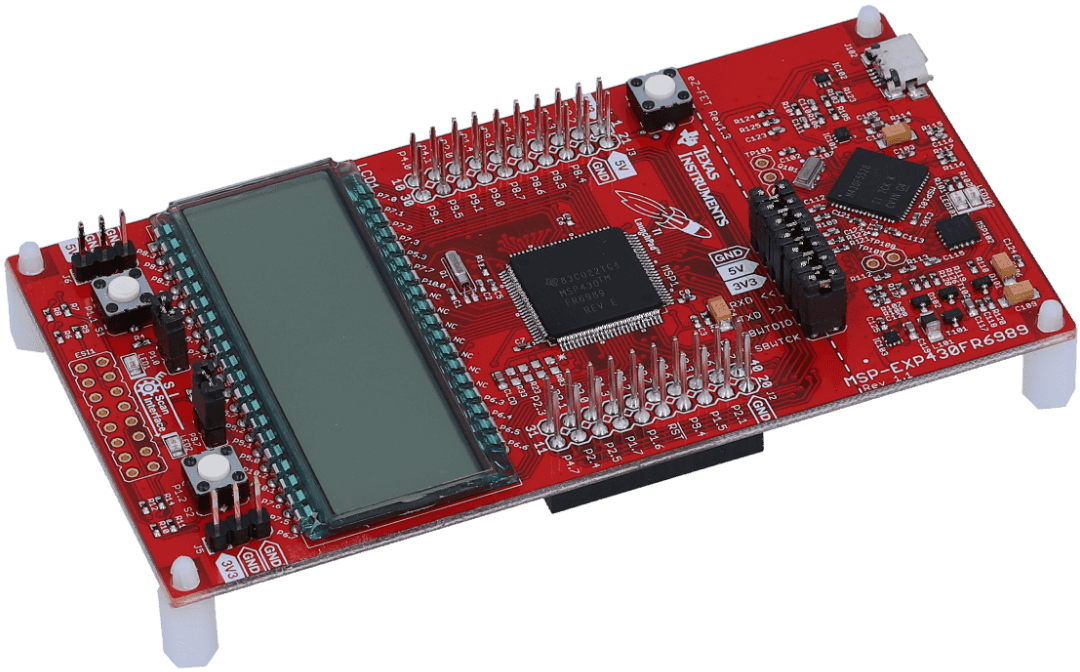

Figure 15: MSP430FR6989 Development Board (Texas Instruments Inc., 2020)

The MSP430FR6989 from Texas Instruments (TI) was also a viable option given its reliability and power. The board is easy to implement, with the thorough documentation provided by TI along with experience with development using this board for Embedded Systems labs at the university. Regarding the specifications of this microcontroller, the roughly $5.00 controller has a 16-bit RISC architecture

running on a 16MHz clock. The controller also has 83 GPIO pins, the most amongst the boards being considered. Regarding memory the controller has 128KB of FRAM and another 128KB of flash. In active mode the controller has a maximum power consumption of 100μA/MHz at worst operating conditions, and in low power the maximum consumption is approximately 17μA/MHz at worst operating conditions. Speaking of worst conditions, the controller has temperature tolerance of between -40°C and 80°C, meaning the board has the worst peak operative temperature of the considered boards. Operating voltage is between 1.8V and 3.6V.

For this project, the MSP430FR6989 microcontroller would work well regarding low power consumption, lots of GPIO pins, communication interfaces and onboard memory.

4.13.3 Raspberry Pi Pico

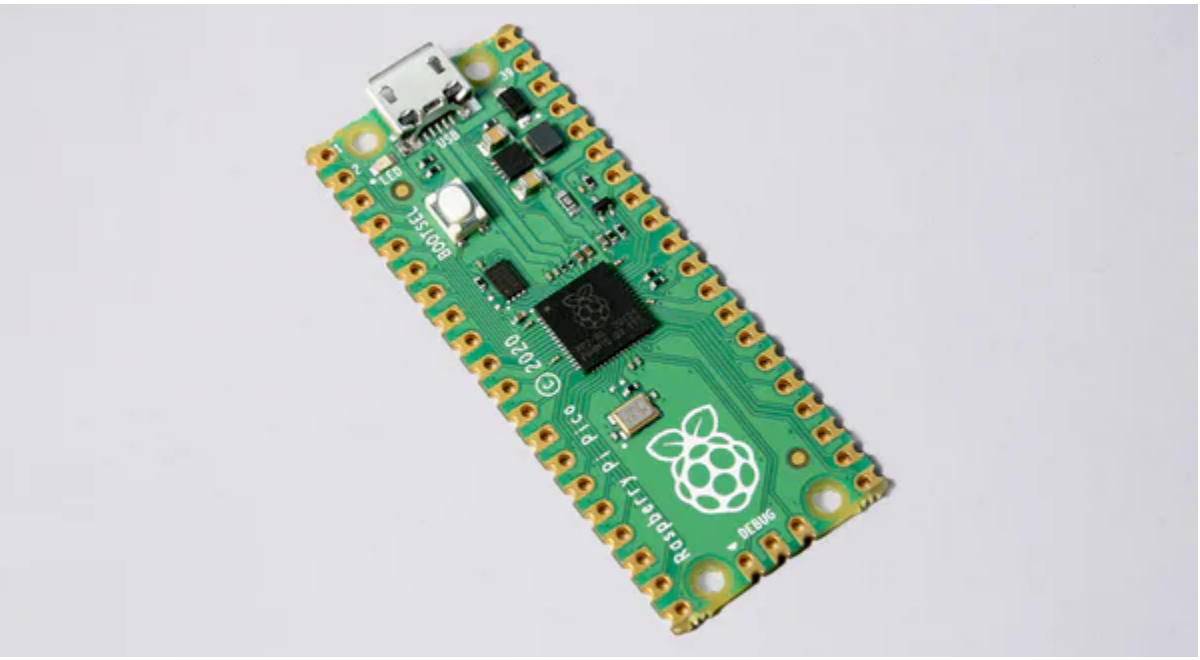

Figure 16: Raspberry Pi Pico Board (Raspberry Pi Trading LTD, 2021)

The Raspberry Pi Pico is the inaugural microcontroller from the developers of the Raspberry Pi line of single board computers. The microcontroller utilizes the RP2040 SoC, which runs on a 32-bit RISC architecture ARM processor with a 133MHz clock and 264KB memory (but no onboard flash memory). Compared to other ARM processors the power efficiency of the chip is strong but compared to the other options explored this is still quite power hungry. This board also contains around 30 GPIO pins, also lacking when compared to the other reviewed boards. The board is also not as great regarding

temperature tolerance compared to the Arduino, but on the high-end of the scale it still does slightly better than the MSP430. For operating voltage, the board, the range is from 1.8 – 3.3V, which would require more consideration regarding how the board is powered.

As such this board tends to be used in Internet-of-Things (IoT) applications where the high clock and memory are in higher demand than lower power consumption. For this application the board was likely to be overpowered and may not be resilient enough given the conditions that the board would experience.

4.13.4 Microcontroller Comparison

MCU	**ATMega4809**	**MSP430FR6989**	**RP2040**
Cost	$1.58	$5.00	$1.00
Architecture	8-bit RISC	16-bit RISC	32-bit RISC (ARM)
Max. Power Consumption (Active)	425µA/MHz	100µA/MHz	718µA/MHz
Max. Power Consumption (Low-Power)	15µA/MHz	17.1875µA/MHz	-
I/O pins	41	83	30
Clock	20MHz	16 MHz	133MHz
RAM	6KB (SRAM)	128KB (FRAM)	264KB (SRAM)
Operating voltage	1.8 - 5.5V	1.8 - 3.6V	1.8 - 3.3V
UART	1	2	2
I2C	1	4	2
SPI	1	2	2
Flash	48KB	128KB	none, supports up to 16KB external
Temperature Tolerance	-40 to 125°C	-40 to 80°C	-20 to 85°C

Table 5: Comparisons between the considered microcontrollers

4.13.5 Microcontroller Selection

The Arduino Nano Every using ATMega4809 was the board and MCU selected for use in this project. This board/MCU combo is a strong choice for this portion of the project, as the low power draw of the controller combined with the strong development support around this board very much indicate why this is a popular choice overall in various projects. The low cost of the board as well as its current availability are additional pluses for the board. This board also has plenty of documentation with projects that were in some ways related to this project regarding RF control which can be referenced and depending on the project could be adapted for the purposes of this project, making the development process quicker and easier.

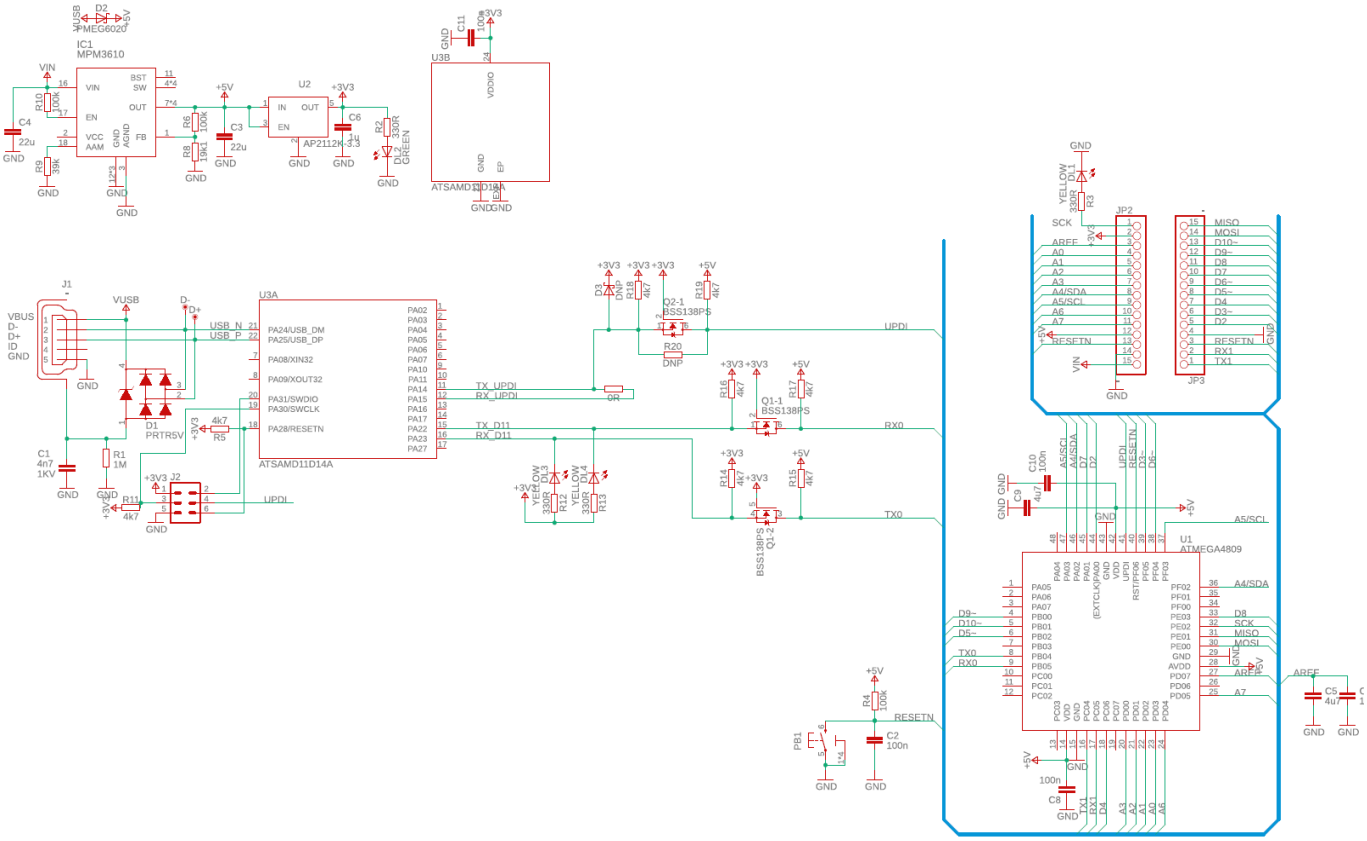

Figure 17: Schematic of the Arduino Nano Every, utilizing the ATMega 4809 microcontroller

5. Similar Products or Projects

This section covers similar projects (academic or enthusiast) and commercial products that exist in the same area as this project, mostly in the area of camera mounts and camera tracking systems.

5.1 Existing Products of Projects

While there is not much in the way of camera mounts used exclusively to track laser beam profiles, there are plenty of examples of robotic and automatic camera mounts that can be used to either track a subject or complete a specified series of motions for filming. These mounts are used in a variety of different fields of photography, from capturing the movement of celestial bodies to tracking the movements of someone walking around a lecture hall. These devices utilize the input of whatever camera is connected to them and depending on the mount's capability can either automatically track a subject, follow a set of preconfigured movements, or be actively adjusted by a user remotely. One of the projects shows a great design of a pan tilt mount which points us into the right directions on how to create a movement for our system. The next project provides the techniques and implementation options to add a third motion to the previous project mentioned. In this project the sliding rail is bought in one piece, which alleviates time to focus on the motor implementation and electric connection. As mentioned before, the second example project utilizes a sliding rail already built, but in order to control the budget of our system, investigation was done in order to see the possibility of building a sliding rail. Matt, who has it's own youtube channel "DIY" perks has a great video about building a sliding rail, which gives a great option for our group, since the materials used are not complicated to obtain or can be relatively affordable

5.2 Robotic/Automatic Camera Mounts

Some of the closest products to the basic function of this project are camera mounts that are developed to utilize remote operation of a camera, shifting movements to track the motions of certain subjects or to combine images into a form of panorama. There are plenty of commercial solutions available for various types of cameras and applications, whether they are for DSLR cameras used for professional photography, film cameras steadily moving through a scene, or for amateur photographers using small digital cameras. The more high-end professional solutions tend to be somewhat cost prohibitive, leading to some DIY solutions, such as the *Pan-Tilt-Mount* project on GitHub from isaac879

(2020). These solutions may or may not implement automatic tracking of a subject, which when implemented can be used for tracking the subject in the camera's range of view (with some limitations). Like what would be expected in the stretch goals for this project, some specialized camera mounts are developed for tracking celestial bodies (stars, planets, etc.), whether it be for purposes of tracking the position of a body in the sky over night, making sure no ICBMs are approaching during the Cold War, or just for some nighttime time lapse photography.

5.3 Commercial Video Drones

Video drones can be seen as a rather elaborate form of camera mount, with the technologies developed for it being very beneficial for our purposes. As video drones operate remotely from the operator, usually at a distance from the operator, the technologies that allow the operator to control the drone's movements and to view what the camera of the drone is capturing are rather useful to our applications of operating a device at a distance while also requiring a video input from the device. These drones also operate on a minimal amount of power in order to operate, providing another point of similarity. Understanding how these drones work and are able to do so at the lower costs they are now available for is beneficial for determining how to implement our solutions.

6. Design

This section covers what design considerations are made and what we propose for this project based on the prior research and technical investigations.

6.1 Design Overview

The design of the remotely controlled diffused surface laser beam imaging system aims to find, track, and characterize important data of the beam. A live image of the beam will be captured by the camera within its field of view, as depicted in **Figure 18**. The live image will be transmitted to the user who is remotely controlling the zoom and movement of the device. The movements are comprised of an up-down rotating motion, and a left-right rotating motion. These movement help the user manually locate the beam on the target board from the remote location, likely at the laser output. The zooming 'in-out' motion will also be controlled manually by the user. The field of view will become narrower as the zoom increases.

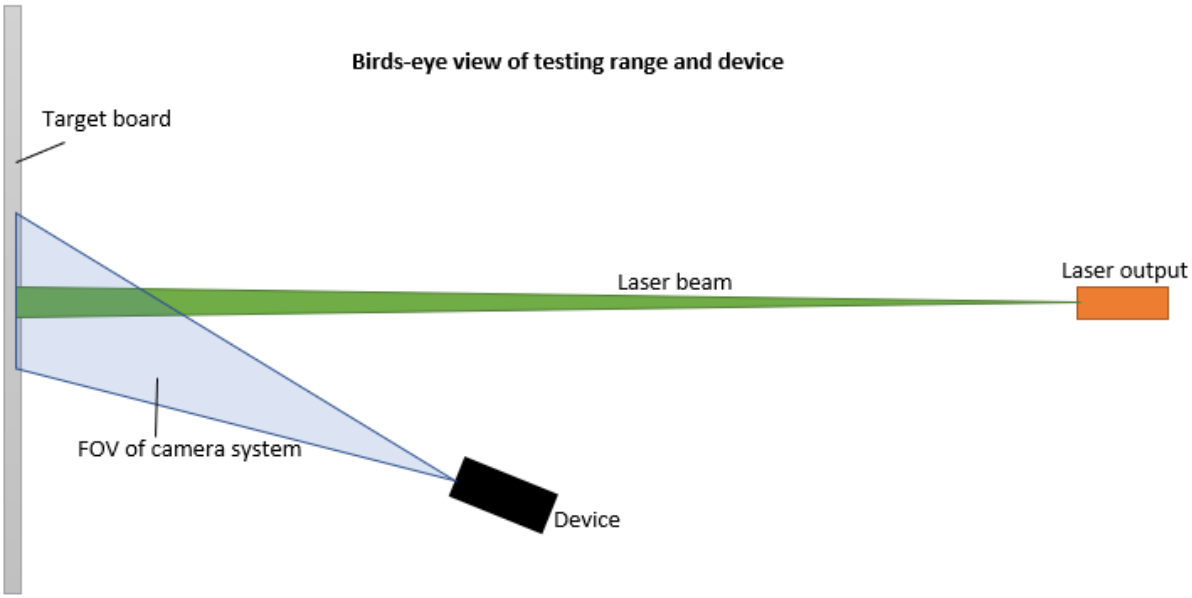

Figure 18: Birds-eye view of device being tested

The design of the remotely controlled diffused surface laser beam imaging system is comprised of several key subsystems. An overview of the final design of these systems are recorded below. The main systems are the zoom-camera system, filtration system, motor movement, data transmission, and power source.

The zoom- camera system is comprised of three lenses. Two bi-convex lenses and a bi-concave lens. The zoom lens system will contain two moving lenses and one stationary lens. Two small motors move the lenses to 5 pre programmed distances from the camera, ensuring an in-focus image at 5 zooms. Allowing the lens movements to be continuous introduces complexity to the code, due to the nonlinear path that the third lens, the compensator lens, needs to travel. Additionally, it would require a high precision in the motors' movement which is not guaranteed.

The optical filters are designed to filter out ambient light introduced to the system and have cut on and cut off wavelengths when superimposed to strictly allow the 532 nm wavelengths to propagate through the system to the camera.

The PIN photodiode is going to be an external element which will measure the ambient light of the environment and map out an accurate intensity profile of the ambient light. This data will be used to determine how much radiant flux is introduced from the ambient light versus the diffused reflected laser light.

6.2 Surface

The current outdoor experimentation being done with the 800 nm laser uses a Lambertian surface. The Lambertian surface used in the current outdoor experimentation is a ceramic cloth. A piece of this exact type of ceramic cloth will be used for lab experimentation of the device. In conjunction with the ceramic cloth and for a more in-depth analysis of the working properties of the experiment a separate Lambertian surface will be designed. The Lambertian surface designed for lab experimentation will consist of an aluminum surface which is covered in a matte paint. The aluminum surface will have some thickness to it. The matte paint will be sourced from a local paint store. The specifics of the type of paint and the exact aluminum are still being discussed. The type of paint and aluminum must be selected carefully because of how the light will diffuse with the materials.

6.3 Zoom System (Zemax Simulation)

The overall simulation and design process were a work in progress over the entire semester and consisted of three rounds of computer modeling and improving designs. This process is recorded here, ending with the finalized design that was the basis of purchased equipment and official demonstration. Zemax is an optical design studio software used for the lens design simulations.

6.3.1 Zemax simulations (1)

Round one preliminary Zemax simulation is recorded here. The current simulation and calculations are not complete and are a work in progress. The main issue that needs to be overcome before the end of this semester and the purchasing of lenses is the spherical aberrations.

To start, a three-group zoom design was chosen for its advantages in aberration correction and design flexibility discussed in research and investigation. A four-lens design increased the control over aberrations, while maintaining relatively low complexity. The PNP design was chosen because a fixed positive prime lens can focus incoming light to one point better than a negative prime lens.

The Zemax simulations uses Thorlab lenses, to ensure that they are accurate to what the real experimental results would look like. Additionally, it was important to ensure that designed lenses would be easily obtained without being too expensive. The total cost of the lenses used in the simulation did not cost more than $200, as was the goal in the initial budget. The first group, the compensator, is a ½ in. plano-convex lens with a radius of curvature of 51.5mm. The second, variator group is comprised of two plano-concave lenses, the first of which is a 1/2 in. lens with a radius of curvature of -51.5mm and the second that is a 1 in lens with 38.6mm radius of curvature. The final prime lens is a ½ in. biconvex lens with radius of curvatures 30.4 and -30.4 mm. The lens data and distances between each lens at each of the three positions in the simulation are shown **Figure 19**.

	Surface Type	Comment	Radius	Thickness	Material	Coating	Clear Semi-Dia	Chip Zone	Mech Semi-Dia	Conic	TCE x 1E-6
0	OBJECT Standard		Infinity	Infinity			0.000	0.000	0.000	0.0...	0.000
1	STOP Standard		Infinity	20.480			10.000 U	0.000	10.000	0.0...	0.000
2	(aper) Standard		51.500	2.200	N-BK7		12.700 U	0.000	12.700	0.0...	-
3	(aper) Standard		Infinity	20.000 V			12.700 U	0.000	12.700	0.0...	0.000
4	(aper) Standard		-51.5...	4.000	N-BK7		12.700 U	0.000	12.700	0.0...	-
5	(aper) Standard		Infinity	0.500 V			12.700 U	0.000	12.700	0.0...	0.000
6	(aper) Standard		Infinity	3.500	N-BK7		17.124 U	0.000	17.124	0.0...	-
7	(aper) Standard		38.600	54.000 V			17.068 U	0.000	17.124	0.0...	0.000
8	(aper) Standard		30.400	6.000	N-BK7		12.700 U	0.000	12.700	0.0...	-
9	(aper) Standard		-30.4...	31.990			12.700 U	0.000	12.700	0.0...	0.000
10	IMAGE Standard		Infinity	-			33.725 U	0.000	33.725	0.0...	0.000

	Surface Type	Comment	Radius	Thickness	Material	Coating	Clear Semi-Dia	Chip Zone	Mech Semi-Dia	Conic	TCE x 1E-6
0	OBJECT Standard		Infinity	Infinity			0.000	0.000	0.000	0.0...	0.000
1	STOP Standard		Infinity	20.480			10.000 U	0.000	10.000	0.0...	0.000
2	(aper) Standard		51.500	2.200	N-BK7		12.700 U	0.000	12.700	0.0...	-
3	(aper) Standard		Infinity	40.000 V			12.700 U	0.000	12.700	0.0...	0.000
4	(aper) Standard		-51.5...	4.000	N-BK7		12.700 U	0.000	12.700	0.0...	-
5	(aper) Standard		Infinity	0.500 V			12.700 U	0.000	12.700	0.0...	0.000
6	(aper) Standard		Infinity	3.500	N-BK7		17.124 U	0.000	17.124	0.0...	-
7	(aper) Standard		38.600	30.000 V			17.068 U	0.000	17.124	0.0...	0.000
8	(aper) Standard		30.400	6.000	N-BK7		12.700 U	0.000	12.700	0.0...	-
9	(aper) Standard		-30.4...	31.999			12.700 U	0.000	12.700	0.0...	0.000
10	IMAGE Standard		Infinity	-			33.725 U	0.000	33.725	0.0...	0.000

	Surface Type	Comment	Radius	Thickness	Material	Coating	Clear Semi-Dia	Chip Zone	Mech Semi-Dia	Conic	TCE x 1E-6
0	OBJECT Standard		Infinity	Infinity			0.000	0.000	0.000	0.0...	0.000
1	STOP Standard		Infinity	20.480			10.000 U	0.000	10.000	0.0...	0.000
2	(aper) Standard		51.500	2.200	N-BK7		12.700 U	0.000	12.700	0.0...	-
3	(aper) Standard		Infinity	42.500 V			12.700 U	0.000	12.700	0.0...	0.000
4	(aper) Standard		-51.5...	4.000	N-BK7		12.700 U	0.000	12.700	0.0...	-
5	(aper) Standard		Infinity	0.500 V			12.700 U	0.000	12.700	0.0...	0.000
6	(aper) Standard		Infinity	3.500	N-BK7		17.124 U	0.000	17.124	0.0...	-
7	(aper) Standard		38.600	10.000 V			17.068 U	0.000	17.124	0.0...	0.000
8	(aper) Standard		30.400	6.000	N-BK7		12.700 U	0.000	12.700	0.0...	-
9	(aper) Standard		-30.4...	31.990			12.700 U	0.000	12.700	0.0...	0.000
10	IMAGE Standard		Infinity	-			33.725 U	0.000	33.725	0.0...	0.000

Figure 19: Table of lens data, simulation 1: Position 1, at the front of the zoom path (top). Position 2, at the center of the zoom path (center). Position 3, that the back of the zoom path (bottom)

As the simulation shows in figure (5), the variator moves from the front of the system to the back as it zooms. The entire length of the system is maximum at 14.2 cm, which is within the design parameters for this project. The camera will sit beyond the image plane.

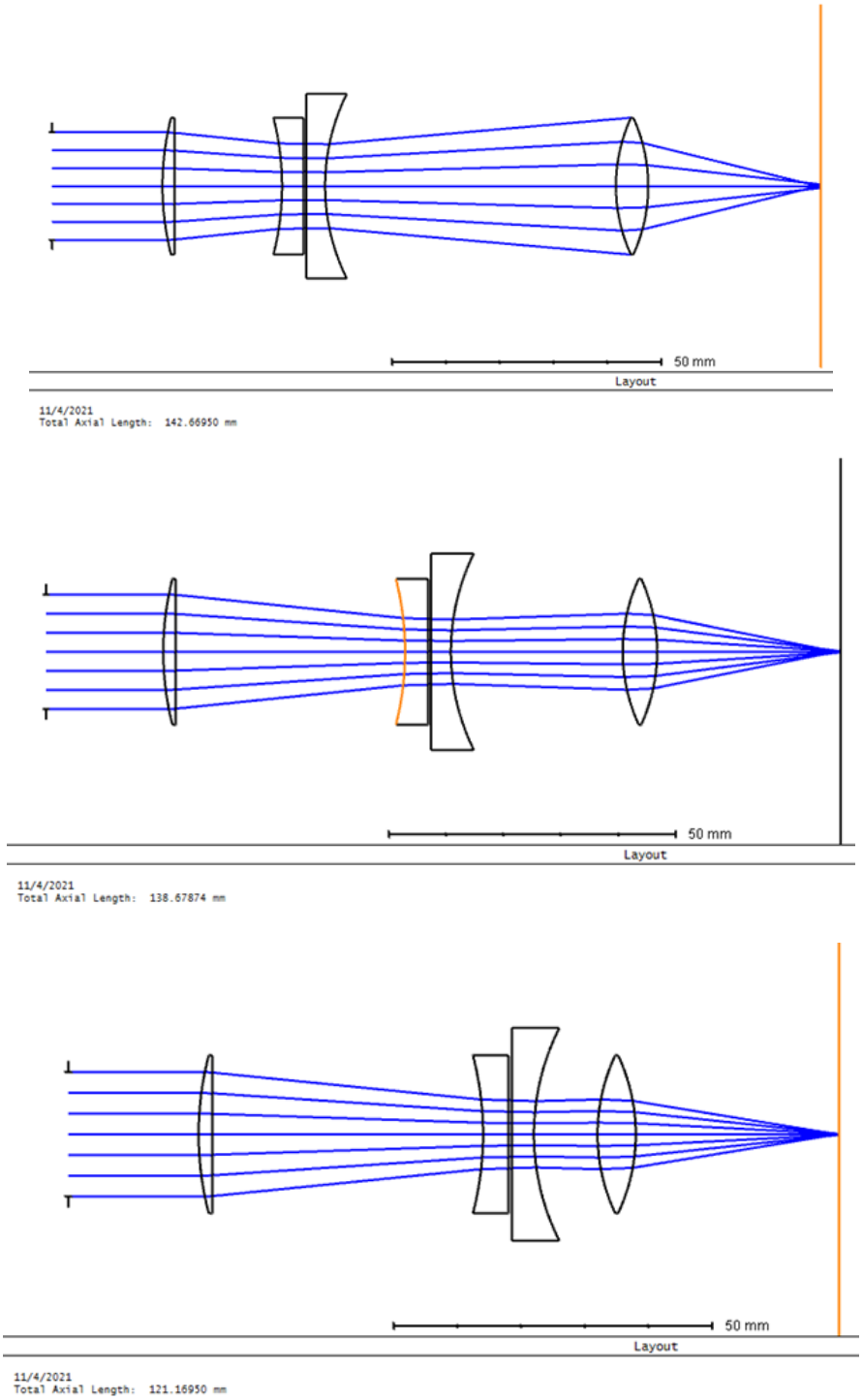

Figure 20: Simulation of focal zoom system: Position 1, at the front of the zoom path (top). Position 2, at the center of the zoom path (center). Position 3, that the back of the zoom path (bottom). The incoming light is from the left, and outgoing light to the right, where it will hit the image plane. The camera will sit at or beyond the image plane.

Although the simulation appears to focus on one spot in the image plane, spot size analysis shown in figure (6) shows a large RMS radius. The RMS radius is a sufficient measure of resolution and is used to tell if the beam is focused to one spot on the image plane. The smaller the RMS spot size, the more focused the image is. The RMS radius for the first position is 108.43, while the second position is 699.261, and the final

position is 59.827. The large RMS radius for the first and second position needs to be resolved before the design can be confirmed.

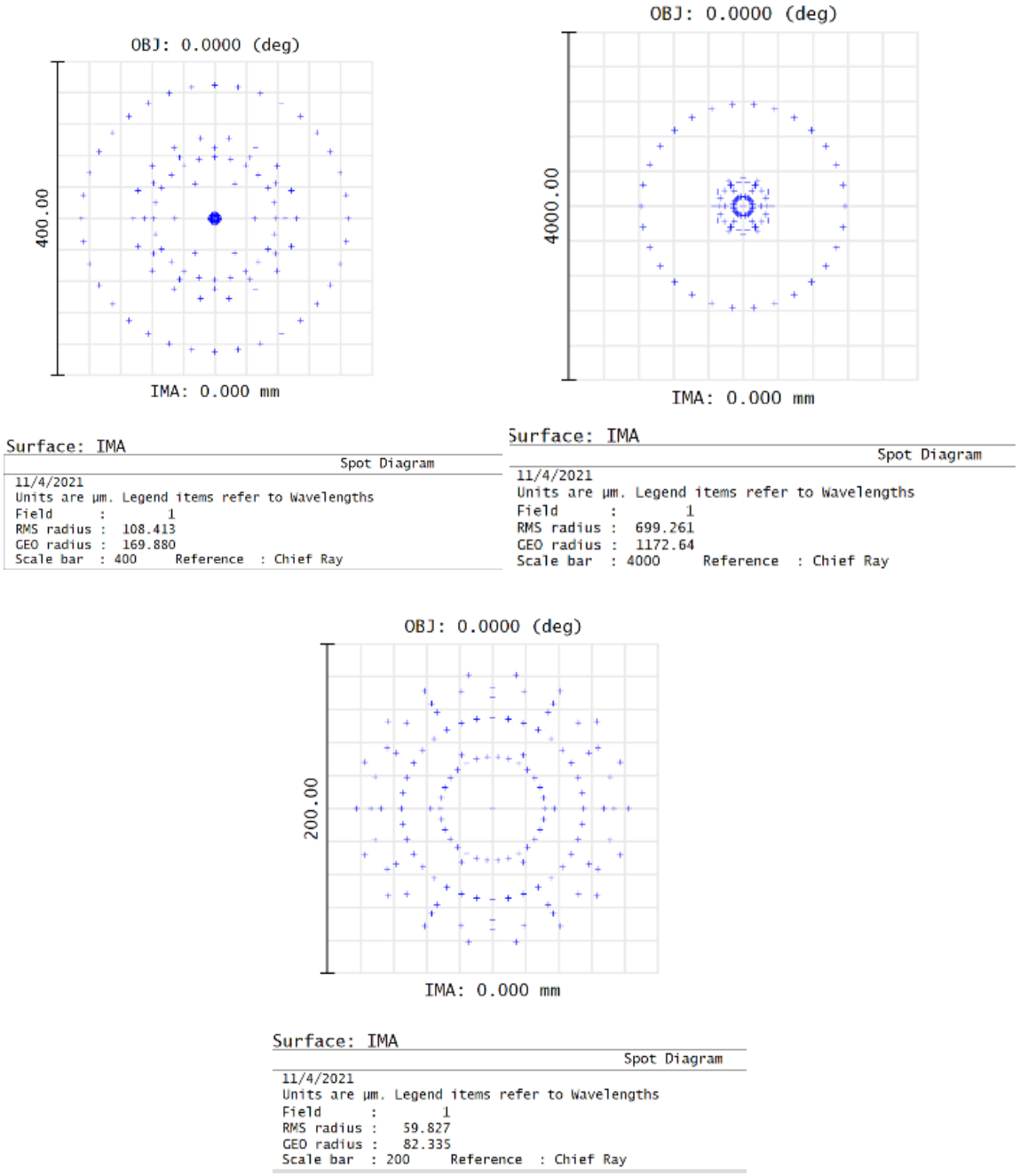

Figure 21: Spot size analysis, simulation 1: Position 1, at the front of the zoom path (top left). Position 2, at the center of the zoom path (top right). Position 3, that the back of the zoom path (bottom).

Future Zemax simulations will adjust the lenses and distances used. The design is based off a cook triplet, a common starting point for zooming designs. This may need to be looked into further and adjusted for a more accurate focus.

The main issue is the spherical aberration that is occurring due to the light rays not all converging to one point. This will affect the intensity profile made at the output of our project design because the image data will not be completely accurate. More research needs to be conducted on some of the functions within the zemax software, so that astigmatism can be checked and corrected as well. Coma should not be an issue in this design because we will be reading a narrow line of frequencies, however it can be checked in future simulations.

6.3.2 Zemax simulations (2)

Once again, the Zemax simulations uses Thorlab lenses, that are commercially available for ease of use and acquisition. Additionally, the total cost of the lenses used in the simulation did not cost more than $100, which is within initial budgetary goals. The first group, the compensator, is a 1 in. biconvex lens with a radius of curvature of 76.6 mm and focal length of 75 mm. The second, variator group is a 1 in. biconcave lens with a radius of curvature of -39.6 mm and focal length of -25 mm. The final prime lens is a 1 in. biconvex lens with radius of curvatures 179.8 mm and focal length of 175 mm. The lens data and distances between each lens at each of the three positions in the simulation are shown **Figure 22**. The entire length of the system is 14.0 cm throughout the entire simulation, which is within the design parameters for this project.
The main difference in this simulation vs the simulation ran initially is that the variator group is no longer split into two lenses. Though, the variator doublet design may be revisited, a single lens reduced cost and complexity while giving sufficient results. Additionally, the zoom system is afocal rather than focal. A focusing lens may need to be added, though the camera might be built in such a way that a focusing lens is already in front the sensor. This will need to be determined before assembling our device. However, the afocal zoom is a separate entity from this lens and the focusing lens is not considered a lens group in the zoom system.

	Surface Type	Comment	Radius	Thickness	Material	Coating	Clear Semi-Dia	Chip Zone	Mech Semi-Dia	Conic	TCE x 1E-6
0	OBJECT Standard		Infinity	Infinity			0.000	0.000	0.000	0.0...	0.000
1	STOP Standard		Infinity	5.000			10.000 U	0.000	10.000	0.0...	0.000
2	(aper) Standard		76.600	4.100	N-BK7		12.700 U	0.000	12.700	0.0...	-
3	(aper) Standard		-76.6...	3.000 V			12.700 U	0.000	12.700	0.0...	0.000
4	(aper) Standard		-39.6...	3.000	N-BK7		12.700 U	0.000	12.700	0.0...	-
5	(aper) Standard		39.600	92.000			12.700 U	0.000	12.700	0.0...	0.000
6	(aper) Standard		179.8...	2.900	N-BK7		12.700 U	0.000	12.700	0.0...	-
7	(aper) Standard		-179....	30.000 V			12.700 U	0.000	12.700	0.0...	0.000
8	IMAGE Standard		Infinity	-			21.028	0.000	21.028	0.0...	0.000

	Surface Type	Comment	Radius	Thickness	Material	Coating	Clear Semi-Dia	Chip Zone	Mech Semi-Dia	Conic	TCE x 1E-6
0	OBJECT Standard		Infinity	Infinity			0.000	0.000	0.000	0.0...	0.000
1	STOP Standard		Infinity	50.000			10.000 U	0.000	10.000	0.0...	0.000
2	(aper) Standard		76.600	4.100	N-BK7		12.700 U	0.000	12.700	0.0...	-
3	(aper) Standard		-76.6...	22.000 V			12.700 U	0.000	12.700	0.0...	0.000
4	(aper) Standard		-39.6...	3.000	N-BK7		12.700 U	0.000	12.700	0.0...	-
5	(aper) Standard		39.600	28.000			12.700 U	0.000	12.700	0.0...	0.000
6	(aper) Standard		179.8...	2.900	N-BK7		12.700 U	0.000	12.700	0.0...	-
7	(aper) Standard		-179....	30.000 V			12.700 U	0.000	12.700	0.0...	0.000
8	IMAGE Standard		Infinity	-			8.075	0.000	8.075	0.0...	0.000

	Surface Type	Comment	Radius	Thickness	Material	Coating	Clear Semi-Dia	Chip Zone	Mech Semi-Dia	Conic	TCE x 1E-6
0	OBJECT Standard		Infinity	Infinity			0.000	0.000	0.000	0.0...	0.000
1	STOP Standard		Infinity	72.000			10.000 U	0.000	10.000	0.0...	0.000
2	(aper) Standard		76.600	4.100	N-BK7		12.700 U	0.000	12.700	0.0...	-
3	(aper) Standard		-76.6...	24.000 V			12.700 U	0.000	12.700	0.0...	0.000
4	(aper) Standard		-39.6...	3.000	N-BK7		12.700 U	0.000	12.700	0.0...	-
5	(aper) Standard		39.600	4.000			12.700 U	0.000	12.700	0.0...	0.000
6	(aper) Standard		179.8...	2.900	N-BK7		12.700 U	0.000	12.700	0.0...	-
7	(aper) Standard		-179....	30.000 V			12.700 U	0.000	12.700	0.0...	0.000
8	IMAGE Standard		Infinity	-			6.664	0.000	6.664	0.0...	0.000

Figure 22: Table of lens data, simulation 2: Position 1, at the front of the zoom path (top). Position 2, in the middle of the zoom path, (center). Position 3, at the back of the zoom path (bottom)

As the simulation shows in figure (8), the variator moves from the front of the system to the back as it zooms. The camera will sit at or beyond the image plane, highlighted in orange. Both the incoming and outgoing light rays are focused at infinity, however are closer together as the variator lens moves closer to the image plane and the zoom increases. The compensator lens moves to compensate the rays and keep the image plane stationary. The final lens group, the prime lens, does not move and fixes the image on the image plane.

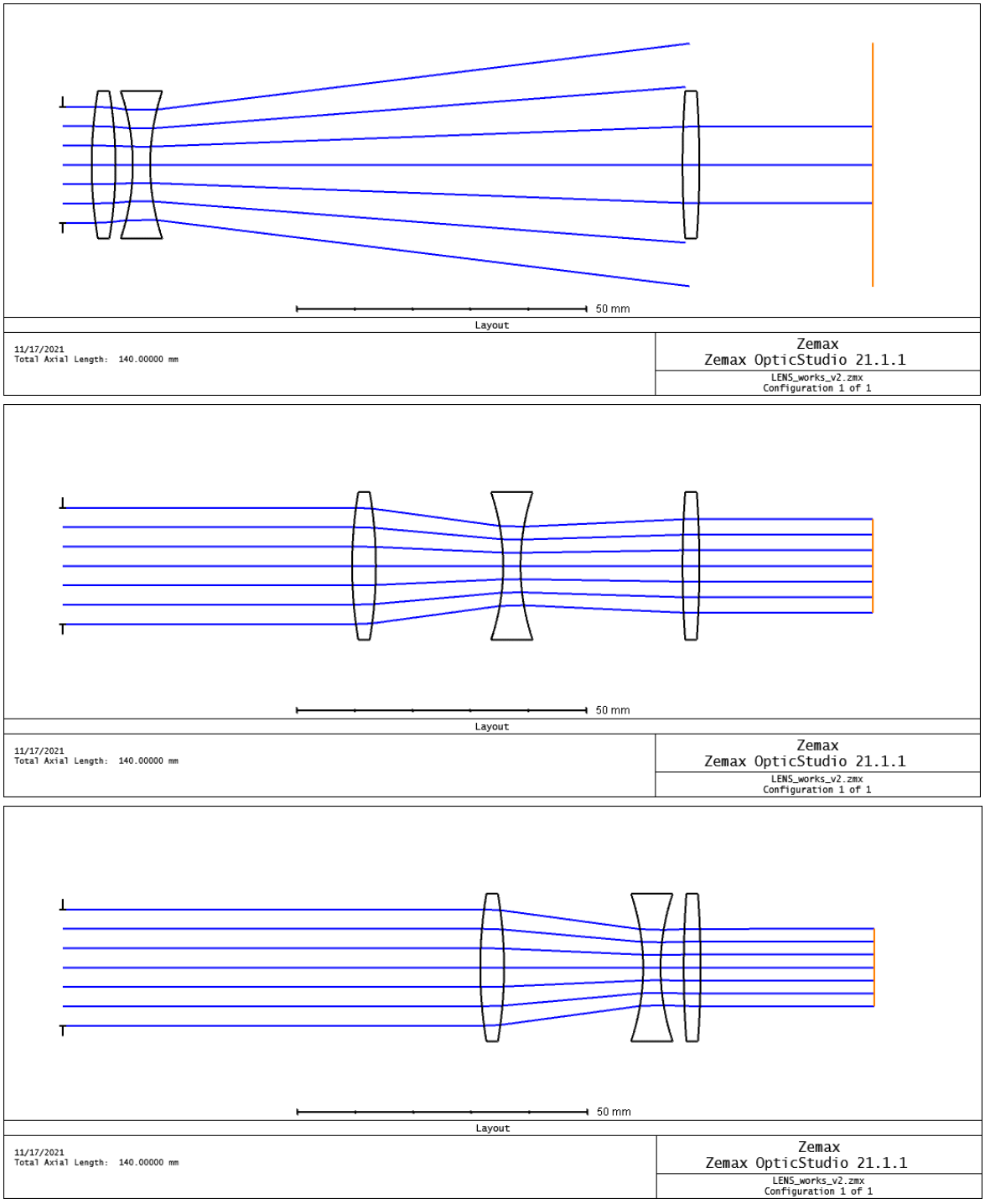

Figure 23: Simulation of afocal zoom system: Position 1, at the front of the zoom path (top). Position 2, at the center of the zoom path (center). Position 3, that the back of the zoom path (bottom). The incoming light is from the left, and outgoing light to the right, where it will hit the image plane highlighted in orange. The camera will sit at the image plane.

The Zemax simulation ran 9 positions that developed coherent output beams, mapped in **Figure 23**. As shown in **Figure 23**, the movement of lens A, the biconvex lens at the front of the system (left) is nonlinear. Lens B, the biconcave lens (center) moves in a linear path. This is consistent with design principles found in preliminary research. Lens C, the biconvex lens at the back of the system (right) is stationary and stabilizes the rays on the image plane. Lens B will move at a constant rate to and away from Lens C in the zooming process. The distance Lens A moves will need to be mathematically calculated and simulated through zemax to ensure it compensates the variator lens correctly. It is essential that the image plane remains stable for a clear image to be formed.

Figure 24: Graph depicting the movement of compensator lens A, and variator lens B, relative to stationary prime lens C. Imagine lens C laying along the x axis, and each point representing a different location along the optical axis. The trend line represents the movement of the lens being linear in the case of the variator lens and nonlinear in the case of the compensator lens.

The RMS spot size is not a sufficient measure of focus in an afocal system. this is due to the parallel output beams incident to the image plane. The RMS spot size shows the entire beam diameter. This analysis, **Figure 24**, shows the parallel rays and illustrate the zoom of the system. At position one the rays are spread out and fewer in number, as this is where the zoom will be the tightest. The smallest amount of light will be collected in this position, because it is dependent on the number of photons reflecting off the surface toward the lens system. This may mean that the closest zoom that can be obtained may not be

practical or collect a sufficient amount of light to resolve an image. If this is the case, the closest zoom that can be used will be the minimum light require to be collected to resolve an image. The second position has rays tighter together and more numerous, which is what is expected when zooming out. The third position is tighter, though has the same number of rays. The amount of light collected in position two and three are the same, due to all of the rays of light successfully traversing the lens system. this is depicted in **Figure 25**, where some rays are angled above and below the prime lens.

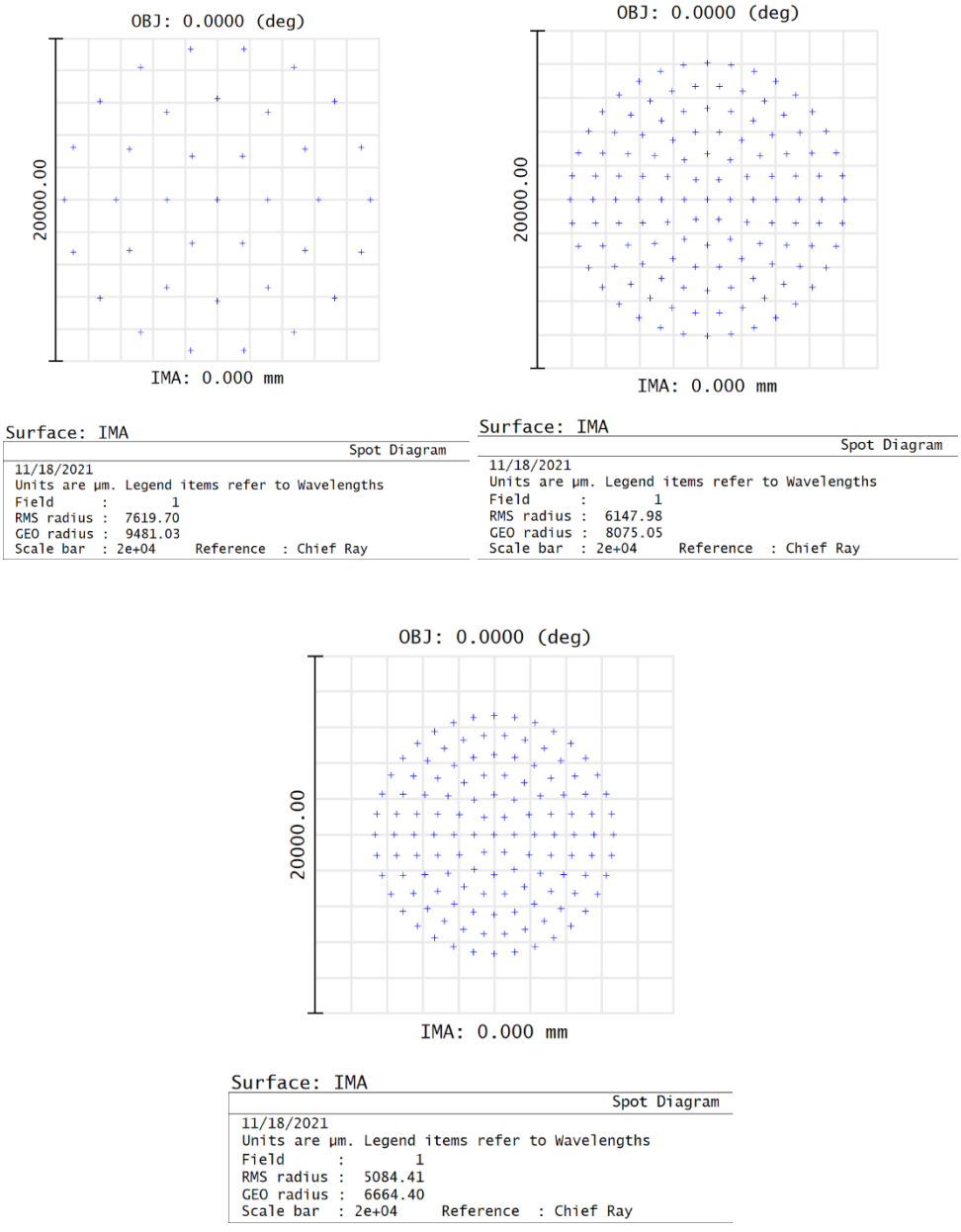

Figure 25: Spot size analysis, second simulation: Position 1, at the front of the zoom path (top left). Position 2, at the center of the zoom path (top right). Position 3, that the back of the zoom path (bottom).

Initial Zemax simulations, that did not work and were later scraped, included a split variator group design to allow for compensation of aberrations, as well as a focal zoom system. The spit variator group led to higher complexity without great effects. It also increased the cost which impeded on budgetary constraints. The focal system is unnecessary and introduced too many aberrations to compensate for, given the limited budget.

Aberrations were a main concern when initial Zemax testing was conducted. However, adjusting the parameters and realizing that an afocal system is a simpler and cost-effective solution, aberrations are no longer a main concern. Light rays do not need to converge for the zoom system to work. This configuration with parallel rays on the image plane is common in telescopes and binoculars, which influenced the design of this system.

6.3.3 Zemax simulations (3)

The main concern from the previous simulations was that it relied on the chosen camera, the ZWO ASI 385 Color CMOS Telescope Camera, having a focusing lens built in front of the sensor. If the camera does not have a focusing lens, the need for a one will be crucial for a clear and focused image. Prior to initial lab testing, elaboration of which will occur in a future section, the camera focusing lens was not a priority. This is because typical consumer ready cameras have one built in, however lab accessible testing cameras did not, so a focusing lens is explored here. The addition of focusing lens to the design will simply require a focal point that falls incident to the camera sensor. The focusing lens would be stationary and lay between the afocal zoom and the camera. The main change that would occur if the focusing lens is needed is the length of the overall system. The current lens system design is 14 cm before the camera. The focusing lens would add that lens' focal length to systems length. The following simulations serve two purposes, proof of concept that the zoom system does in fact produce parallel light rays that then can be focused on the camera sensor, and selects a fitting focusing lens, in the case it is needed.

The requirement of the focusing lens is that it is a biconvex lens. Several focal lengths were tested, and the resulting focus is tabulated in **Table 6.**. The highlighted lens resulted in the smallest rms spot size, meaning it focused to the smallest point on the image plane, where the camera sensor will lay.

Focusing lens (ThorLabs)	*Focal length (mm)*	*Back Focal length (mm)*	*RMS spot size (μm)*	*Distance from camera - added length to the system (mm)*
LB1761	*25.4*	*22.2*	*287.8*	*19.25*
LB1471	*50.0*	*48.2*	*58.2*	*46.98*
LB1901	*75.0*	*73.6*	*14.07*	*73.09*
LB1676	*100.0*	*98.8*	*4.48*	*98.59*
LB1904	*125.0*	*123.9*	*15.9*	*123.94*

Table 6: Focusing Lens

The simulation design uses the same afocal zoom lenses as the previous round of simulations, however, introduces a 1 in. biconvex focusing lens with a radius of curvature of 128.2 mm and focal length of 100.0 mm. The lens data and distances between each lens at each of the three positions in the simulation are shown **Figure 25**. The entire length of the system is increased by cm to be 24.2 cm total throughout the entire simulation, which is within the design parameters for this project.

	Surface Type	Comment	Radius	Thickness	Material	Coating	Clear Semi-Dia	Chip Zone	Mech Semi-Dia	Conic	TCE x 1E-6
0	OBJECT Standard		Infinity	Infinity			0.000	0.000	0.000	0.0...	0.000
1	STOP Standard		Infinity	3.000			10.000 U	0.000	10.000	0.0...	0.000
2	(aper) Standard		76.600	4.100	N-BK7		12.700 U	0.000	12.700	0.0...	-
3	(aper) Standard		-76.600	3.000 V			12.700 U	0.000	12.700	0.0...	0.000
4	(aper) Standard		-39.600	3.000	N-BK7		12.700 U	0.000	12.700	0.0...	-
5	(aper) Standard		39.600	92.000 V			12.700 U	0.000	12.700	0.0...	0.000
6	(aper) Standard		179.800	2.900	N-BK7		12.700 U	0.000	12.700	0.0...	-
7	(aper) Standard		-179.800	30.000 V			12.700 U	0.000	12.700	0.0...	0.000
8	(aper) Standard		102.400	3.600	N-BK7		12.700 U	0.000	12.700	0.0...	-
9	(aper) Standard		-102.400	98.596			12.700 U	0.000	12.700	0.0...	0.000
10	IMAGE Standard		Infinity	-			10.000 U	0.000	10.000	0.0...	0.000

	Surface Type	Comment	Radius	Thickness	Material	Coating	Clear Semi-Dia	Chip Zone	Mech Semi-Dia	Conic	TCE x 1E-6
0	OBJECT Standard		Infinity	Infinity			0.000	0.000	0.000	0.0...	0.000
1	STOP Standard		Infinity	52.000			10.000 U	0.000	10.000	0.0...	0.000
2	(aper) Standard		76.600	4.100	N-BK7		12.700 U	0.000	12.700	0.0...	-
3	(aper) Standard		-76.600	22.000 V			12.700 U	0.000	12.700	0.0...	0.000
4	(aper) Standard		-39.600	3.000	N-BK7		12.700 U	0.000	12.700	0.0...	-
5	(aper) Standard		39.600	28.000 V			12.700 U	0.000	12.700	0.0...	0.000
6	(aper) Standard		179.800	2.900	N-BK7		12.700 U	0.000	12.700	0.0...	-
7	(aper) Standard		-179.800	30.000 V			12.700 U	0.000	12.700	0.0...	0.000
8	(aper) Standard		102.400	3.600	N-BK7		12.700 U	0.000	12.700	0.0...	-
9	(aper) Standard		-102.400	98.596			12.700 U	0.000	12.700	0.0...	0.000
10	IMAGE Standard		Infinity	-			10.000 U	0.000	10.000	0.0...	0.000

	Surface Type	Comment	Radius	Thickness	Material	Coating	Clear Semi-Dia	Chip Zone	Mech Semi-Dia	Conic	TCE x 1E-6
0	OBJECT Standard		Infinity	Infinity			0.000	0.000	0.000	0.0...	0.000
1	STOP Standard		Infinity	52.000			10.000 U	0.000	10.000	0.0...	0.000
2	(aper) Standard		76.600	4.100	N-BK7		12.700 U	0.000	12.700	0.0...	-
3	(aper) Standard		-76.600	24.000 V			12.700 U	0.000	12.700	0.0...	0.000
4	(aper) Standard		-39.600	3.000	N-BK7		12.700 U	0.000	12.700	0.0...	-
5	(aper) Standard		39.600	7.000 V			12.700 U	0.000	12.700	0.0...	0.000
6	(aper) Standard		179.800	2.900	N-BK7		12.700 U	0.000	12.700	0.0...	-
7	(aper) Standard		-179.800	30.000 V			12.700 U	0.000	12.700	0.0...	0.000
8	(aper) Standard		102.400	3.600	N-BK7		12.700 U	0.000	12.700	0.0...	-
9	(aper) Standard		-102.400	98.596			12.700 U	0.000	12.700	0.0...	0.000
10	IMAGE Standard		Infinity	-			10.000 U	0.000	10.000	0.0...	0.000

Figure 26: Table of lens data, simulation 3: Position 1, at the front of the zoom path (top). Position 2, in the middle of the zoom path, (center). Position 3, at the back of the zoom path (bottom)

As the simulation shows in **Figure 27**, the variator moves from the front of the system to the back as it zooms. The focusing lens is the final lens before the image plane, where the camera sensor will sit, highlighted in orange. For the afocal zoom, both the incoming and outgoing light rays are focused at infinity, however are closer together as the variator lens moves closer to the image plane and the zoom increases. The lens motion is the same as the last simulation where the compensator lens moves to compensate the rays and keep the image plane stationary and the third lens group, the prime lens, does not move and fixes the image on the image plane. The final lens is the focusing lens which is stationary through the entire zoom range. At each position, the rays focus to a single point on the image plane.

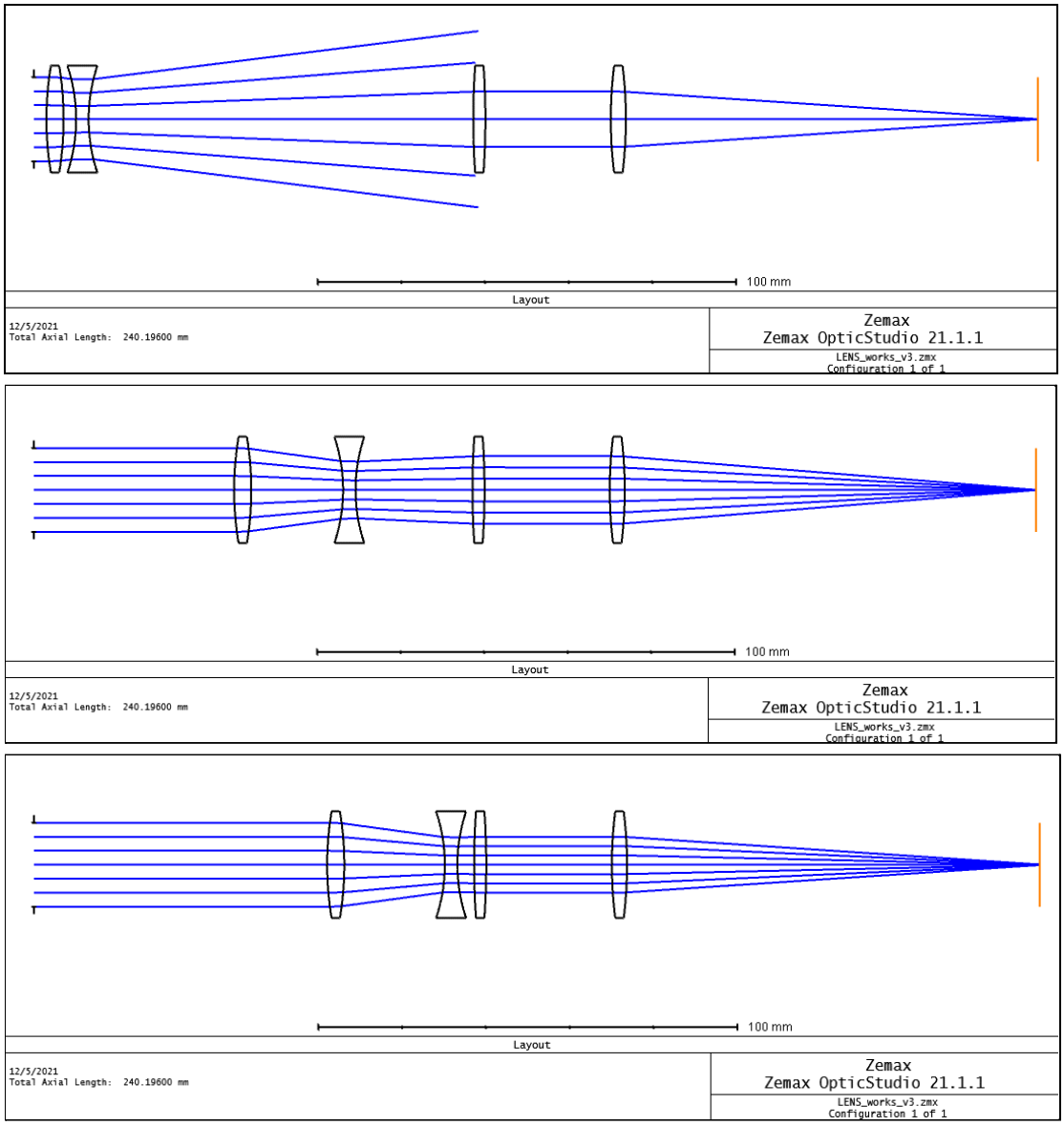

Figure 27: Simulation of focal zoom system with focusing lens: Position 1, at the front of the zoom path (top). Position 2, at the center of the zoom path (center). Position 3, that the back of the zoom path (bottom). The incoming light is from the left, and outgoing light to the right, where it will hit the image plane, highlighted in orange. The camera sensor will sit at the image plane

The simulation focuses the beam to one spot on the image plane more tightly than previous simulations. The spot size analysis shown in **Figure 28** shows small RMS radiuses for all three positions. The RMS radius is a sufficient measure of resolution and is used to tell if the beam is focused to one spot on the image plane. The smaller the RMS spot size, the more focused the image is. The RMS radius for the first position is 42.03 μm, while the second position is 4.486 μm, and the final position is 2.147 μm. The large RMS radius for the first is relatively small and is expected when the rays are far apart.

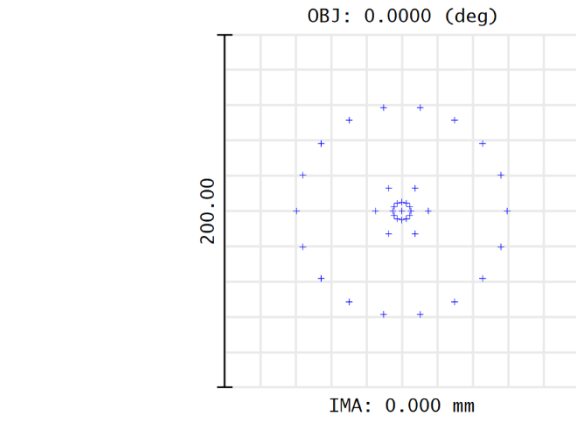

Surface: IMA

Spot Diagram

12/5/2021
Units are µm. Legend items refer to Wavelengths
Field : 1
RMS radius : 42.030
GEO radius : 59.497
Scale bar : 200 Reference : Chief Ray

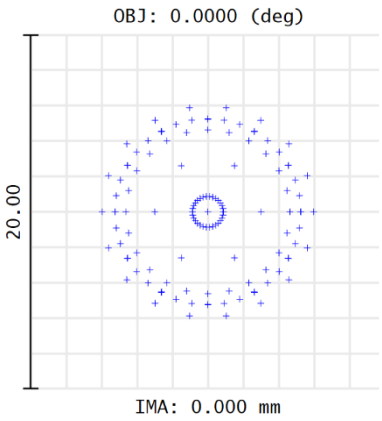

Surface: IMA

Spot Diagram

12/5/2021
Units are µm. Legend items refer to Wavelengths
Field : 1
RMS radius : 4.486
GEO radius : 5.970
Scale bar : 20 Reference : Chief Ray

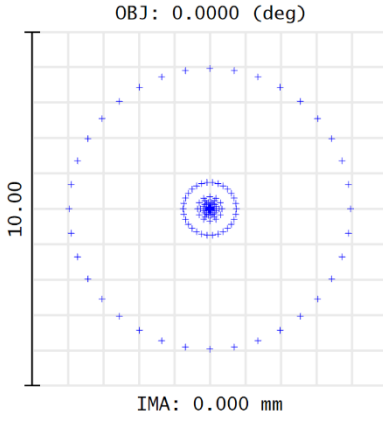

Surface: IMA

Spot Diagram

12/5/2021
Units are µm. Legend items refer to Wavelengths
Field : 1
RMS radius : 2.147
GEO radius : 3.965
Scale bar : 10 Reference : Chief Ray

Figure 28: Spot size analysis, third simulation: Position 1, at the front of the zoom path (top left). Position 2, at the center of the zoom path (top right). Position 3, that the back of the zoom path (bottom).

6.3.4 Future Zemax simulations and design considerations

Future design considerations that need to be explored and simulated are a collection lens, a focusing lens and reintroduction of split variator group design. The need for a collecting lens must be explored because the incoming light into the system is small. The small amount of light collected is because the light is coming from a diffused surface and at a distance. Additionally, the lenses and housing are small, around 1 inch in diameter, so there may be a need for a large collecting lens to sit in front of the zoom system to focus in as much light as possible. Also, introducing a split variator group to may be needed to account for aberrations if the addition of a collector lens or focusing lens introduces those issues.

6.3.5 Lens design 1

The concern between simulation 1 and simulation 2 was that the camera chosen would not have a focusing lens in front of the imaging sensor. The only real change between these two designs added a focusing lens in the rear of the design to compensate for the camera if needed. After the camera was received, it was confirmed that the camera had a focusing lens built in. So, zemax simulation 2 was finalized as our lens design 1. The prescription of the lenses used are listed in table **Table 7.**

Lens	Radius of curvature (mm)	thickness (mm)	diameter (mm)	focal length (mm)	back focal length (mm)
A	76.6	4.1	12.7	75.0	73.6
B	-39.6	3.0	12.7	-25.0	-25.6
C	179.8	2.9	12.7	175.0	174.0

Table 7. Design 1 lens prescription

6.3.6 Initial Lab Testing

Once the lenses were purchased, initial lab testing began to zoom in on an image using a camera provided by the university testing labs. The schematic of the experiment is depicted in **Figure 29**. The set up consisted of an optical rail, on which an image screen is position on one end and the camera on the opposite end. On the optical rail the three lenses that make up the zoom system are positioned before the camera. The lenses are held up by lens mounts that can

move along the optical rail. The test contains four positions of the front two moving lenses. Three of these four positions are used in the simulations contained in the Zemax simulation section, though all four were simulated prior to testing, and are tabulated below in **Table 7.**

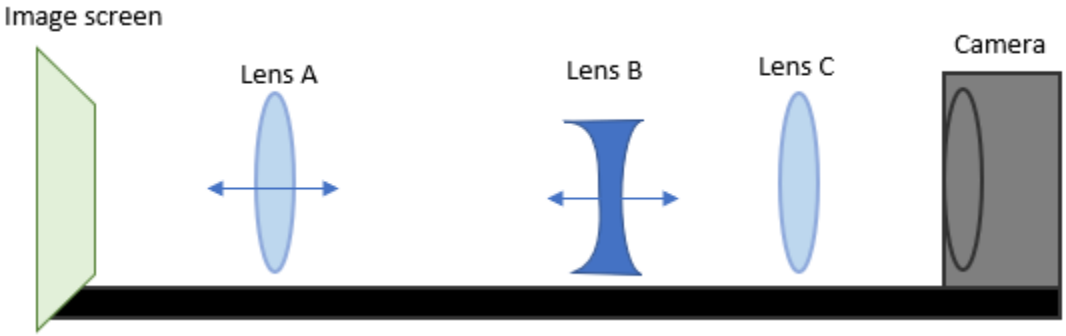

Figure 29: Zoom experiment schematic

Position	*Distance between lens A and B (mm)*	*Distance between lens B and C (mm)*	*Simulated RMS spot size (μm)*
1	*3*	*92*	*42.03*
2	*18*	*53.7*	*0.4*
3	*22*	*28*	*4.48*
4	*24*	*7*	*1.355*

Table 8: Simulated Distances between Lenses

Several issues with the current state of the design stood out right away. The camera used does not have a focusing lens in front of the sensor and cannot develop a clear or focused image. This is not the camera that will be purchased for this project, it was a testing camera provided in the lab. However, this revelation caused additional simulations that introduced a focusing lens to occur. This issue is easily remedied by adding the lens that was optimally chosen via Zemax simulations. Another issue is that the distances between lenses, the closest of which is 3 mm at position one, is too close to be feasible while using the optical rail and lens posts. In fact, in all positions the distance between lens A and B are too close to be feasible given the current equipment available. The posts and rail sliders are too thick, and the lenses cannot get close enough to each other to successfully be in any of the four positions. Because the design relied on using the same equipment that is available to test with, several solutions need to be explored as to not waste time or money jumping to an unviable solution. To overcome the bulky equipment issue, various solutions to this problem are explored below, along with each's pros and cons.

One solution, may be the simplest, is to use different posts. Newport offers A-line Keyed guide rods and A-line fixed lens mounts which would eliminate the need for bulky mounting equipment. The mounts are designed to be self-aligning as there is a hole parallel to the optical axis through the face of the lens mount where a guide rail will run through all subsequent lens mounts. The optical axis would therefore be the guide rod rather than the optical rail in this design. The clearance of the lens mount is the only equipment that would need to be considered when testing different positions. This is the simplest solution, however, may cause an issue with movement using the motors. Additionally, all the mounting equipment would need to be purchased before further testing, as these are not readily available in university labs. However, the cost for the Newport mounts cost about half as the Thorlabs mounts that the tests were conducted with, which would also help with the budget.

Another solution would be to use translation stages in the place of an optical rail. This was a solution tested in the lab. Two translation stages positioned butt to butt are able to move at different distances, as is needed for lens A and lens B's movement paths and provide mounting holes close enough together to reach the smallest gap of 3 mm in position 1. The main issue is that translation stages are extremely expensive, and this design would employ two translation stages. For this reason alone, though its confirmed to be a working solution that can meet all other design need and reach close distances, the price is too high and cannot be chosen.

An untested but feasible solution would be to use two rails rather than the one so that the lenses are horizontally suspended over the optical axis. To illustrate the concept,**Figure 30** shows the horizontal suspension. The lenses would only need to consider the clearance needed by the mounts themselves rather than the posts or slide rail mounts, which caused the main issues. The movement would be easier than with the A-line mounting rod because the motors would be able to shift the rail-mount along the fixed rail rather than the lens-mount along the rod. However, the optical axis will be hard to maintain because there will not be a rail or rod in this design to adhere the lenses to it. For this reason, it may be too difficult to maintain a proper optical axis given the nature of the device's movement in several directions and being outside.

Figure 30: Horizontally suspended lens (Image taken from ThorLabs)

Finally, the last solution would be to redo the simulations with new lens taking into account the need for 15 mm minimum clearance for the available rail-mounting equipment. This option is a backup option and other solutions should be exhausted before this one is taken, given the amount of time required to redo the simulations.

6.3.7 Design flaws discussion and rectification

This semester the lenses for lens design 1 were purchased and tested. This is the design used in the midterm demo. The prescription of the lenses used in design 1 are listed in **Table 8,**. The main issues with design 1 that came up during testing is the field of view and the magnification. The field of view was about 12% of the total vertical image. Additionally, the magnification was only about 1.8x when the goal was 4x. The field of view was a design constraint that was initially overlooked but proved to be a major factor in image quality for image analysis.

To rectify the design flaws, nine new simulations in Zemax were run to try and optimize the field of view and magnification. The main change is that the front compensator lens was doubled in size, to collect more light and to increase the field of view. The magnification was increased by changing this front lens's power as well. These nine simulations illustrated that there is a direct relationship between field of view and length of the system. The field of view is best when the length of the entire lens system is minimized. The nine simulations' best system length ranged between 44.2 mm and 54.1 mm. If the lens design was able to keep the lens movement within this system length range, the field of view would be 100% of the image height throughout all positions. Unfortunately, this did not prove to be feasible given that the lenses used were prefabricated and available off the shelf. The lenses used would have had to be custom made and larger than the available 25.4 mm and 50.8 mm diameters.

The field of view and the magnification had an inverse relationship, where the best magnification had the worst field of view and vice vera. On the magnification extreme, the simulation with the best magnification gave 5.3x, while the field of view was only 14% of the image height. The optimal length of the system was a maximum of 48.2 mm, but the maximum length of the simulated system was 214.8 mm. Another issue with this design is that the movement would have had to be significant for the magnification to change. The magnification stayed above 5x despite large lens displacement. This design would not "zoom" as intended and would have progressively worse field of view throughout the lens movement.

On the field of view extreme, the magnification was about 1.8x, which was not an improvement from the original design. The field of view, however, was 39% of the total image height. The optimal length of the system was a maximum

of 44.2 mm, but the maximum length of the simulated system was 77.8 mm. Even the most optimal field of view simulation did not achieve more than 40% the image height with the prefabricated lenses.

It was decided for the final lens design that there should be a compromise between these two constraints. Despite the magnification goal of 4x, it was decided that any magnification of 3x and above, while having a field of view over 20% of the image, would be an optimal compromise for image processing and analysis. The magnification was able to achieve 3x and the field of view was 24% of the image height.

6.3.8 Final lens design and Zemax simulation (4)

The Zemax simulations use Thorlab lenses that are prefabricated and commercially available. The front compensator lens is the only change from the previous design. The first group, the compensator, is a larger 2 in. biconvex lens with a radius of curvature of 101.4 mm and focal length of 100 mm. The second, variator group is a 1 in. biconcave lens with a radius of curvature of -39.6 mm and focal length of -25 mm. The final prime lens is a 1 in. biconvex lens with radius of curvatures 179.8 mm and focal length of 175 mm. The lens data and distances between each lens at each of the three positions in the simulation are shown **Figure 31**. The entire length of the system is 13.0 cm throughout the entire simulation, which is within the design parameters for this project.The magnification was able to achieve 3x which is a large improvement from the initial magnification of 1.8x. The field of view was 24% of the image height, which is twice the initial design's field of view of 12% the image height.

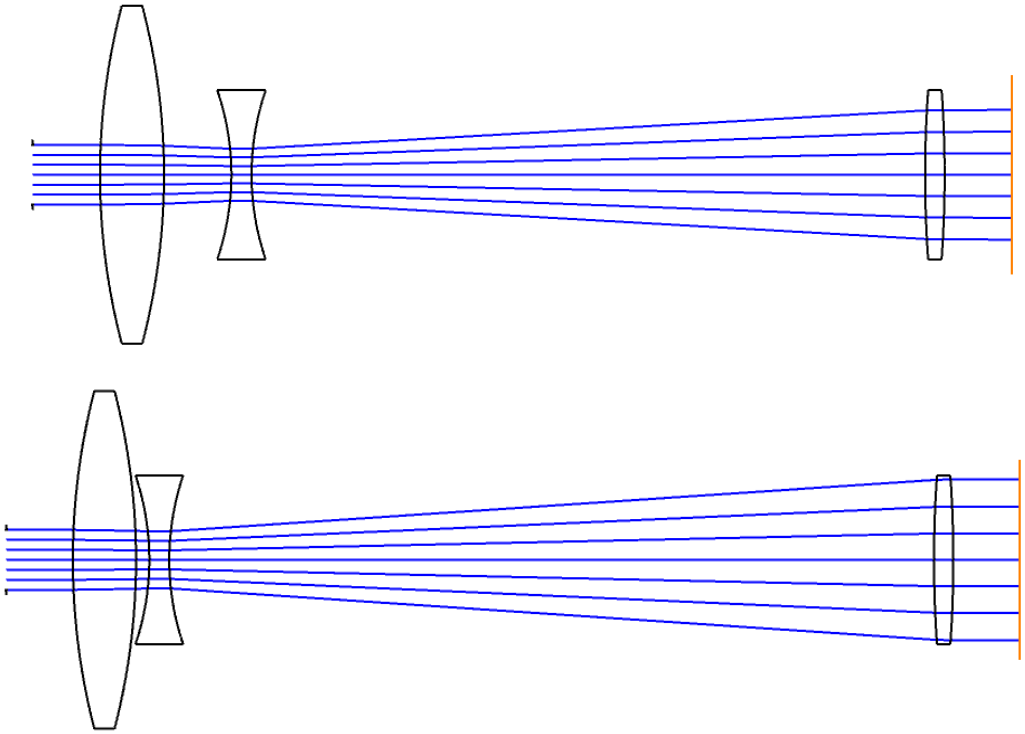

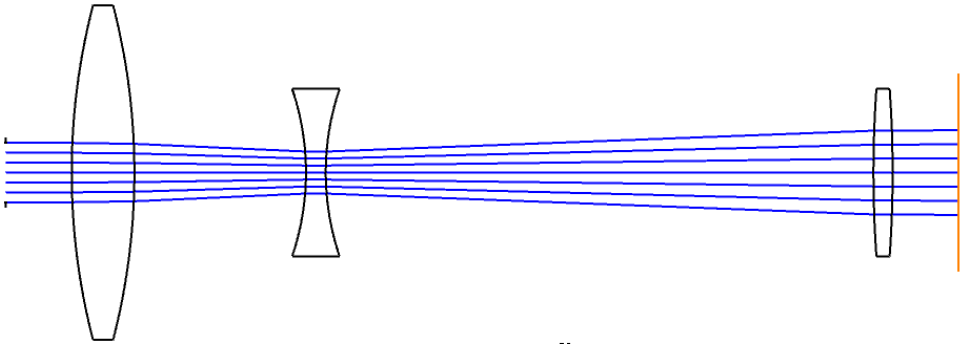

Figure 31: Simulation of focal zoom system with focusing lens: Position 1, at the front of the zoom path (top). Position 2, at the center of the zoom path (center). Position 3, the back of the zoom path (bottom). The incoming light is from the left, and outgoing light to the right, where it will hit the image plane, highlighted in orange. The camera sensor will sit at the image plane

6.3.9 Lens Mount and Movement system

After initial testing, it became clear that the lens mounts typically employed in lens designs would not be suitable for our design. The lens mounts were too bulky and would not allow the lenses to be positioned in the proper locations. Several solutions were explored, such as the translation stages, A-line lens holders with guiding rods, and horizontally suspended lens holders. Optical cage system is utilized for our final lens design, illustrated in **Figure 35**.

Like the A-line lens holders, the cage system has guiding rods to maintain a rigid optical axis. However, the design for the movement of the lenses required two rails with two motors, because the two front lenses move at different speeds and distances. The A-line lens holders contain one guiding hole and would be oriented opposite each other which would not line up the lenses. The cage system however, utilizes four guiding rods to fix the optical axis in the y- and z-directions, while allowing the two front lenses to freely move forward and backwards in the x-direction. The third lens is fixed to the back of the system but is maintained to the optical axis by the guiding rods. This system takes away the variability of y and z- directional movement that was of concern in the horizontally suspended solution option.

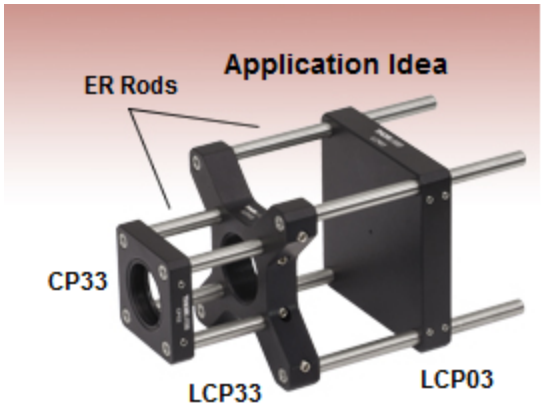

Figure 32: Optical cage system (Image taken from ThorLabs)

6.4 Camera

6.4.1 Initial Camera design

In our beam profiler, care will be needed to balance the need for low read noise and higher frame rate. Though, as previously mentioned, a frame rate of 60+ fps is unlikely to be necessary, it is important to keep in mind any relationships that will affect the image (Andor, 2019).

In our demo we plan to use a green or red laser pointer. Because the quantum efficiency is highest in the green frequencies, it is likely that a green laser pointer is most practical for proof of concept. Also, a high quantum efficiency is high priority when choosing and comparing camera options, especially in low power scenarios. Low power laser pointer beams will not be as easy for the camera to pick up because less photons will be diffused from the target surface. Therefore, a high peak quantum efficiency is needed in our demo (Andor, 2018).

Specification	Goal	ZWO ASI 385 Color CMOS Telescope Camera	ZWO ASI120MM-S Monochrome CMOS Astrophotography Camera	Celestron NexImage 10 Color Solar System Imager	Orion StarShoot AutoGuider
Price	<300	$350 ($299)	$179	$435.95 (274.95)	$299.99
ADC	12 bit	12 bit	12 bit	12 bit	8 bit
Back focus		12.5 mm	12.5 mm	13.1 mm	
Connection		Female M42x0.75	Female M42x0.75	C thread	1.25" Nosepiece
Color/mono		Color	Mono	Color	Mono
Dynamic range		12 stops	11.6 stops		
Frame rate (full res)	30+ fps	120 fps	60 fps	15 fps	
Frame rate (max)		120fps	254 fps	200 fps	15 fps
Full well	Large ke	18.7 ke	20 ke		
Mega pixels		2.1 mp	1.2 mp	10.1 mp	1.3 mp
Peak QE	High QE	80%	78%	39%	
Pixel array		1936 x 1096	1280 x 960	3664 x 2748	1280 x 1024
Pixel size		3.75 microns	3.75 microns	1.67 microns	5.2 microns
Read noise	Low e-	0.7 e-	6.6 e-		12 e-
Sensor diagonal		8.3 mm	6 mm	7.6 mm	8.5 mm
Sensor type	CMOS	CMOS	CMOS	CMOS	CMOS
Sensor		Sony IMX385LQR	CMOS AR0130S monochrome sensor	ON Semi MT9J003	Micron MT9M001
Weight	Low lbs		0.2 lbs		

Table 9: Camera specifications comparisons. Taken from (CMOS Cameras, 2021)

Due to the considerations mentioned above, the ZWO ASI 385 Color CMOS Telescope Camera fits the design needs the most. Key considerations included the ADC, frame rate, full well, peak QE and read noise. Ultimately, the read noise and peak QE are the parameters that this camera rose above compared to the other options and were the reason this was chosen. The frame

rate and peak QE eliminated the Celestron NexImage 10 Color Solar System Imager from consideration. The read noise eliminated the ZWO ASI120MM-S Monochrome CMOS Astrophotography Camera, despite all other specifications meeting the design requirements. The read noise and frame rate of the Orion StarShoot AutoGuider were nowhere near the requirements needed for this application, and therefore eliminated this option as well.

6.4.2 Final Camera Design

While the ZWO ASI 385 Color CMOS Telescope Camera fits the design needs the most, the software or post imaging processing caused the displayed feed to be in only primary colors with no image definition or details. This made the camera unusable for the project needs. an alternative that was affordable was required because the original camera used nearly all of the budget allotted to the camera.

The solution was the web camera Logitech C615, which allowed us to receive a live feed with high camera resolution and high frame rate. resolution and frame rate were the two specifications that this new camera could not compromise on. The logitech was very light weight which was a bonus for the electronics and movement design.

6.5 Optical Filter (Initial Design)

The design for this experiment will consist of two optical filters. One filter will be a long pass optical filter and the other a short pass optical filter. The two optical filter stacked will create a custom bandpass filter. The goal is to have as narrow of a bandwidth as possible only allowing in the laser wavelength being used for experimentation and blocking all other frequencies outside of the bands. These two filters will need to be compatible, have a high enough optical density to block the outer bands sufficiently, and have a high enough transmission rate of the pass band. The calculated threshold transmission rate for the design is at least 70% to have an intense enough optical signal to reach the camera. Interference filters were not chosen because of their extreme angle sensitivity. The ideal choice are absorptive filters that require no angle of incidence, and they must fall within the budget for the lenses of roughly 250.00$. For lab testing of this experimental design a high intensity laser pointer of 532 nm wavelength will be shone upon a diffused surface backboard. The diffused surface will be made of material that is used on the outdoor range for the stretch goal. The main objective of this design is to capture as much diffused laser light as possible from the diffused surface through the lens system and filter system by the camera. During lab experimentation there will be ambient light from a light source that is in the room. This light source will introduce a broad range of visible wavelengths into the system that will be considered noise and must be filtered out by an

optical filter. By stacking both an optical short pass filter and an optical long pass filter a custom optical bandpass filter will be created. It is ideal to have the smallest bandwidth of allotted wavelengths being introduced to the camera for analyzing the data. After searching around on many websites, to name a few, Newport, OmegaFilters, OceanInsight, Alluxa, OpticalfiltersUS, EdmundsOptics, many optical filters and design combinations are available on the market. The prices of each optical filter and there working properties ranges from as low as forty dollars US to as high as a few thousand dollars. The price difference is due primarily to the types of materials, the thickness of the optical lens, the type of filter, and the working properties. Many rare metal coatings on optical filters will give the optical filter unique transmission windows, but in turn significantly increase the costs. There are many optical filters online that are the exact transmission spectrum with the required central wavelength for this experiment, but unfortunately the cost makes them unrealistic to add to the budget. These types of optical filters are traditionally used in specialized experimentation. The option to design an optical filter on many of the websites is also available for the company will create the necessary lens per specification. This process through shopping around is quite costly and can potentially be even more than purchasing all other components individually for the design. Instead of purchasing an expensive optical filter for the experiment or just buying a bandpass filter that is centered at the 532 nm, the approach taken is to create an optical bandpass filter using both an optical short pass filter and optical long pass filter. By stacking these two types of optical filter a unique bandpass filter will be created and will allow the proper range of spectrum to travel through the optical system designed. Below is a table of many combinations of optical filters that were attempted.

For the stretch goal a similar approach can be attempted to build a band pass filter with a narrow transmission band allowing only the desired 800 nm frequency transmitted. After having already looked at multiple websites to find a similar design for the stretch goal it has been challenging to find a combination that narrows the bandwidth as small as that with the 532 nm design. The smallest bandwidth combination found was larger than thirty nanometers which is not ideal. This stack combination also was much more expensive than that of the filters being used for the green laser experimentation. In compassion to the 156.00$ of the green filter design the 800 nm design costs nearly double. Through looking on many different optical filter websites there are multiple band pass filters already on the market which are quite affordable. When it comes to the stretch goal instead of designing a bandpass filter it may be the most reasonable decision to just purchase an already prefabricated 800 nm central bandwidth filter.

Manufacturer	Long Pass Optical Filter	Short Pass Optical Filter	Peak Transmission Bandwidth	Cost
Edmunds	#49-026 D = 12.50 mm Cut on 500 nm Transmission: 520 – 2000 nm > 85% @ 532 OD = 2 Angle of Incidence: 0	#47-813 D = 12.50 mm Cut off 550 nm Transmission: 400 – 535 nm > 85% @ 532 OD = 2 Angle of Incidence: 0	520 – 535 nm	LP = 64.75 $ SP = 92.50$ Total = 157.25$
Omegafilters	SKU: W4583 501AELP D = 12.50 mm Cut on 501 nm Transmission: 505 – 600 nm > 90% @ 532 OD = 4 (484 – 492 nm) Angle of Incidence: 0	SKU: W6045 540SP D = 12.50 mm Cut off 805 nm Transmission: 432 – 538 nm > 90% @ 532 OD = 4 (540 - 1100 nm) Angle of Incidence: 0	505 – 538 nm	N/A Requested Quotes.
Thorlabs	FEL0500 D = 25.4 mm Cut on 500 nm Transmission: 502 - 2200 nm > 88% @ 532 OD = 2: (200 – 502 nm) Angle of Incidence: 0	FES0550 D = 25.4 mm Cut off 550 nm Transmission: 380 – 550 nm > 85% @ 532 OD = 2: (560 – 2200 nm) Angle of Incidence: 0	502 – 548 nm	LP = 80.62$ SP = 80.62$ Total = 161.24$
Dyanasil	LP-500-25 D = 25 mm Cut on 500 nm Transmission: 500 – 2200 nm > 80% @ 532 Angle of Incidence: 0	SP-550-25 D = 25.4 mm Cut off 550 nm Transmission: 400 – 550 nm > 80% @ 532 Angle of Incidence: 0	505 - 545	LP = 70.00$ SP = 70.00$ Total = 140.00$

Table 10: Filter Comparison

Choosing which combination is both the best for application as well as for cost efficiency the The Edmunds set of edge filters will give the narrowest bandwidth, and the transmission is 72.25% (above the 70% threshold sought for design). The optical density will be a little higher than two for the band reject region and the price is within budget. The omegafilters have the highest transmission rate of 81% and the highest band reject region with optical density of a bit more than four when stacked. These two optical filters have an acceptable bandpass window, but without knowing the pricing it is hard to say if

they are within the budget. The Thorlabs short pass and long pass optical filters have an acceptable bandpass transmission of 74.80%. The optical density of for the band reject region will be just above two. The pricing is comparable to the Edmunds but the bandpass transmission window is a little wider than desired for the design. The Dyanasil edge filters have a bandpass transmission of 64%. The bandpass region is also the broadest of the four filters compared. The pricing is reasonable but because of the wide bandpass region and the transmission lower than the desired 70% threshold this option will not be chosen. It is in the best interest of the design to have the highest possible transmission rate. The laser light signal will already be lower intensity as it will be diffused light, and highly attenuated by the optical lens system design. These two factors will make it harder to get quality data. If the pricing for the omegafilters optics are comparable to that of the Edmunds than those may be the stack combination of choice choice. These optical filters have a higher bandpass transmission rate as well as a higher optical density to block out the undesired frequencies Currently the bandpass filter design combination of choice is the Edmunds set. The total transmission of the stack is 72.25% which is what is being sought (over the 70% threshold mark). Also, the cost of the filters is reasonable and within budget. The optical density reject region is high enough to block out the undesired frequencies from entering the camera. If the pricing for the omegafilters optics are comparable to that of the Edmunds than those may be chosen. These optical filters have a higher bandpass transmission rate as well as a higher optical density to block out the undesired frequencies The images below show the spectrum of both the Edmunds #47-813 short pass filter and the Edmunds #49-026 long pass filter.

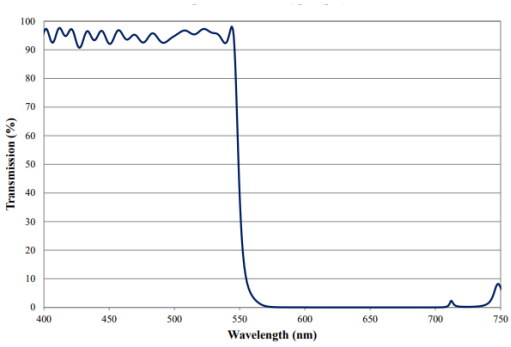

Edmunds #49-026
Picture taken from Edmunds website

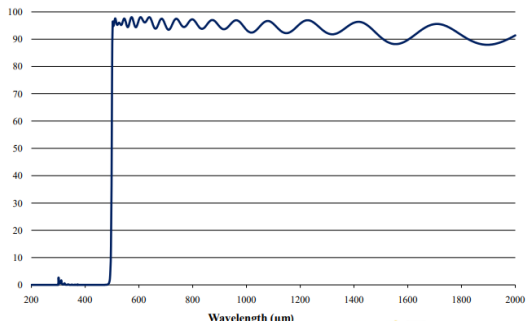

Spectrum of long pass filter used in device
Edmunds #49-026
Picture taken from Edmunds website

Figure 33: Short Pass and Long Pass filter acceptance band

The stacking of these two filters will be the linear multiplication of the two filters which can be written as a unit stepwise function. Let H_1 be the long pass optical filter dimensions and let H_2 be the short pass optical filter dimensions. Below the unit stepwise function of the designed bandpass filter

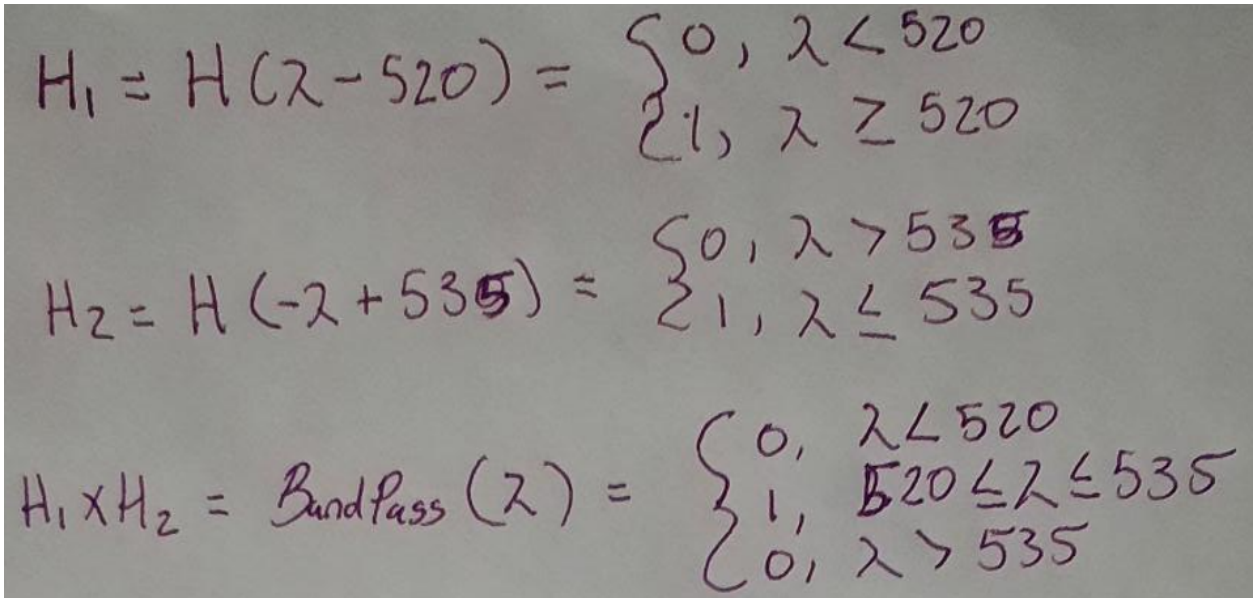

Figure 34: Stepwise function for bandpass filter design
Depicts the linearity of stacking a short pass and long pass optical filter to create a unique band pass optical filter

For the stretch goal of working with the 800 nm laser a similar approach with the filter design can be achieved. There are many band pass optical filters on the market that are made with a central wavelength of 800 nm. Doing the same process as before searching low pass and long pass optical filters online there are many combinations from different optical lens distributers that can be stacked to achieve a narrow bandpass linewidth for the 800 nm laser. The problem with these combinations is that the optical lenses are a bit more expensive than that of the ones used for the 532 nm optical band pass design. The types of optical filter materials used to reach this infra-red region are what add onto the additional cost making them out of budget. For the stretch goal it will be much cheaper to buy one of the already fabricated optical bandpass filters designed for this bandwidth.

6.5.1 Optical Filter (Final Design)

The executive decision was made to instead of stacking two filters to create an optical filter, one that was already fabricated with the required specifications will be purchased. This decision was made based on cost efficiency, the need for it to work up to the specs designed, and errors found in the initial design. The bandpass filter that was chosen for this design is the Edmunds 25 mm 532 nm CWL mounted bandpass filter. This filter checks all of the boxes when it comes to the five requirements. The filter has a central wavelength of 532 nm + or – 2 mm and a bandwidth of 10 mm + or – 2. The bandwidth is narrow enough for the application with cut on and cut off frequencies at 527 and 537 mm respectively. The optical density of the filter is 3

which is high enough for the application of this design. An optical density of 3 attenuates the undesired bandwidths ranging from 200 nm – 1200 nm by a factor of 103. The transmission percentage is ≤ 45%. The transmission is on the cuff of the desired minimum transmission percentage but is also acceptable for this application. The last parameter is the size of the filter which is a diameter of 25mm. This is more than enough size to match the smallest optics in the lens system and plenty of room for the camera and light dependent resistor sensor to both sit behind completely. There were many other filters with higher transmission rates and higher optical densities, but the pricing ranged from double to triple the pricing of the filter chosen which was out of budget. Shown in **Figure 35** are the properties of the bandwidth filter.

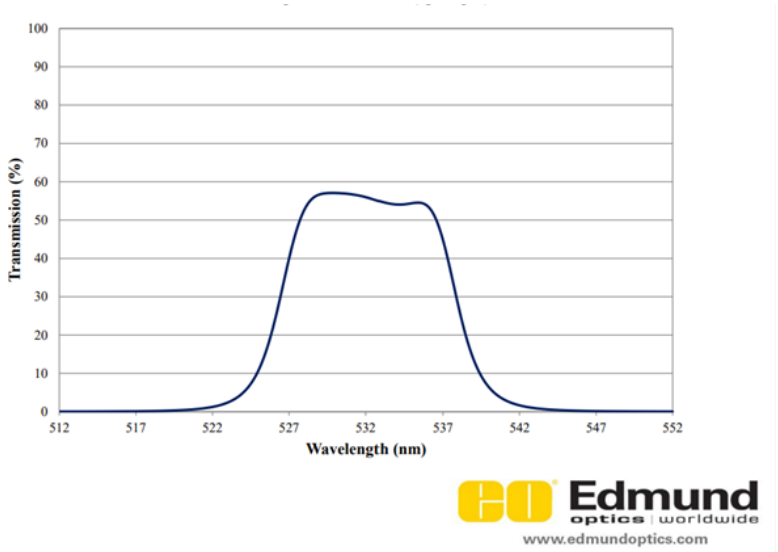

Figure 35: Bandpass region of 532 nm Bandpass filter provided by Edmund Optics

6.6 Ambient Light Sensor (PIN Photodiode)

The proper photodiode for this experimentation is a silicon PIN photodiode that is sensitive to both visible light and near IR. Below is a list of the many different PIN photodiodes on the market that have been researched for the design.

Brand	Model	Operating Voltage	Functioning Temperature	Cost	Response Time	Spectral Range
CivilLaser	1.2mm Si PIN Photodiode	0 – 15 V	-40 – 85 C	20.00 $	8 ns	200 – 1100 nm
Osram Opto	SFH2704	0 – 5V	-40 – 85 C	0.65 $	46 ns	400 – 1100 nm
Advanced Photonix	PDB-C152 SM	0 – 10 V	-40 – 105 C	1.97 $	50 ns	400 – 1100 nm
Advanced Photonix	PDB – C154SM	0 – 10 V	-40 – 80 C	1.47 $	10 ns	400 – 1100 nm
CivilLaser	3.2mm Si PIN Photodiode	0 – 15 V	-40 – 85 C	11.00 $	6 ns	400 – 1100 nm
CivilLaser	3mm Si PIN Photodiode	0 – 10 V	-25 – 85 C	6.00 $	15 ns	300 – 1200 nm

Table 11: Photodiode Comparison

The Civil Laser 3mm SI PIN photodiode seems to be the appropriate photodetector for the ambient light measurements for the design. This light sensor has a relatively quick response time of 15 ns and will be able to be operated with a low voltage of 5 volts. This photodiode was chosen over the other because it does have a much broader bandwidth reaching into the UV. This photodiode will be used to measure the intensity of the full spectrum light source as well as the sun for the stretch goal. The ability to get an accurate full spectrum intensity profile of the ambient light will allow for the true intensity profile of the laser beam being measured to be calculated by neglecting the ambient light of the same intensity as the laser source. This photodiode has the highest responsivity to the 532 nm spectrum as well so an additional photodiode within the system can be used to aid in determining the intensity of the diffused light travelling through the system. This photodiode also has a relatively low dark current (V_R = 10V) of 10 nA. The cheaper options are still being investigated but unfortunately were not in stock or had a delivery time that would be way outside the window of building the project. The only drawback is to order these photodiodes they must be purchased with a minimum of ten per order which places the cost at 60.00$. This cost is not necessarily out of budget but would be ideal to find cheaper photodiodes that can be ordered in smaller batches. As of right now it seems this photodiode will be the appropriate fit and with having multiple there is room for mistakes in case one burns out in testing. Below is the spectral profile of the photodiode in operation.

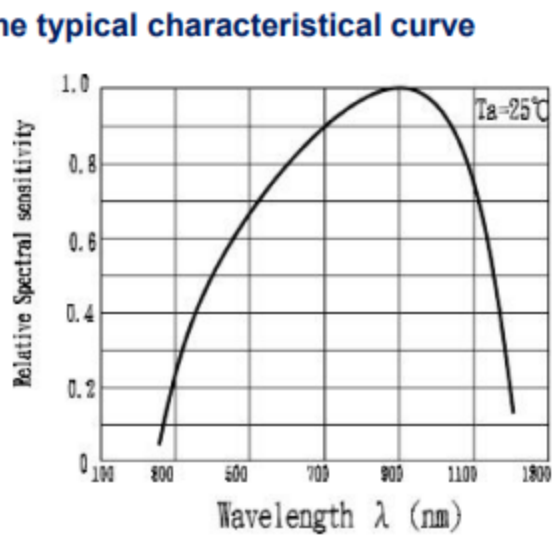

Figure 36: PIN photodiode sensitivity graph (taken from civillaser.com)

The stretch goal is to be able to block out the undesired wavelengths of light through the optical system and then sense, how much of the wavelength is actually being measured from the 800 nm laser versus the full spectrum visible light source. In the lab setting it is possible set a control variable when the lights are off compared with when the full spectrum light is on. Since there is no way to get a true control outside in the sun the device will need to be able to differentiate the blackbody radiation through the optical filter from the diffused laser light. The problem with this is the inconsistent fluctuation of light intensity as the brightness, cloud coverage, and position of the sun changes. This means that every time a test is run the results will be unique to the weather conditions at that time. Since the light intensity is affected by a multitude of factors relating to weather the system needs to be able to record the data and by design differentiate the diffused wavefronts of the laser from the infrared black body radiation of the sun. This approach is still being worked out to find the most effective sensor and approach to single out only the diffused laser light for the stretch goal outdoor laser testing.

6.6.1 Optical Sensor (Final Design)

Three different light dependent resistors (LDR) were examined in the lab to find the best suited for the application. LDR's have very few electrons when not illuminated resulting in a high resistance. As light is shone upon the surface of the LDR the photon energy allows for the electrons to jump energy bands and dramatically drop the resistance. Three LDR's 5506, 5516, and 5549 all composed of cadmium sulphide (CdS) were tested. CdS is used due to it's very high spectral sensitivity to 532 nm light. When the CdS is set up in a voltage

divider circuit with another resistor, the voltage across the voltage divider branch is used to calculate the approximate luminous intensity upon the surface. The unit for luminous intensity is lux and the logarithmic relation between the voltage and lux measurement are shown in Equation (). In the lab all three LDR's were examined under different conditions; measured with an intensity variable fiber light source (Fiber Light High Intensity Series 180 Dolan-Jenner Industries) with out any bias, measured with the same fiber light under a 5V bias in a voltage divider circuit with 10k ohms, measured without bias by two 532 nm green laser sources of varying intensities with varying optical densities applied and the 532 nm bandpass filter, and lastly with a 5V bias in a voltage divider circuit with 10k ohm and two different green 532 nm laser sources of differing intensities under varying optical densities and the 532 nm bandpass filter. All lab testing was conducted under dark light conditions with the only light being supplied coming from the tune able fiber source and lasers. Each test was accompanied by a lux meter (Dr. Meter Model LX1330) which was limited in capabilities maxing out at about 2000 lux which can be seen in **Figure 37**. After all the lab testing the 5506 LDR resistor was chosen. Each LDR examined had a high sensitivity to the 532 nm wavelength with the 5549 having the highest resistance, which inevitably responded to the voltage divider with a higher output voltage as illuminance increased. The 5506 responded with a much lower output voltage which is the biggest reason it was chosen for this application as to not negatively impact the components in the Arduino. Table () and () compare the LDR's response to the fiber light shone through the bandpass filter with and without the bias. **Figure 38** shows the relationship between the lux and resistance. That data of that graph was than all altered to a log scale to get a linear slope which is used for calibration of the Arduino to create the luxmeter. The lab data collected of the 5506 resistor is shown below.

Intensity	Resistance (K-Ohms)	Lux (Lx)
0	1M	0
1	9.97	7.4
2	8.65	9.5
3	7.55	11.9
4	6.56	15.1
5	5.81	18.6
6	5.11	23.2
7	4.43	29.8
8	3.85	38.1
9	3.37	48
10	2.93	60.9

Table 12: Resistance Vs Lux of Fiber Light with Bandpass Filter, No Bias

Intensity	Resistance (K-Ohms)	Voltage Output (V)	Lux (Lx)
0	0.968	0.18	0
1	5.16	2.50	7.3
2	4.83	2.66	9.0
3	4.50	2.83	11.3
4	4.15	3.01	14.4
5	3.83	3.12	18.1
6	3.53	3.29	22.6
7	3.19	3.46	29.3
8	2.90	3.61	37.3
9	2.62	3.75	47.5
10	2.37	3.85	60.0

Table 13: Resistance, Voltage, and Lux Measurements with Fiber Light through bandpass filter, 10k ohm resistor, and 5V Bias.

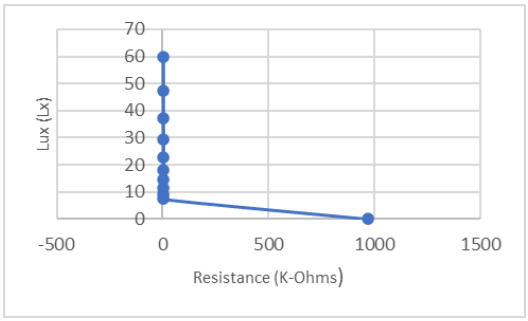

Figure 37: Lux vs Resistance of 5506 LDR with Fiber light of varying intensities, Bandpass filter, 10k ohm resistor and 5 V bias

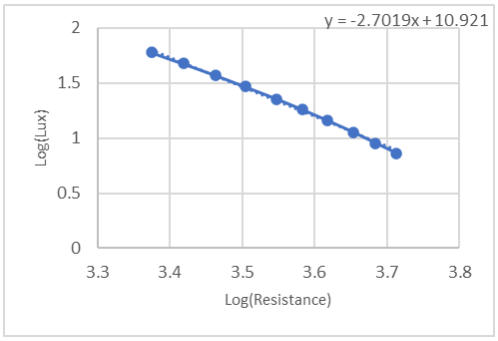

Figure 38: Log(Lux) Vs Log(Resistance). The slope equation is used for calibration of the Lux Meter.

6.7 Power Supply and Distribution

A design for a power supply is needed for the system. Batteries of a range of 12-24 volts were compared along with the chemical composition of the battery. Calculating a comfortable amount of output power for the overall load of our system, allowed us to find the right battery's amps per hour which allows the system to run without any interruptions or damage. Our system does not require a high voltage as a power supply, but it does require the right distribution of power to the components making up the system. Since our system powers a number of different components (i.e., motors, sensors), DC-to-DC converters were designed using TI's Webench software, in order to provide a stable voltage and current to the component. Providing power to the motors was the biggest challenge in terms of providing power to the system. There are two motors providing two movements, with each movement holding a different weight. Comparing types of motors, as well as an understanding of each motors' rated values (voltage, current and torque) was key to be able to combine supplied power given to the motor, and output work from the motor. Although the microcontroller needs power from the battery, the controller is also connected to a laptop in order to read values from the camera, as well as powering it. The

microcontroller is connected to two motors in order to move them when needed for calibration.

6.7.1 Power Supply

The total amount of power consumption based on each component of our system was calculated. Carefully detecting what components consumed the most power from the system is key, then moving on the rest of the components that will need to be powered by the battery. Our system is implemented with two stepper motors, giving motion to two 70x70 mm lenses which are mounted to a platform. From all the components used in the project, the raspberry and the two motors consumed the most energy, which means we will design a capable power supply that can provide the right currents in order to run with no errors.

Our system requires a variety of magnitudes for voltages and currents, which is not possible by just connecting the battery to these components. DC-to-DC conversion is required to be designed, in order to distribute and amplify the power going through these components. The motors for instance, which are our heaviest component required currents that range from 1.4 amps to 3.0 amps. In the figure below, Webench was utilized in order to get an acceptable circuit schematic for an input voltage ranging from 11.3 V to 12 V. This circuit design results in an output of 13.8 V and 3.0 A.

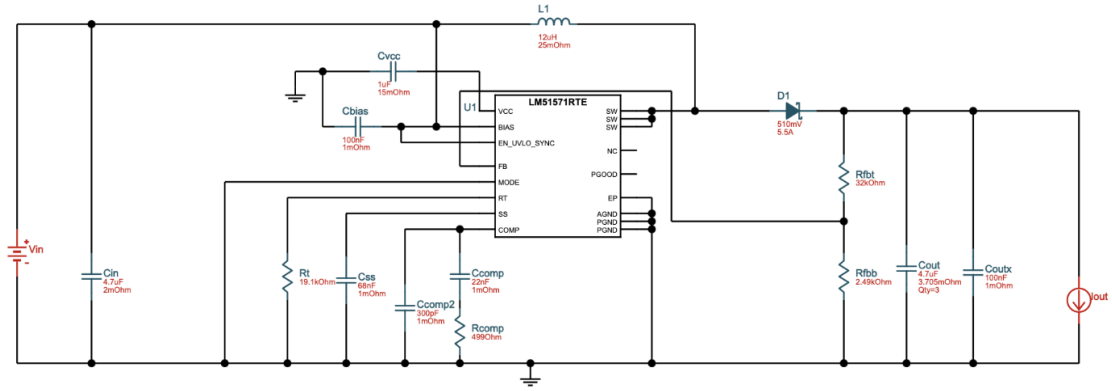

Figure 39: Webench Circuit Design

6.7.1.1 Battery

It is important to size the battery with enough capacity, that it could keep running for longer than what it expected. One of the main parameters is the length at which the system will be in use. For our system, each session will last around ten minutes, leaving enough room for error when it comes to the battery

charging and discharging. It is important to understand how much power the system is estimated to consume, this value is 39.34 W which is mainly added from M1 and M2. Knowing the total power conceded by the system, the capacity of the system can be calculated and compared to see if we have enough energy. Another key component is the discharge time. Our system will be tested outside, where the environment can affect certain components. The battery is one of those components that our group has to pay attention to. At this moment, our group has decided to power the system with an Eco-worth Lithium iron battery, which is rated at 12 volts, with 10 Ah. Its temperature ranges from 0 - 55 Celsius, and for discharge temperatures ranges from -20 - 55 Celcius.

As we made a decision for a battery of the right size, **Figure 40** illustrates a schematic where a 12 volt battery energizes each component. Our system has two motors, The schematic illustrates the connections. As it can be seen, after the microcontroller is powered by the battery, the stepper driver A4988 is connected to the microcontroller at one end, and at the other end is connected to the coils of the motor. Another component from the figure, is DC-to-DC converters which will scale down the voltage coming from the battery and allow the voltage to be more managle. One of the motors, M1 as can be seen below, takes as an input 3.0 volts, from the DC-to-DC converter output. This converter described in earlier sections steps down the battery voltage three times its size. For the other motor M2, a separate DC-to-DC converter is displayed, where it will scale down the battery's voltage four times its own. As our group gathered all the components and decided on what implementation of electronics to go about, the PCB design is explained and illustrated further in the report.

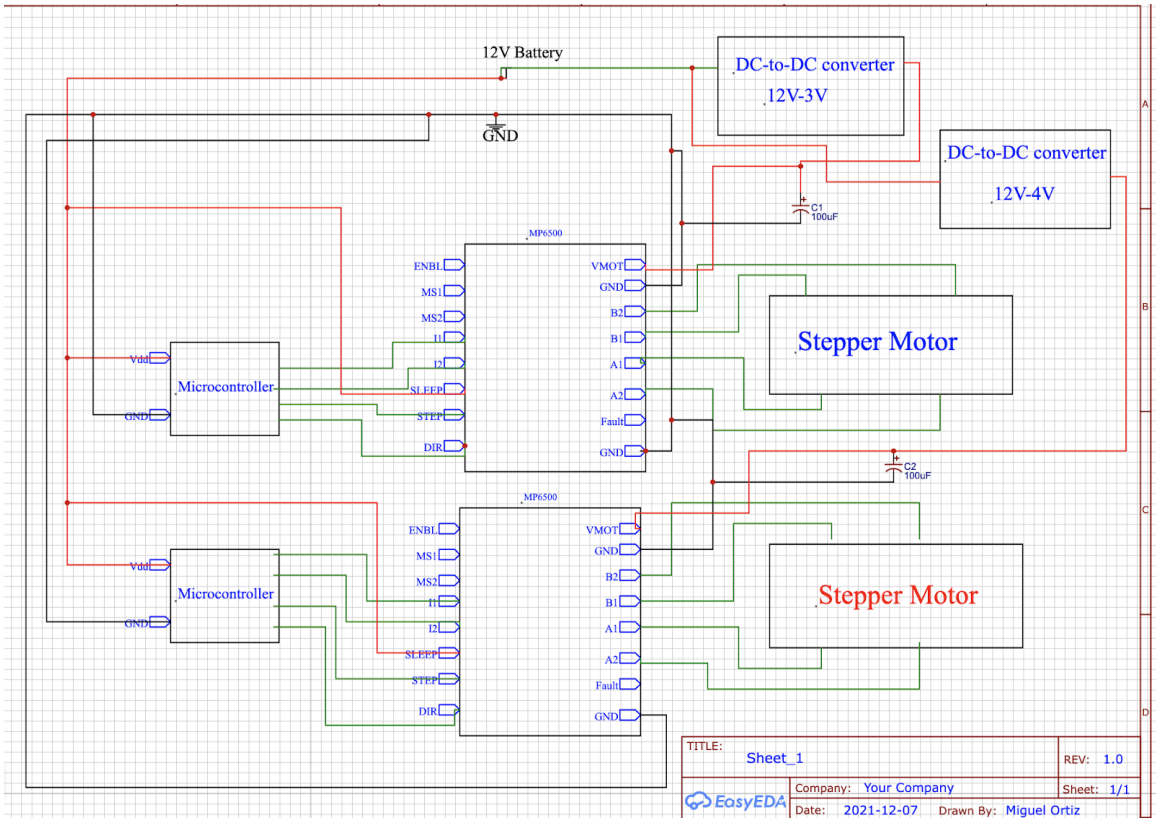

Figure 40: Schematic

On the table below, we have listed batteries which were researched for the project. We can see that the list consists of 12 volts, but the capacity of each battery varies. The capacity is important to note, because our motors will require a constant amount of current in order to work without any interruption or failures.

Name	Type	Voltage	Capacity(ah)	Power (w)
ExpertPower	Sealed lead acid	12	7	84
MightyWax	AGM Deep Cycle	12	12	144
Weize	SLA AGM	12	18	216
Weize	Lead Acid	12	20	240
Weize	Lead Acid	12	100	1200
Lossigy	Lithium ion	12	8	96
Miady	Lithium ion phosphate	12	6	72
ECO-Worthy	Lithium ion phosphate	12	20	240

Table 14: Battery Comparison

6.7.2 Motor Consumption

As mentioned before, the system creates motion utilizing two different motors. We implemented stepper motors to create these motions. Looking independently to each motor we will be able to make a decision for how much power each motor requires from the battery. As we can see one motor implements a linear motion on the same axis to one of the two lenses requiring motion. The other motor used to create movement to our system is shown this motor allows movement to the second lens, also on the same axis. Each motor will move independently and carry the weight of the lens, mount and platform.

6.7.4 Filter System Motion Motors

Inside the 'arm' of our system, as detailed in previous sections a filter subsystem is implemented. Careful calculations were conducted to describe the lengths each non-static filter will move, inside the 'arm'. As described earlier, the filters will be light weight (ranges of 50 to 100 grams). With this in mind, a high torque is not the main priority to implement for this subsystem, since the weight of the filters is low. An important characteristic for these two motors is the weight of the motors themselves, by searching for stepper motors of around 140 to 180 grams.

Below, the table provides a few of the options that are out in the market. As it can be seen there are a range of stepper motors with a wide variety of torque created, as well as weight of each individual motor. Two servo motors are also shown in the table below, the table shows that servo motors can produce a large torque within one motor, which also gives the group an option to utilize both motors in the system. A stepper motor was a greater option for our system's motion since the motors were found at a more affordable price. At the time of designing servon motors were not chosen, due to budget.

Name	Type	Torque (Oz.in)	Voltage	Current (Amp)	Weight(g)	Dimensions(mm)
Nema 17	Stepper	18.4	2.9	1.4	180	42x42x25
Nema 17	Stepper	22.6	3.7	2.0	140	42x42x20
Nema 17	Stepper	63.74	13.8	3.0	280	42x42x39
LD-20Mg Digital	Servo	277.6	7.4	1	66	54.5x20x47.5
Deego-FPV	Servo	11.65	7.2	1.0	55	40.7x19.7x42.9

Table 15: Motor Motion Comparison

6.7.5 Torque

For our system, we understand that the correct torque will be calculated from effects of both gravitational force and angular acceleration. A point to consider is that commonly the torque needed for gravitational force is notably higher than the torque needed to opposite angular acceleration. This gives us guidance to look into the design of our case, which inside holds the filter system including rails, a motor and other electronic connection between components. The overall system's weight and the length between the end of the filter and the axis of rotation, will dictate the size of the motor needed for the up/down movement. The next step for sizing the motors implemented for our system is calculating Torque. Torque will be calculated into two, load torque and acceleration torque. Load torque is the energy used to hold our system, or the load. The load held by the load torque can be split into two categories, gravitational and frictional loads. Acceleration torque only exists when there is a need for our system's body to move from a stationary position, or stop the body to a stationary position. Acceleration torque is very dependent on the moment of inertia. For the motors M1 and M2, the acceleration torque was manageable. Acceleration will be easier to achieve, having to move significantly lighter loads than M1 and M2. The following will calculate both load and acceleration torque, it will also illustrate the system with each torque being clearly labeled.

6.7.6 Load Torque

Looking into motors M1 and M2, we focused on the filtering subsystem, constructed by a linear rail connected to a platform, which slides back and forth in a linear motion. Before calculating the load torque, each external force was recognized. **Figure 41** illustrates the two forces that result in load torque, gravitational and frictional force. Illustrated in the image, the vertical arrows show the gravitational force acting on the body of the system, and the rail creating friction. The arrows going in a horizontal direction depicts the frictional force acting on the platform and the load it is carrying. Gravitational force is calculated by utilizing the formula used earlier, which multiplies the mass of the load at around 5 grams with the gravitational acceleration of 9.8 m/s^2. This results in a gravitational force of 0.049 N, which is the body of the system pushing against the platform and rail. Frictional force must be calculated for this type of motion, The rail used to allow the movements of both lenses is a V-slot aluminum rail. Also, a platform which is designed to slide within the rail contains wheels allowing rolling, it was key to analyze how much friction the platform will add to the motion.

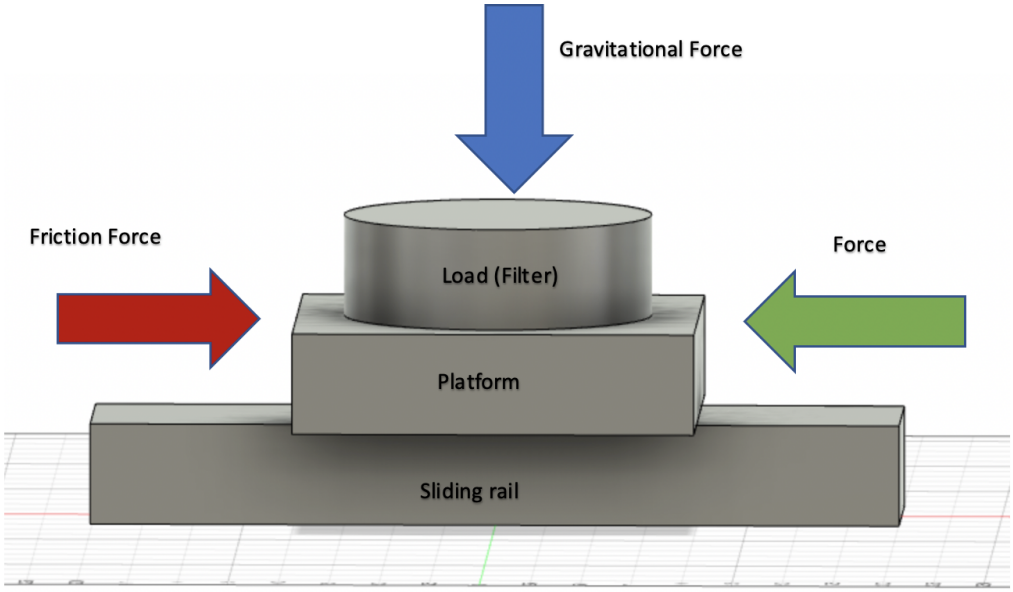

Figure 41: Gravitational and friction force acting on the load and rail

Force (N)	Diameter (m)	Efficiency	Gear ratio	Load Torque (Nm)
0.098	0.0381	0.85	10	2.2×10^{-4}
0.098	0.0508	0.85	5	5.86×10^{-4}
0.098	0.0635	0.85	5	7.32×10^{-4}

Table 16: Load torque with different gear diameter and ratios

A timing belt along with a gear reduction strategy was utilized, in order to create motion for the two filters along the rail. Having that in mind, use of the load torque formula mentioned is as follows;

$$T_L = (F * D)/(2 * \eta * i),$$

Where F is the force needed move the load, D is the pulley diameter, η is the efficiency of the system, and i is the gear ratio. We can estimate a set of diameters and gear ratios in order to obtain the load torque. The following formula is also utilize, in order to find the force that acting on the filters;

$$F = F_{fric} + F_{grav},$$

Where F_{fric} is the friction force acting on the platform when sliding, and F_{grav} is the gravitational force acting vertically on the rectangular casign, which was

calculated above. Table 12 calculates a load torque varying gear dimension, and gear ratio. From the table it can be seen that as the diameter of the output gear increases, the load torque also increases. On the other side, it is also possible to design a gear reduction system, which will result in a gear ratio large enough that will help reduce the overall force needed to move the rectangular casing.

6.7.7 Acceleration Torque

Now we focus on the torque which is responsible to accelerate and decelerate a body of mass. In our system we have two moving parts, where acceleration torque is needed. As mentioned before acceleration torque is linearly affected by the moment of inertia given by the mass needed to be moved. For our system, the moment of inertia for the lenses inside the was calculated earlier. Having this results, acceleration torque is calculated by using the formula described in previous sections which equals,

$$T_a = J * A,$$

Where J is the moment of inertia, body of mass, and A is the acceleration rate to start moving the body. Motors M1 and M2, produces a torque large enough that will cover the acceleration torque, when the filters need to be adjusted. Below, table 5.1.3 calculates the acceleration torque with varying moment of inertia, and acceleration rates. The table shows that by reducing the moment of inertia, acceleration torque can be affected linearly, but as our system extends to house the filtering system, it will be very difficult to adjust the dimensions of the overall body of the system. Another option to reduce the acceleration torque is to reduce the acceleration rate, which will be affected when choosing the right implementation for the gear reduction system. The acceleration and speed graph for our system. It visually labels the acceleration rate increasing at a time (s), till it reaches constant speed, and finally decelerates till it gets to a speed of zero.

Moment of inertia	Acceleration rate	Acceleration Torque (Nm)
0.033	0.209	0.0069
0.033	0.109	0.0036
0.0008	0.076	6.08×10^{-5}
0.0008	0.096	7.68×10^{-5}

Table 17: Acceleration torque from inertia and acceleration rate

6.8 Gear reduction and motor selection

After calculating all different types of torques for our system, the required torque is calculated by using the formula mentioned in earlier sections which is;

$$T_M = (T_L + T_a) \times S_f$$

Where, T_L is the load torque, T_a is the acceleration torque found earlier, and S_f is the safety factor which will be defined as 0.85. For the filtering system, as mentioned before in the load torque section, we use the formula where we double the gravitational force acting on each filter. Also, a diameter of 0.0382 meter for the output gear, along with an efficiency of 85% and designing a pair of gears which give a gear ratio of 5. Plugging this into the equation above, the load torque for motors M1 and M2 is 2.20×10^{-4} Nm. Now combining the load torque with acceleration torque of 6.064×10^{-5} Nm and a safety factor of 0.85, results in a required torque of 1.33×10^{-8} Nm.

Figures 42a and **42b** below, shows the prototype of the four gears which are used to increase the torque given to the system in order to change positions. The figure illustrates two driver gears and two driven or output gears. The driver gear will have an estimate of eight teeth, and will drive power to two driven gears which have a diameter of 1.5 inches or 0.0381 meters. For motors M1 and M2, not much torque was required, since the dimensions and weights of the loads inside the filtering system are small. It is important to realize that a gear reduction in the filtering subsystem helped our group to purchase smaller and lighter motors. Our system can benefit from implementing small motors for the filtering system, since the overall system decreases in weight. As we talk about torque and gear reduction, it is important to have an understanding of the motor's speed effects over its torque.

Illustrating the effects of the increase of speed to the torque, which are available on the motors datasheet. We could see that as we increase the speed, the motor starts to lose torque. This highlights the importance of keeping a balance over speed and torque when selecting the motor. The table also gives different implementations for the gear reduction system. Adjust the diameter of a gear, or changing the gear ratio affects the load torque needed for the motor to overcome

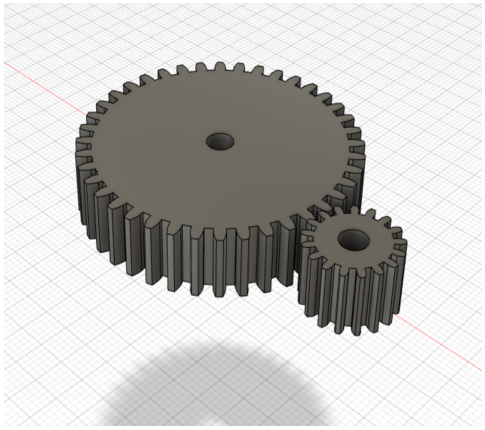

Figure 42a: Gear reduction system using Spur gears

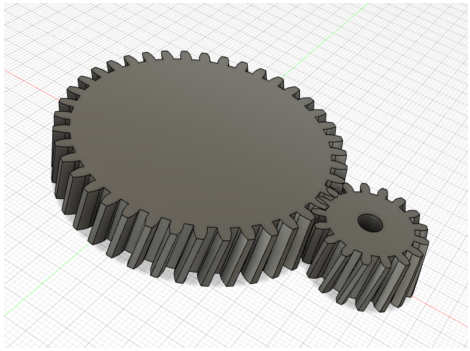

Figure 42b: Gear reduction system using Double helical gears

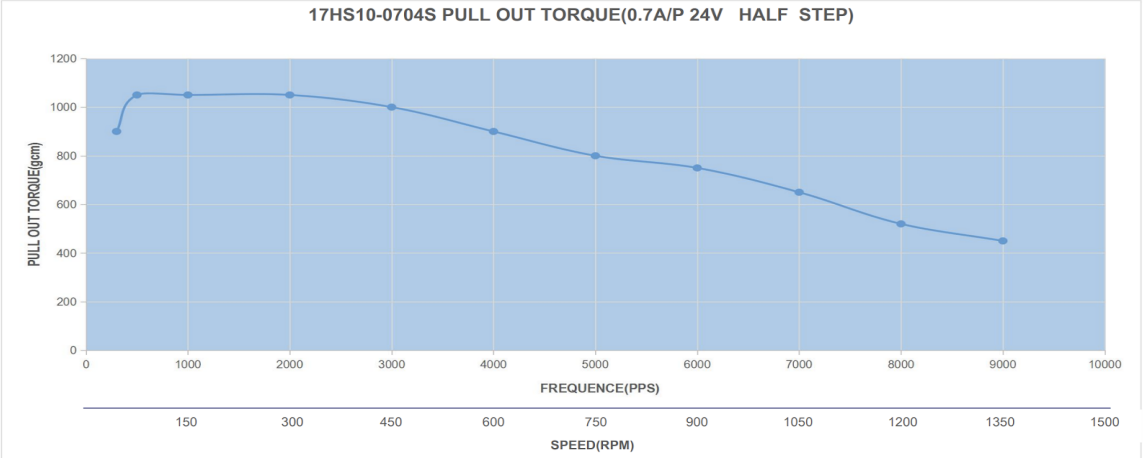

Figure 43: Effect of speed over torque for Nema 17 (18.4 oz. in)

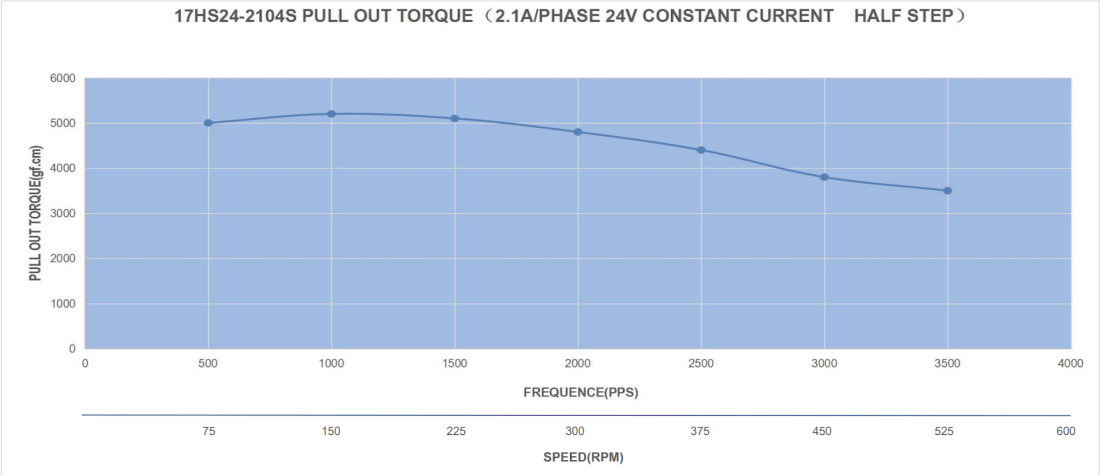

Figure 44: Effect of speed over torque for Nema 17 (92 oz. in)

6.9 Sliding Rail

In order to provide a platform that provides movement to the filters, two v slot rails are implemented into the system. There are a total of twop filters. Two of these filters contain motion, and there's one stationary. Each filter's motor will be sized in order to consume the least power, add the least weight to the system and be as precise as possible. The filters, by having a light weight it is very promising to find two motors which will allow us to find small size motors. As mentioned previously, the sliding rail is 16 cm long, having this in mind, the motors are sized correctly in order to give the right amount of power and provide enough torque to move the filters smoothly through the sliding rail. What makes our system unique from another laser profiler besides being controlled electronically, is the fact that a filter system is implemented in order to capture the refracted laser beam from the target accurately. From the engineering investigation that our group conducted, the distance for the extension starting from the lens of the camera will be around 16 cm. Four lightweight filters compose the filter system, which will sit on a two rail sliding rail. **Figure 45** below, shows the filter system, here it illustrates the two rails on each side of the system. It can be seen the distance each lens has to change positions, where it can also be seen how each lens is mounted to the platform which is attached to the rail.

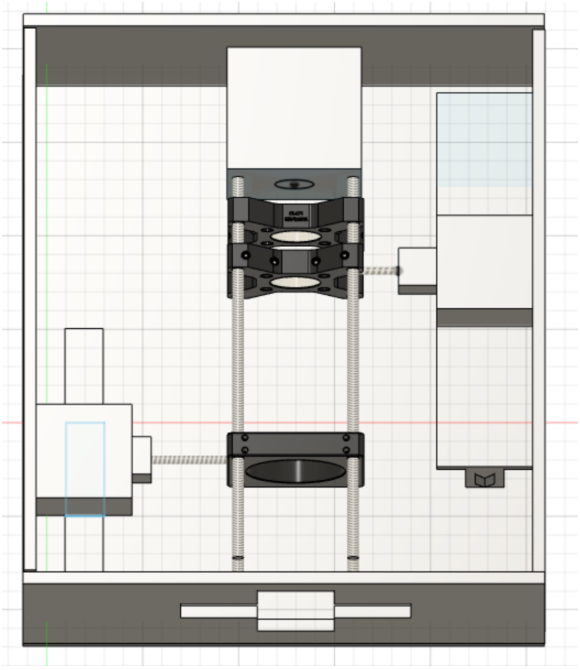

Figure 45: Lens Sliding Rail

From the figure above, four metall rods are used in order to allow each of the lenses and the camera lens to be aligned. This gives the freedom for the motors to just pull the lenses back and forth without having to worry about misalignment. For future reference, better mounting of the rods, would allow for better precision and less errors.

6.9 System Alignment

Precise alignment is key for the system, in order to avoid the laser beam to be distorted by hitting the custom filter composed of varying lenses. In a case of misalignment, the laser beam would hit each lens at a different angle where if not aligned correctly, will create disturbances to the beam's response to the line of lenses. The filter system consists of a camera sharing the same axis with three lenses. A lens will be mounted in front of the camera. The remaining two lenses can move linearly in order to adjust the zoom and quality of the image. Detail to distances between all components that compose the filter system is key for the project, to obtain cleaner data and reduce weight consuming less power.

A 2040 V-slot rail is used in this project, in order to allow linear moment to each of the lenses that make up the filter. The rails' height is 40 mm, with a width of 20 mm. The lenses farthest distance between each other is 10 mm. In order to

aid the alignment and reduce the most movement for each of the lenses, 6 mm of diameter and 8 mm of length rods are mounted in order to guide the lens cage. Taking into consideration the space taken by the rails, motors and the proper alignment for the lenses. The box will have a length of 30 cm, width of 27 cm and a height of 12 cm. This gives enough spacing, as well as keeping the load weight to a minimum.

6.9.1 Top View

The distance between components that compose the filter system are very precise, where the least space is utilized in order to decrease weight of the overall system. **Figure 46** gives a view from the top of the box, labeling the dimensions where each component is layed out. A Nema 17 motor with a horizontal length of 5.5 cm, and vertical length of 5.0 cm is attached at the bottom left corner. Aligned with the motor, the V-slot rail takes a horizontal space of 2.0 cm, and a vertical space of 16.0 cm. Attached to the rail, is a platform with dimensions of 5 cm both horizontal and vertical. An extension to the platform was designed and 3D printed. The extension is replicated the same size as the horizontal and vertical dimensions of the platform, but it extends 4cm of the z axis or width. The platform extension has an extrusion on its side facing the lens. This extrusion extends as a square of 2 cm on each side. The extension printed coming away from the rail connects to the lens cage creating a distance of 7.03 cm from the midpoint of the cage holding the lens, and the edge of the rail closest to the lens. At the other end of the v-slot rail, the driven gear is mounted on a designed 3D printed mount, with dimensions of 2x4x6 mm.

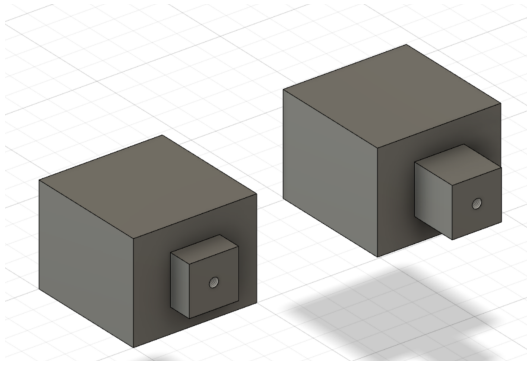

Figure 46: Designed and 3D printed lenses mounts

6.9.2 Front

The alignment in the point of view from the perspective of the camera is very important for the camera's lens to align with the midpoint of the three lenses extending away from it. The goal for the system is to be precise enough where the laser beam coming into the camera is as close to perpendicular to the plane of the camera's lens. **Figure 47** shows the alignment sketch from the front panel.

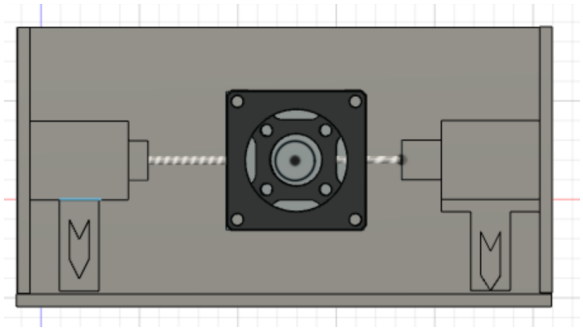

Figure 47: Front View alignment

6.10 Power distribution

The power provided to the project is produced by two 12-volt Lithium Iron Phosphate batteries, made by ECO-WORTHY. Each battery is rated at 10 Amp-hours and has an overall power of 120 watt-hours. At the end of this section,The final product from all the components connected to the designed PCB, allowing the connections for the motors used in the project.

6.10.1 Voltage Regulator

As the 12-volt battery is powering the project, a regulator is utilized to step down from 12 to 5 volts, in order to provide the correct voltage to some of the components. This project implements the LD1085V50, providing the correct voltage to the motor, drivers, processors, raspberry pie, and Lux meter.

6.10.2 Motors

One battery provides power for the four Nema 17 motors. Two of the motors are attached to the lenses allowing the filter system to adjust distances between lenses. Two other motors will provide the pan and tilt motion that allows the outside box to adjust its distance vertically and horizontally. The current limit for the motors is of a max current of 1.5 Amps, and minimum current of 0.4 Amps required.

6.10.3 Drivers

Four A4988 drivers are also powered by the battery. The max voltage that the driver will allow is 5.5 volts. With this in mind, a LD1085V50 **Figure 48** voltage regulator in order to step down the voltage from 12 volts to 5 volts.

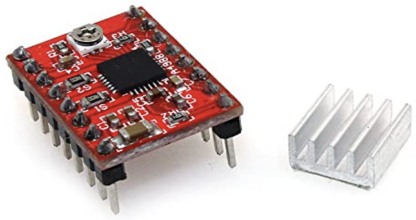

Figure 48: A4988 Stepper driver

6.10.4 Processor

The same battery that powers the motors and the drive, also powers the ATMEGA4809. With a maximum of 5.5, and a minimum voltage of 1.8 volts, the regulator will provide stability to the power coming into the microprocessor, avoiding overload and any burning of components.

6.10.5 Raspberry Pi

The second battery powers the raspberry pi, which allows the laser beam tracking software to run. In order for the raspberry pi to run with the battery a LD1085V50 regulator connects the battery to the microcontroller, taking 12 volts coming from the battery as input, and with an output of 5 volts to the microcontroller.

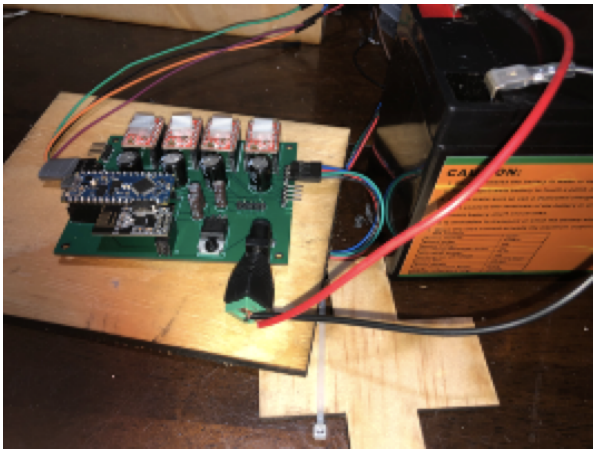

Figure 49: PCB holding connection for motors

6.10.6 Lux Meter

The Lux meter circuit measures the amount of light going into the camera lens besides the laser beam, demonstrating the amount of light pollution at the point where the laser beam is measured. In order for the circuit to run, a LD1085V50 is connected with its input to the battery and the output to the input of the Lux meter circuit.

6.11 Mechanics

The project implements a zoom mechanism designed by our Optics and Photonics group members. The lenses move individually while adjusting their position. This allows the image received by the camera to be able to zoom in and out from the target reflecting the laser beam.

6.11.1 Pulley System

The system transfers rotational motion, coming from the two separate motors, to linear motion allowing the lenses to move along the same axis directed by the rail. Along the 13 cm rail, at the end a driven gear is mounted. Using a CAD software tool, a (BlahXBlah) mount was designed and 3D printed for the driven gear. A 5 cm x 5 cm platform is then attached to a belt with a 5 mm width belt, with the proper tension, since slack in the belt could cause inaccurate position for each lens. The inside of the project, the two rails are separated by a distance of 8 cm. The two lenses' midpoint meet in the middle measured from the rails. Two customized mounts were designed using the CAD software tool in order to get the right dimensions, seeing that the cases where each lens is attached have different dimensions. **Figure 50**, illustrates the time belt attached to the motor shaft, with enough tension to avoid stalling.

Figure 50: Pulley connected to Motor Shaft

6.10 Camera Control Setup

The camera control setup will consist of the following systems:

- Lens Control System
- Camera Position Adjustment System

To make things more concise, the lens control system and the camera position adjustment system will be reduced to the Camera Adjustment System (CAS). The CAS will operate with 3 motors, 1 adjusting the lens focus and 2 adjusting the direction the camera is pointing along the horizontal and vertical axes. To operate the set up an MCU will be needed locally to process commands from the control device. There will also need to be a means for the input of the camera to be sent out to the control device that will allow for the control device operator to properly determine what adjustments need to be made and to allow for analysis of the laser beam profile. All these things also need to fit in a device that is at most $4ft^3$ and handle operation in a weatherproofed container and handle the intense Florida heat.

6.11 Control Module Selection

Many cheap and available RF control modules can be used for wireless communications between multiple microcontrollers for extended ranges, with different configurations having maximum ranges varying from 100 meters to 1100 meters.

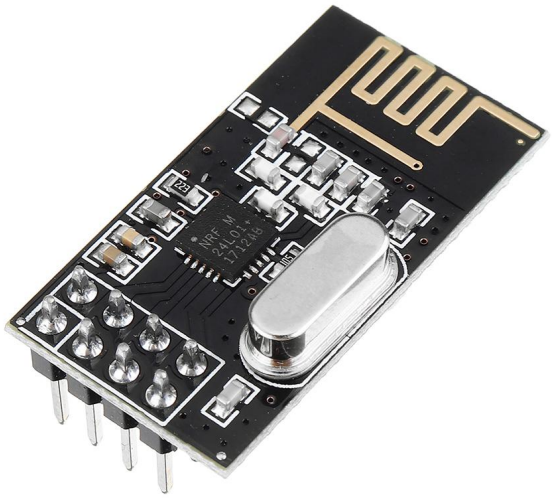

Figure 51: nRF24L01+ TX/RXmodule

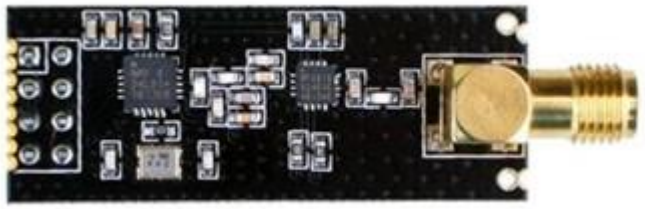

Figure 52: nRF24L01+ PA/LNA TX/RX module

The module used for ours is the nRF24L01+, a RF receiver module developed by Nordic Semiconductor. The module is a popular choice for longer range wireless communications between microcontrollers for its extensive range and cost as low as less than $4 for the module with an included antenna for longer range communications. The device works as a SPI slave device for the MCU. We use the non-long-range version for our prototype as during testing it was found to be easier to establish communications at the range used for our testing and demonstration, although the longer range nRF24L01+ PA/LNA module can allow for ranges measuring above 1 km with optimization.

Frequency Range	2.4 GHz ISM band
Air Data Rates	250kbps, 1Mbps, 2Mbps
Maximum Output Power	0dBm
Supply Range	1.9 - 3.6V
Standby Mode Current (Minimum Operating Current)	26μA
Maximum Operating Current	13.5mA
Input tolerance	5V
Operating Temperature	-40°C - 85°C
Communication Range	~ 100m (> 800m for LA/PNA version)
Serial Interface	SPI
Modulation	GFSK

Table 18: Specifications of Nordic Semiconductor ASA nRF24L01+ (Last Minute Engineers, 2020), (Nordic Semiconductor ASA, 2008)

6.12 Single Board Computer

The device that receives the video feed from the camera allows for the operator to view the adjustments being made and the laser profile over time through tracking of the laser beam. This portion of the project had a lot of potential customization and still has plenty of room for further development, such as means to auto-track the beam in real-time and automatically identify certain characteristics of the beam. The main considerations for this project were simply

to 1) receive the imaging data of the laser beam profile from 3 meters away to track the beam position and determine its characteristics, and 2) to send signals to the Camera Adjustment System to make the necessary adjustments to best attain the necessary imaging data. For this device the following options were considered: Option 1) use separate controller and display devices used in conjunction to perform the necessary operations, Option 2) utilize some already existing device such as tablet and develop software to operate the CAS, or Option 3) utilize a single board computer (SBC) to develop a customized device with the necessary communications, control peripherals, and software.

Option 1 is the absolute bare minimum for the goals specified for this project and is likely one of the cheaper possible solutions but doesn't necessarily impress anyone and can be seen as a weak work around for achieving the basic requirements and doesn't provide much in the way of future development for this project should the need arise.

Option 2 is a possibly less time-consuming and cheaper option as the hardware of the device is already selected. There is also the possibility of already existing applications for the device that can be used for some of the more advanced features that would need to be developed for the device in later stretch goals. The downsides however are that the development may be limited depending on the operating system of the device, as software developed for a device running on Android is incompatible with a device running iOS. There are also different hurdles for application development depending on which operating system is developed for, such as which programs can be used for development and testing, curation (especially if developing for iOS and needing to release the app publicly), and limitations on what hardware can be used for development in the first place (iOS development can only be done using hardware using MacOS). There is also no guarantee that the hardware will have all the necessary capabilities for the project without having to invest in a more extensive MCU for the CAS, leading to other issues on that end. Regarding the project developing a long-term solution, this option may lead to issues with the application over time, as updates to the OS software of the device and changes to newer devices may at some point lead to compatibility issues with the older application software. This would require the software to be continuously updated, lest development become dormant, and the project become defunct well before its time due to planned obsolescence.

Moving onto Option 3, although this would require more development on the hardware end, covering the base requirements the software development may not be as extensive as Option 2. This option would also allow for more customization for the device to cover all the necessary specifications and depending on what hardware is used can allow for more extensive development in the future depending on if the client wants it. If components are chosen carefully the device may come out to be relatively cheap to put together and depending on the compatibility of the components, they may be relatively simple to implement in software. As this device would not be varied like in Option 2, the issues of having to constantly update the software to ensure compatibility of the device would be as much of an issue. Option 3 seemed to be the best option,

however for the prototype implementation we ended up going with Option 1, as this allows for solving the issue of movement commands and the real time video analysis separately, as well as holding off on dealing with the issue of figuring out video transmission for this project.

For the implementation of the control device, there are various options for the SBC depending on a variety of factors including:

- having the capability to run a video analysis program that will automatically save the processed video when finished
- having a means to iterate further for automated analysis of the beam profile
- being able to do all of that still run well

6.12.1 Single Board Computer Options

For the SBC there exist various options at equally varied price ranges. The ones considered below were selected due to aspects such as price to performance, size, and power considerations. These boards also had their own additional draws that will make their use in the project easier to implement.

6.12.1.1 NVIDIA Jetson Nano

Figure 53: NVIDIA Jetson Nano (NVIDIA Corporation, 2021)

The Jetson Nano Development Kit from NVIDIA Corporation is an SBC that is designed for use in Artificial Intelligence applications, having “the performance and capabilities needed to run modern AI workloads” according to the User Guide (ssheshadri, 2019). This board utilizes a GPU that compared to other SBCs in this price range ($60-$118.75 depending on model) is much more powerful, making the calculations necessary in AI based operations and machine learning quicker.

The specs for the board are displayed in the table below:

Architecture	Quad-core 64-bit ARM
Clock	1.43 GHz
GPU	128-core NVIDIA Maxwell GPU
Memory	4 GB
Display	HDMI/DisplayPort
GPIO Pins	28
UART	2
I2C	6
SPI	2
I/O	4x USB3.0, USB 2.0 Micro-B
Power Requirement	5V, 2A
Temperature Tolerance	-25-80°C

Table 19: Board Specs

6.12.1.2 Raspberry Pi 4 Model B

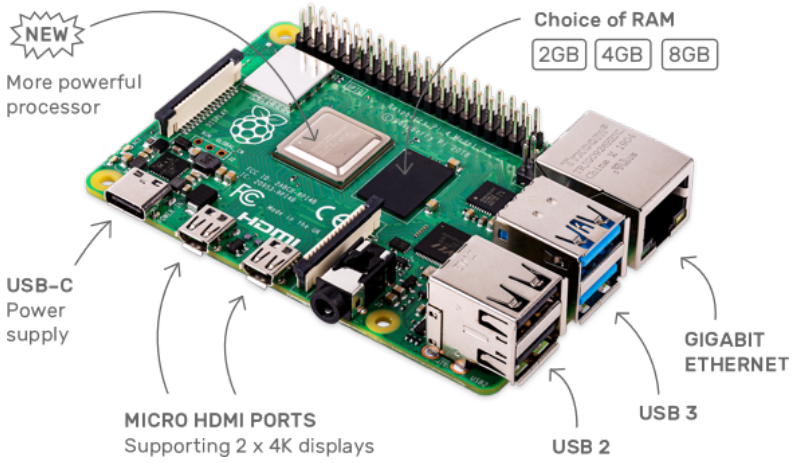

Figure 54: Promotional diagram of the Raspberry Pi 4 (Raspberry Pi Trading Ltd., 2021)

The Raspberry Pi 4 Model B (from this point just referred to as the Raspberry Pi 4) is the newest and most powerful of the popular lineup of SBCs

developed by Raspberry Pi Trading Ltd. Like the board's predecessors this board has plenty of power to run the expected applications while remaining relatively inexpensive with the low end model being $35 and the highest end at $75. The specifications of the device are as follows:

Architecture	Quad-core 64-bit ARM
Clock	1.5GHz
GPU	VideoCore VI 3D Graphics
Memory Options	2, 4, 8 GB
Display	2 micro-HDMI
GPIO Pins	28
UART	6
I2C	6
SPI	5
I/O	2xUSB2, 2xUSB3
Power Requirement	5V, 3A
Temperature Tolerance	0-50°C (do not exceed 85°C)

Table 20: Raspberry Pi 4 Model B specifications (Raspberry Pi Trading Ltd., 2019)

As the specifications show this SBC should have adequate processing power to run the required applications, although also requiring a considerable amount of power. As the control device is not the device in this project being left out outside in the elements the middling temperature tolerance is not a deal breaker and is expected given the possible applications of the SBC being a miniature desktop computer. Along with the prior computers in this series this computer has extensive community support, especially when it comes to customization for the interface.

6.12.1.3 Single Board Computer Comparison

In comparing hardware, the boards are evenly matched, each having the same 40 pin-out set up (allowing interoperability with components designed for the Raspberry Pi to work with the Jetson Nano), similar specs regarding I/O and in power requirements. The Raspberry Pi has the better CPU, being able to run at a higher clock speed than the Jetson Nano, as well as having the option for an 8GB memory model whereas the Jetson maxes at a 4 GB model. The Jetson

Nano is also much larger in comparison, with the board dimensions for each being 3.9 x 3.1 x 1.1 inches for the Nano and 3.74 x 2.76 x 1.1 inches for the Raspberry Pi. This all comes with the top spec versions of each board coming out to $75 for the Raspberry Pi 4B 8GB and $99 for the 4 GB Jetsun Nano. What the Jetson Nano does have going for it is its much more powerful GPU as highlighted in Stephen Cass's article for IEEE Spectrum (2021) that makes the board much better suited for AI and ML applications. That proficiency in AI and ML makes the board a very compelling option for this project.

6.12.1.4 Single Board Computer Selection

The selection for the SBC was ultimately the Raspberry Pi 4B 8 GB. This selection was made as a result of issues regarding availability for both boards, especially at MSRP. Neither was available for purchase at the beginning of the project testing, with the Raspberry Pi not being available until mid-February according to all vendors and the Jetson Nano not having a set date for restock. As a result, the choice was whatever board was available on hand or could be attained easily second-hand. Therefore, the Raspberry Pi 4B 8GB that one of the members of the team had on hand was the resulting choice.

6.13 Controller

In the initial designs it was believed that the SBC would be used for the RF controller at the same time as doing object detection and tracking. As it was found that there would be issues in implementing the video transmission needed to allow for that, it was then determined that the controller could simply be another Arduino controlled device that could handle the user input and transmit them to the receiving Arduino in the camera adjustment device. The controller needed a means for the user to simply and easily adjust the camera's view, the process for determining such is described in the prototyping section.

6.14 Software

For software there are two aspects that need to be coded for: 1) the operation of the motors for the adjustment of the camera, and 2) the tracking of the beam profile. For the motor operation a microcontroller will be used to operate the motors themselves and a separate SBC will be utilized to transmit directions for the microcontroller. For the beam profile tracking the same SBC

from before will also be utilized to perform analysis on the beam profile based on video transmitted back to it from the camera

6.14.1 Development Tools

For the development of software there are necessary tools to aid in the process of development in order to make development simpler and to not lose progress. As such, integrated development environments were utilized for writing and testing code.

6.14.1.1 IDE and Text Editor

Programming for the Arduino board used for the microcontroller operating the motors was handled through the Arduino IDE. The Arduino IDE is an open-source IDE that is the official software developed by Arduino.cc for code composition for the Arduino devices, which have native support with the software. The IDE is notable for its ease of use for those who have no prior knowledge in development. This user friendliness is aided by the extensive free libraries available for Arduino devices. This IDE also contains the necessary tools to program for other microcontrollers. This made this a prime option for development as the software developed initially for Arduino boards can later be used in custom boards utilizing the same controller.

Software development using the Arduino IDE as described before was simple for development. This allowed for development using files referred to as *sketches* that can be written in a C/C++ derived Arduino language. Given the team member in charge of the programming of the microcontroller used in this project has plenty of experience in C programming this was quite convenient. The newcomer friendliness in this IDE is shown in the sample code that exists for various supported Arduino boards, making this welcoming for those who have never coded for Arduino, much less coded ever. As Arduino was not something that the team member in charge of coding was completely familiar with, this was especially helpful in determining the particulars of coding for Arduiono devices. Between the built-in sample code and the code available for reference from various projects performing similar applications from the extensive community around Arduino the software development for the microcontroller will be a much less daunting task.

For programming the SBC used to perform the tracking of the laser beam profile an adequate text editor for writing and evaluating the Python code was needed. As such Visual Studio Code, or VSCode for short, was used. VSCode is a text editor developed by Microsoft that has features such as debugging, syntax highlighting, code completion, and source control support through Git. VSCode is designed to make coding more streamlined and configurable for the use of the developer through extensive customization and numerous available extensions.

6.14.2 Camera Adjustment System

The camera adjustment system takes commands from the controller and executes the movements for the motors to adjust the view of the camera for purposes of tracking the laser beam profile. The microcontroller operating this system was programmed to perform the following:

- Initialize the setup of the camera adjustment system
- Receive transmissions from the transceiver
- Execute the commands broadcast to the device
- Wait for further transmission

The code for the microcontroller handling the camera adjustments utilizes libraries for making the handling of the nRF24L01+ module and the motor controls simpler. The libraries used are the open source RF24 library available on GitHub and the AccelStepper library by Mike McCauley. Both of these libraries are under a GNU General Purpose License, which the use in this project falls under.

6.14.3 Control Device

The control device contains another microcontroller and the necessary transmission modules as well as the controller interface.

6.14.3.1 RF Controller

For the RF controller that communicates with the camera adjustment system to dictate the commands input by the user the following functions are programmed for:

- Initialize the setup of the controller and the RF communication system
- Establish a connection to the camera adjustment system
- Accept inputs from the user
- Transmit signals to the camera adjustment system
- Wait for further inputs from the user

The code for the microcontroller handling the controller also uses the RF24 library described in the camera adjustment system software section.

6.14.3.2 Object Tracking System

For the tracking system the SBC uses the OpenCV library for Python, “an open source computer vision and machine learning software library… built to provide a common infrastructure for computer vision applications” (OpenCV Team, 2020). The library implements object detection by trying to find HAAR features in an image, HAAR features being “rectangular features with regions of bright and dark pixels” (Kumar, 2020).Paraphrasing from Kumar’s article, the algorithm utilizes the calculated pixel difference between darker regions of an image from the lighter regions to identify certain features it is trained to associate with a certain object. The individual features it singles out are referred to as “weak figures,” and with a determined sum of these figures within a certain region in a particular configuration the algorithm can identify some given object. This allowed us to use the library to use the SBC to identify the beam profile from the video feed from the camera usd and to track the laser beam’s movement along the diffused surface.

The program used for object detection is an alteration on an existing free-to-use code from Brad Montgomery, the original version of which implements a simple tracking algorithm that is able to track a red laser pointer dot. This works by taking each frame from a video input and filtering the frame by the HSV values of each of the pixels in the frame. The program goes through the frame and determines where in the given frame there are pixels that fall within a certain threshold of HSV values and filters out the pixels that do not fall within the parameters. After the filtering there should be just the object that is intended to be tracked. The program would then determine the center point of the object it found and overlay the result on the original frame, as well as adding a line to the centerline location of the object as it was detected in the last frame, with all the prior lines also being overlaid.

For the program we used we altered the HSV value threshold to, instead of filtering everything except a strong red light, filtered everything aside from a strong green light. The program used in the project also has the addition of saving the processed video as a .avi file, allowing operators to review the laser tracking for later analysis.

6.15 Prototyping

To sort out what remaining design considerations exist there was a process of prototyping. The prototypes aided in determining what was necessary in the end design that was used in the demonstration. It also helped in determining if there were any major design considerations that needed to be redone if some parts proved to be ineffective or unreliable.

6.15.1 Controller Interface

For the design of the main controller for the camera adjustment system there was a process of prototyping to determine what works best for functionality and in simplifying design. The controller interface needed to perform the adjustments for the camera by having the transceiver's MCU communicating with the receiver's MCU to operate the motors adjusting the camera's magnification. We initially wanted the interface to have a means to see what the camera is viewing to have the camera positioned correctly and allow for a means to see how the SBC is tracking. Given the short range of the prototype it was determined that instead of determining the means to set up video transmission we could simply have it hooked up for displaying the video through wired means that are separate from the controller itself that would allow the user to see what adjustments are done.

There was still a need to implement the nRF24L01+ to allow for the "Remotely Controlled" aspect of the project to work, and therefore weren't negotiable in whether they are implemented unlike the other components. This still left much to be explored in how we could implement an effective controller interface that worked satisfactorily for our project prototype.

For the user input portion of the controller, there were a few options to be considered. One of these options is the use of physical analog controls (such as Joystick controls). This could be used to control the motors responsible for the horizontal and vertical angle adjustments in a way that is simple to learn and easy to operate. Using an analog control mechanism would also allow for some variance in how the adjustments are made, possibly making it easier to get the camera's frame just right to capture the reflection surface and make the set up quicker and easier. An additional plus for this would be that it is not all that difficult to implement, as there were already methods and libraries that already existed to be referenced that allowed for this to be an easy means to control the motors. The only part that would be time intensive is narrowing in on the calibration of how the joystick input translates into motor adjustment. The joystick could also be used for the zoom lens adjustment as well if the implementation could be shown to be useful. A downside for the joystick in the expanded aspects of the project for the purpose to be implemented was how to keep the joystick mechanism free of debris that can inhibit the function of the joystick, as this device is expected to be used outside where such things can be unavoidable. Solutions may already exist that can be implemented, or we may have to come up with ways to handle this scenario. Another is that accidental movement of the joystick when the tracking of the beam profile is already occurring can throw off the data as the whole frame of view of the camera is thrown off if there is not a way to disable joystick inputs after the adjustments are dialed in.

Another option for physical inputs was the use of physical buttons for the interface. Regarding implementation this was probably the easiest as it can operate on Boolean logic to determine what action is to occur. This was the more

versatile physical input for what it could be used for, as they could be implemented for various purposes and individual buttons can work in multiple operations. A duo of buttons could be used for the camera lens zoom, which works quite well as there are only two options for that mode of camera adjustment: zoom in and zoom out. A set of four of them could be utilized as a directional pad that can be an alternative to the joystick discussed prior, although you do lose the benefit of more adjustability in movement that the joystick allows for. Buttons could also be used for other potential functions that can be easily programmed for that something like a joystick would likely be locked out of, such as confirmation or denial of certain functions if that were to be implemented.

It was ultimately decided (prior to determining the implementation of X/Y-axes movements would not be necessary) to implement both buttons and a joystick, buttons for the zooming in and zooming out of the magnification system and the joystick for the X/Y axis adjustments that were not ultimately used.

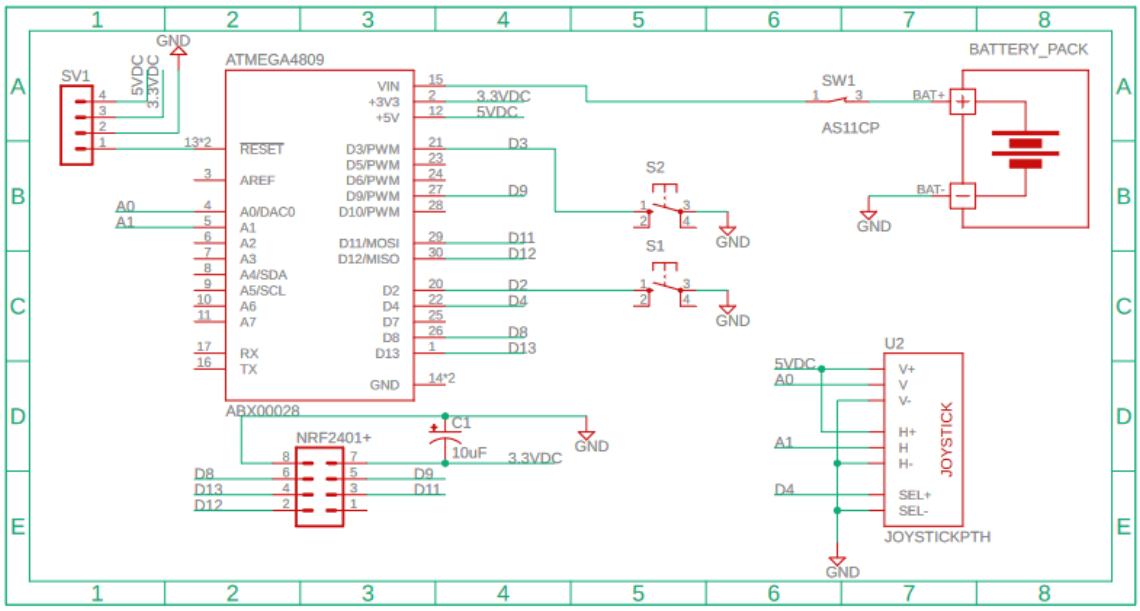

Figure 55: Schematic of the camera adjustment transceiver

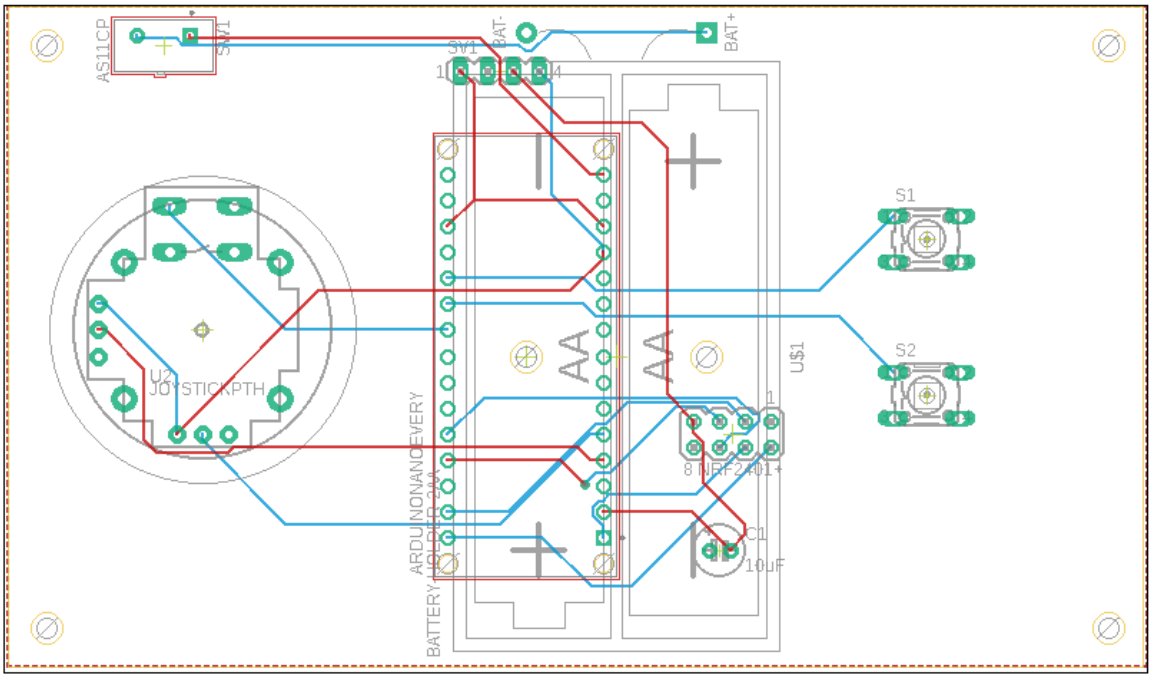

Figure 56: PCB board design of the camera adjustment transceiver

6.15.2 Receiver

Regarding the receiver it was determined that, in the case that there was to be X/Y axis movements, up to 4 motors would need to be implemented. This would entail the use of 4 motor drivers that would need to be added to the designs for the receiver. Implementation of the motor drivers required determining how to properly power them and how to implement their connections to the stepper motors themselves. The receiver board also needs to account for the power needs of the Arduino board and the nRF24L01+, which run in 5V and 3.3V respectively. Accounting for these factors, an LDO voltage regulator also needed to be implemented such that the motors could be powered at an input voltage of 12V, the Arduino and the motor drivers could operate at 5V off the output of the LDO, and the nRF24L01+ could operate on the 3.3V output of the Arduino board in order to simplify the design. The 12V power input for the motors also needed to be regulated through the use of 100uF capacitors, with the nRF24L01+ also needing a 10uF capacitor to better regulate the current flowing into the module and guarantee better operability.

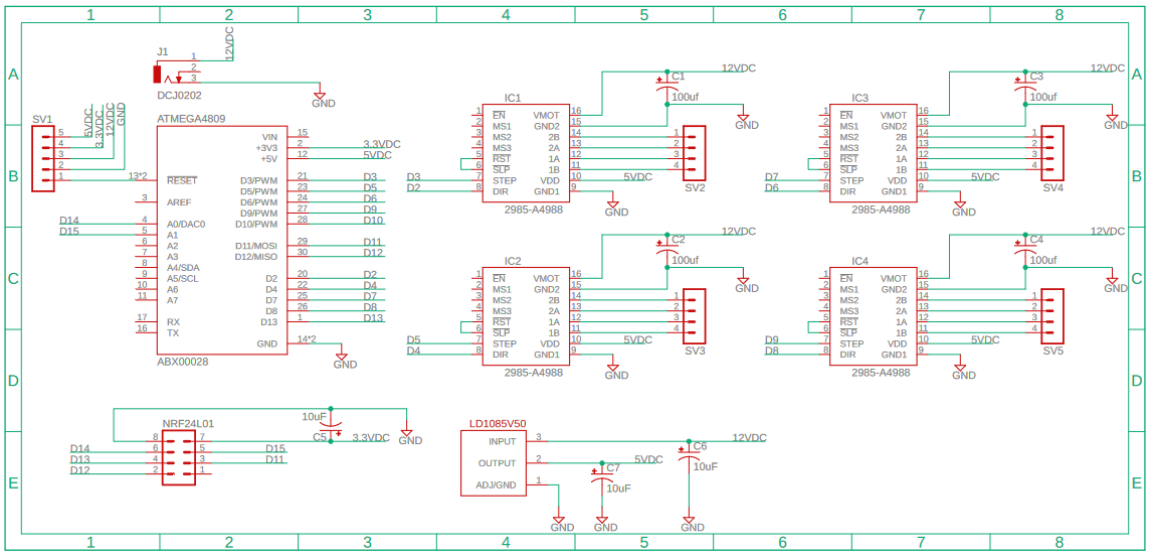

Figure 57: Schematic of the camera adjustment receiver

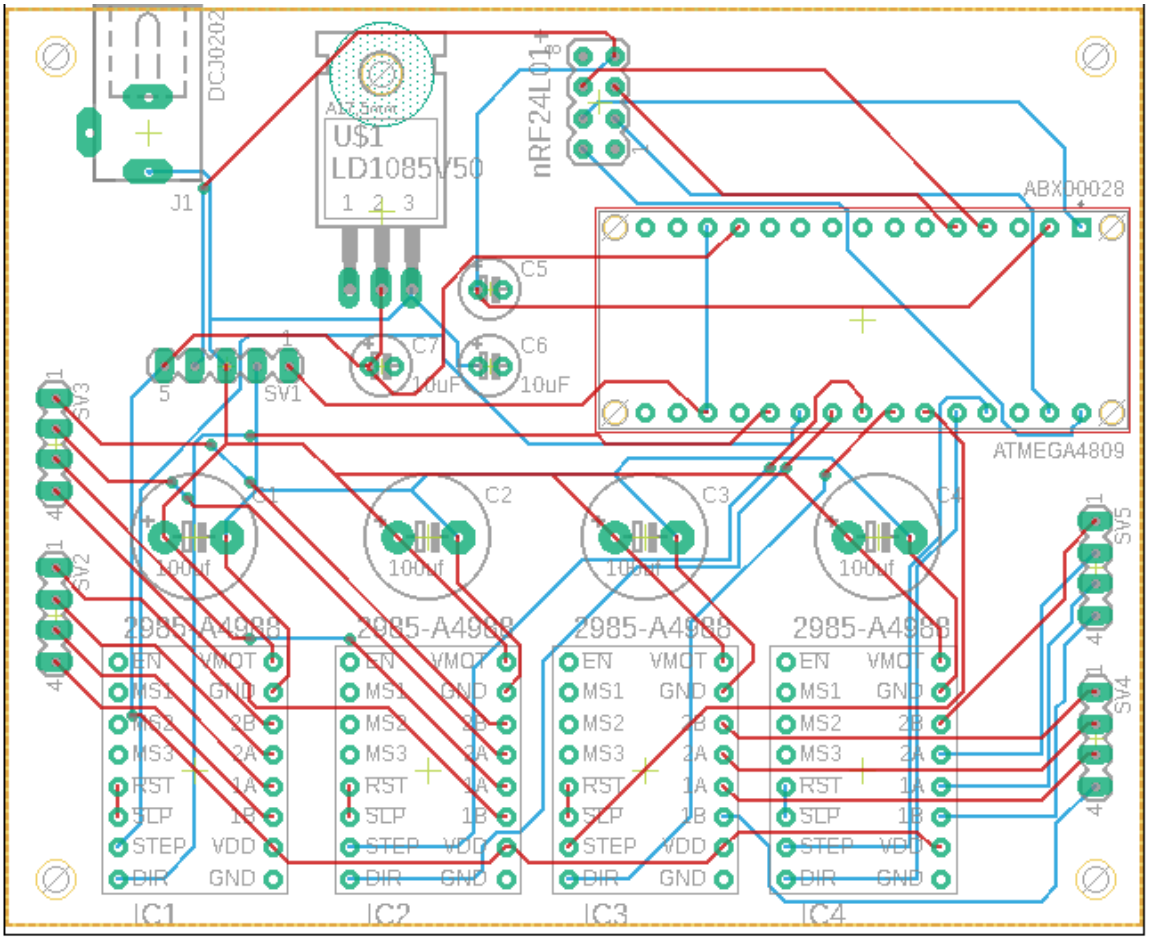

Figure 58: PCB board design of the camera adjustment transceiver

6.16 Cooling Fans

As in all electrical systems, heat is one of the most important characteristics to note. Being able to measure and control is very important for our system, in order to avoid any malfunction or damage to the components. Having that in mind, our system will utilize four motors, sensors among other electrical components. These components when running at the same time, will produce heat, which our system needs to react and respond. Engineering investigation was done into cooling fans. These fans will allow for our system to cool down our components and avoid reaching a temperature limit.

6.17 Post processing - Intensity profile

The intensity profile is obtained via MatLab code that takes frames from the video feed, after it is collected and layers them on top of each other to show how the intensity of the centroid of the laser beam changes over time. Shown in **Figure 59**. three frames taken 20 ms apart from a test video are processed to show how the intensity changes over one second. In **Figure 60**, the processed frames give a layered intensity profile.

This program can be improved to work automatically rather than manually taking the frames of the video that are desired to be processed. it can also be improved by being able to be run during a live feed to give a live intensity profile.

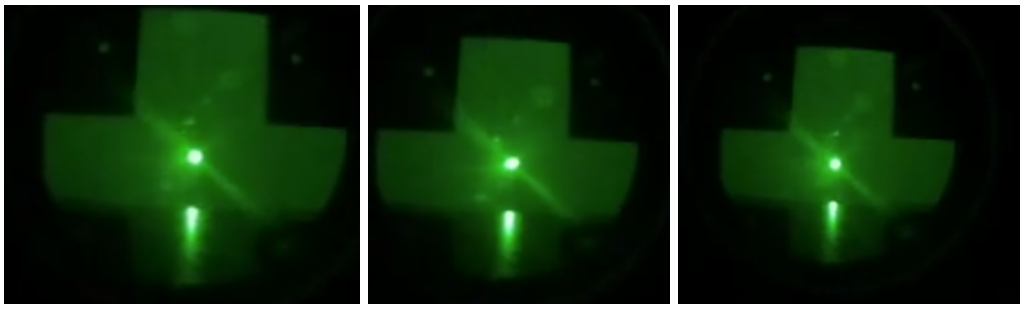

Figure 59: Three frames taken 20 ms apart from a video feed that is processed in the MatLab code to give a figure that shows how intensity profile changes over one second

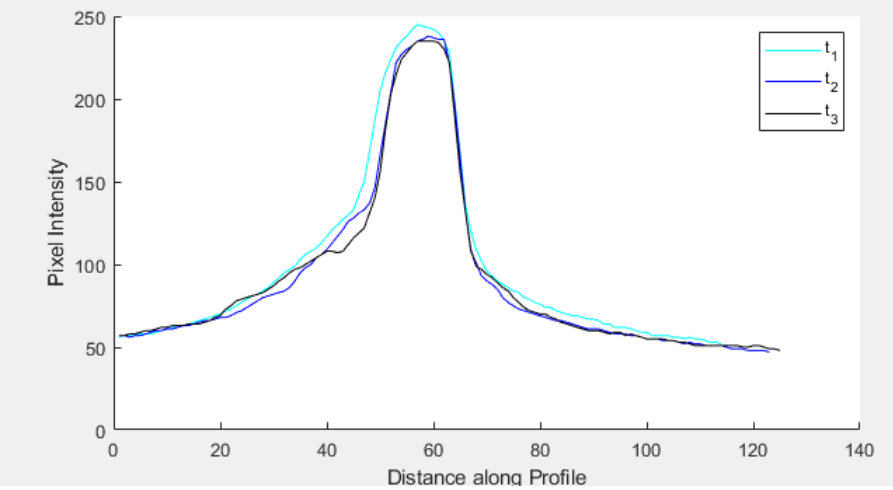

Figure 60: Intensity profile of three frames, taken about 20 ms apart layered to show how the intensity profile changes over one second.

7. Design Diagrams

This section contains visual diagrams for the proposed designs of the project in its various areas spanning from photonics to software.

7.1 Optical System

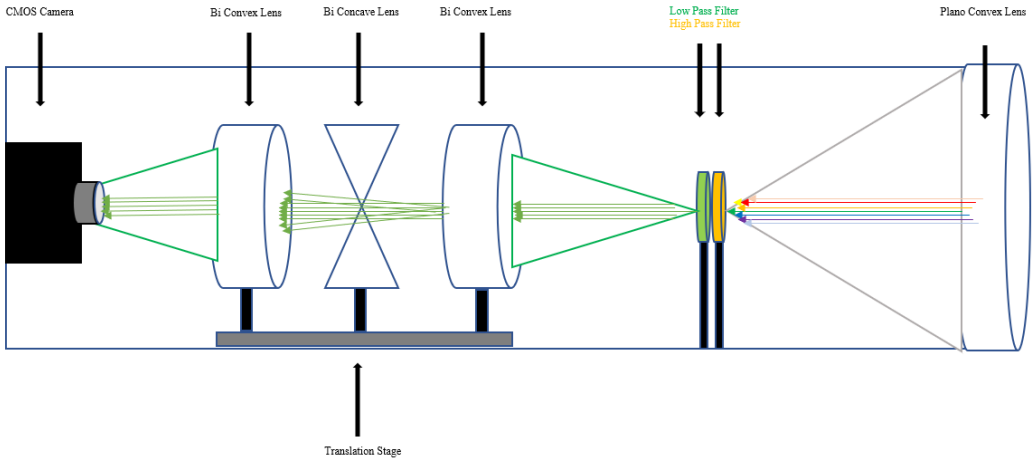

Figure 61: First design of optical cavity for device

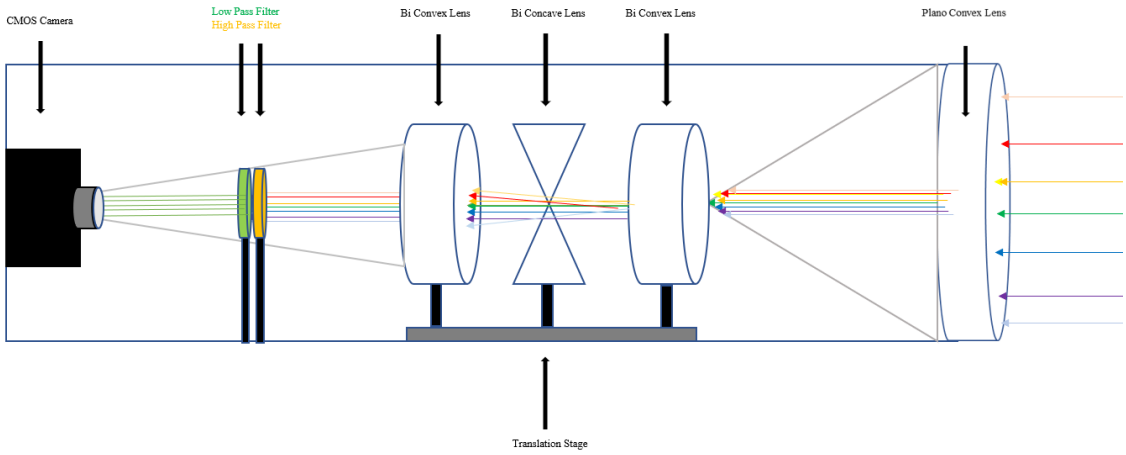

Figure 62: Second design of optical cavity for device

7.2 Camera Adjustment System

Figure 63: RC receiver flowchart

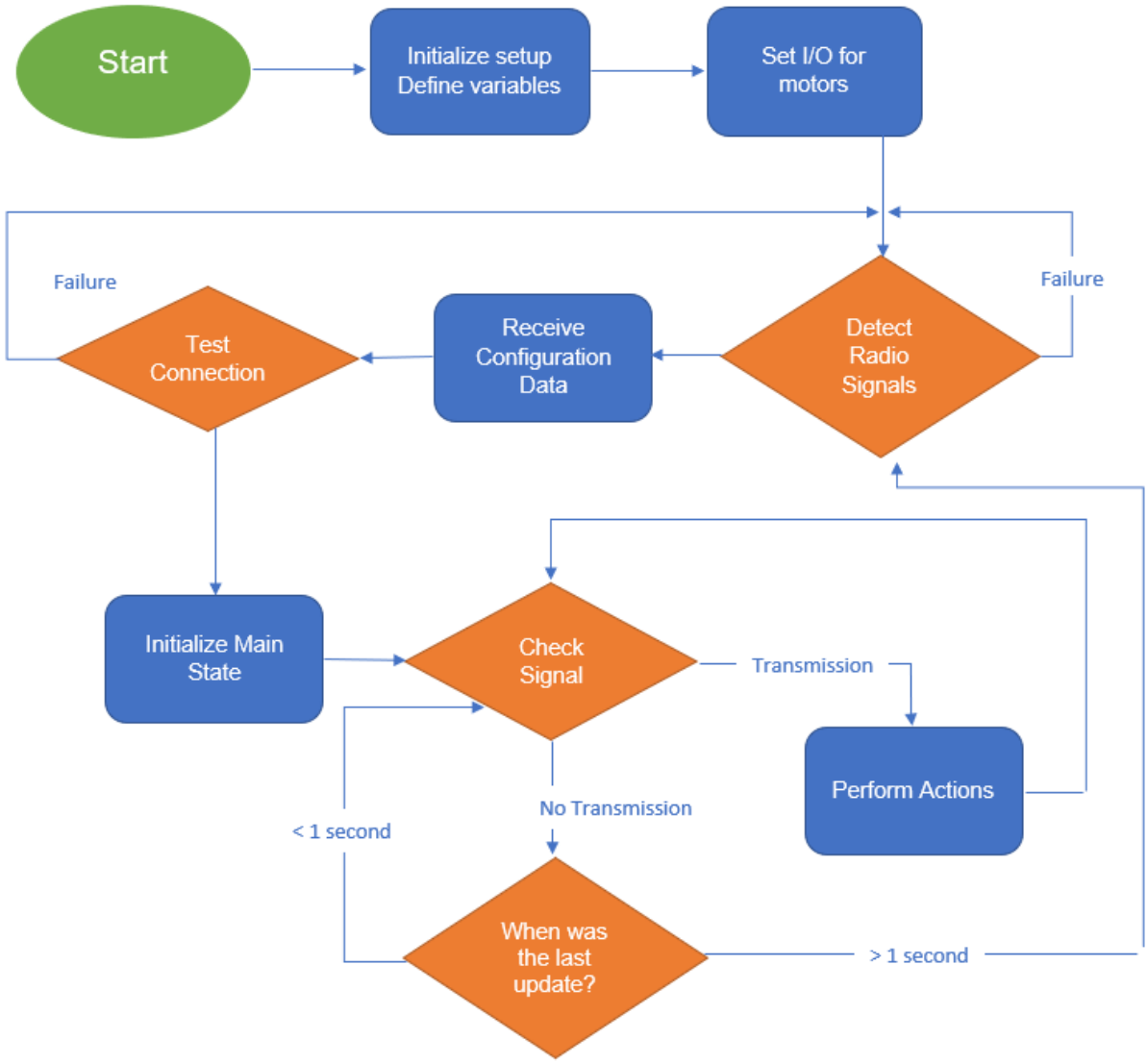

7.3 RC Controller

Figure 64: Flowchart for directing controls

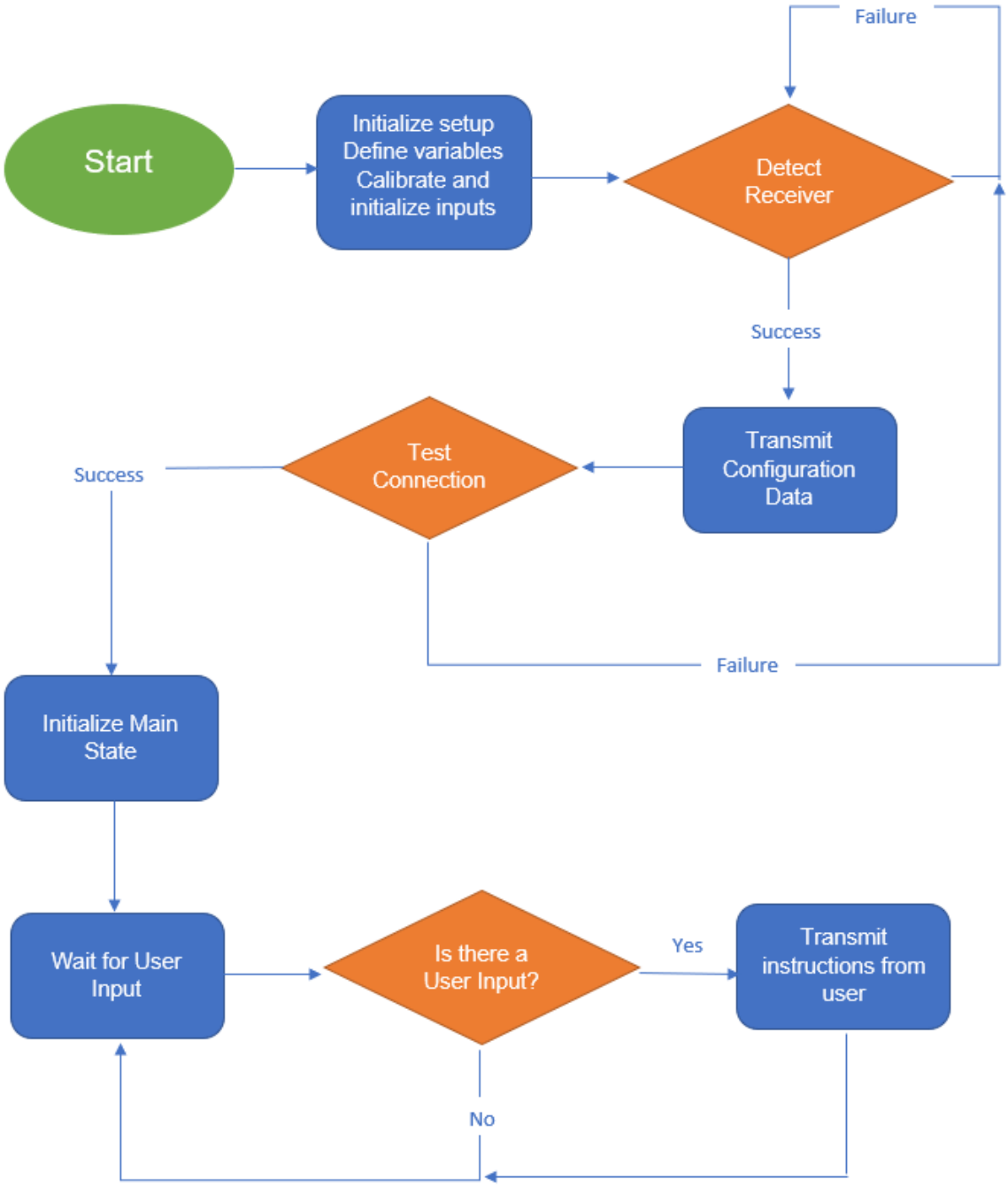

7.4 Object Tracking

Figure 65: Tracking flowchart

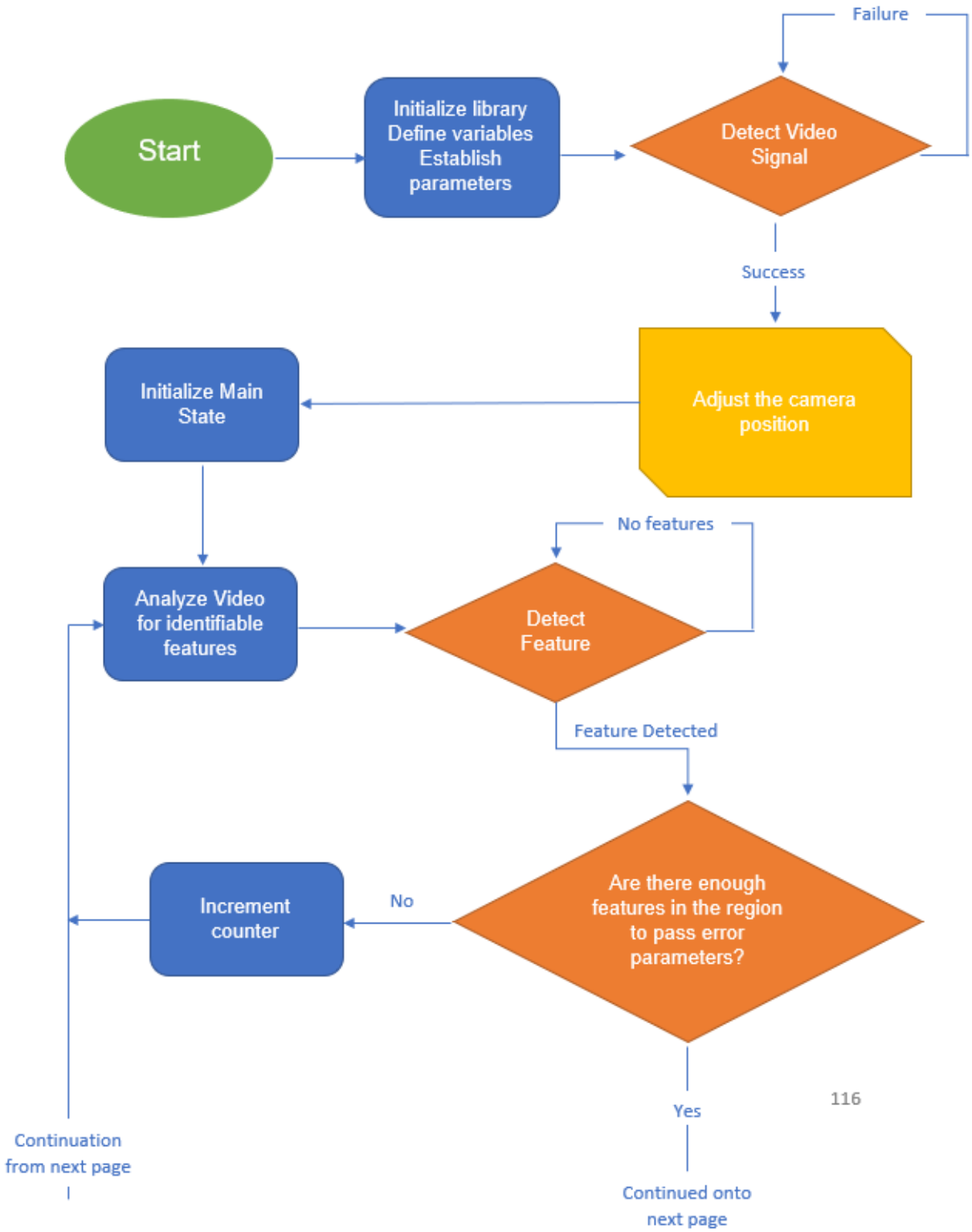

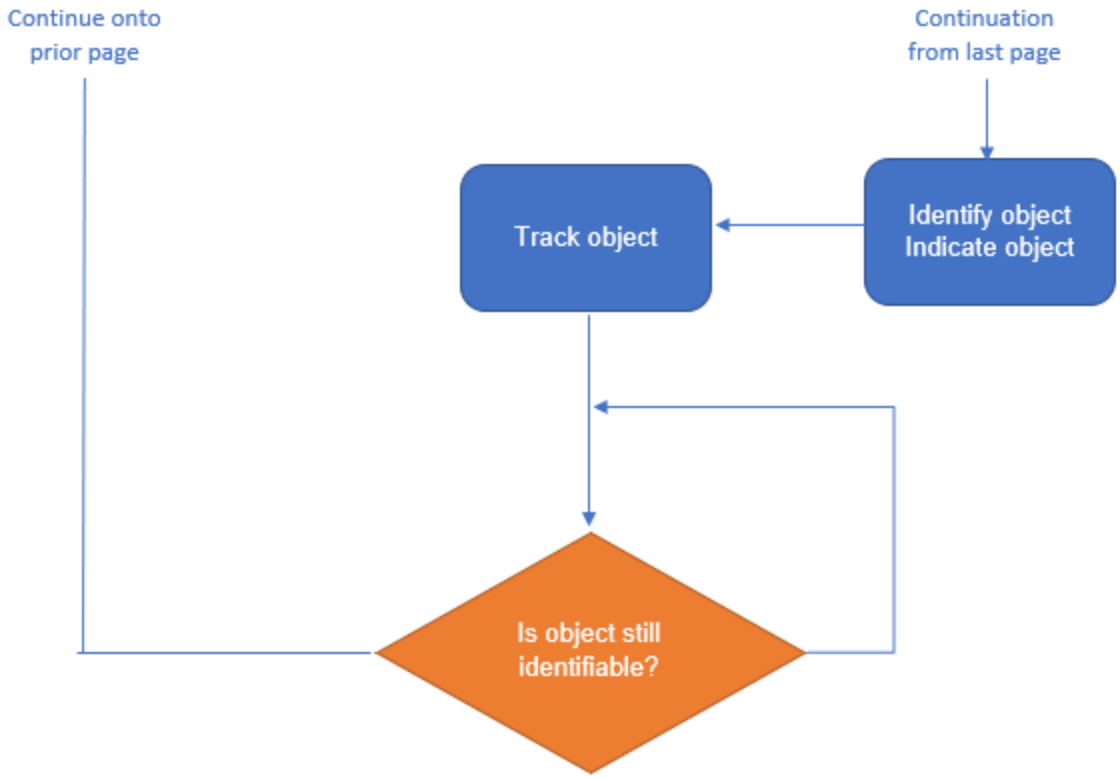
Continue onto
prior page
Continuation
from last page
Track object
Identify object
Indicate object
Is object still
identifiable?

7.5 Power Diagram

Figure 66: Battery and power consumption flowchart

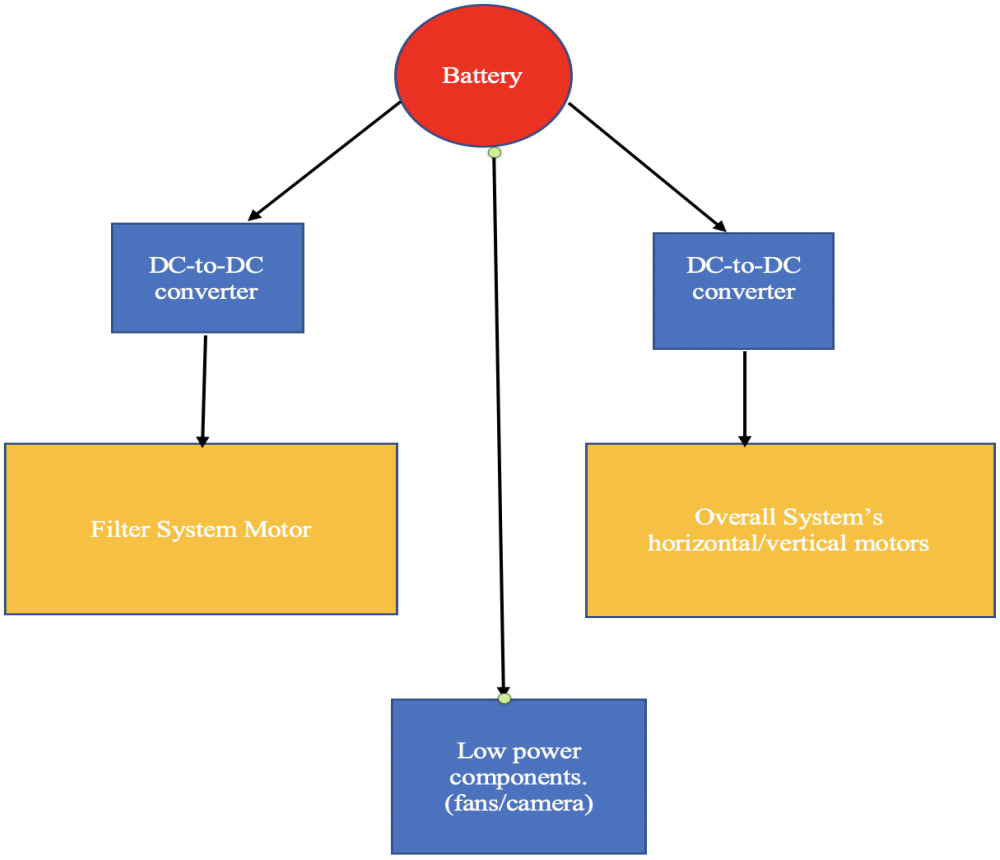

8. Testing

To ensure the end result of the project is that of a demoable product tests will need to be done in various areas to guarantee that the design and the materials used are all sound.

8.1 Hardware

Testing of hardware was a necessary part of guaranteeing the functionality of the components of the project and of the project. Testing was carried out as described in the following sections and the results for each are also shown.

8.1.1 Microcontrollers

For the testing of the microcontroller hardware there are a few areas that needed to be tested to verify the integrity of the microcontroller and its functionality: the functionality of the I/O pins, the power draw of the controller, and its ability to physically operate with other devices.
For the microcontroller the functionality of the pins is obviously quite necessary for the ability to be implemented into the project. There are many reasons why the pins may not be operable, either there is an issue with the connection due to how either the microcontroller or the pins are soldered that may just need to be resoldered, or it could be a manufacturing defect on the chip of the microcontroller that may require the microcontroller to be replaced, which can be a major setback if not handled early. Using a simple circuit composed of the board, a resistor, a button, and an LED as well as using a multimeter and some code that can be uploaded to the microcontroller. the pins were tested for functionality and checking that the current draw from each pin was as expected. Pin testing was necessary not only for the initial test board but also the final PCB implementation. Each of the boards used has each of their main GPIO pins evaluated through code that would test each as an input for the button as well as an output using the LED, with a button press on one pin needed to correspond to the activation of the LED. This simple test verified the functionality of the pins on the boards used and allowed for confidence when using them in further testing and in the final prototype for the course.

The microcontroller also needed to be tested for power consumption, especially based on clock speeds to verify the manufacturer’s specifications and to also guarantee the functionality of the board. For this just a power supply and a multimeter were necessary for measurements themselves, with a computer needed for uploading the necessary code to test at the clock speeds to be tested

at. The boards were tested for their power consumption at the available clock speeds they can run at, and the results were compared to those in the user's guide for the microcontroller to verify how the board functions and to gather our own understanding of what considerations needed to be made regarding power for the system. Tests done found that the boards utilized fell within the expected power specifications set by the board manufacturer, GPIO pins running with an expected 5V logic and the outputs of the board's 5 and 3.3V output pins being accurate.

The microcontroller also needed to be tested with the Radio Control Transmitter module to verify the setup of the module, the interoperability between module and microcontroller, and the ability of the communication module used for the microcontroller to communicate with the other module. The means by which this was to be achieved are covered in the section on the testing of the Radio Control Transmitter.

8.1.2 SBC

For the SBC, the tests done were similar to that of the tests used for the microcontroller, with the areas tested being the functionality of the GPIO pins, the power draw of the SBC, and its ability to physically operate with other devices. For the testing of the functionality of the pins of the SBC, the tests were the same as for the microcontroller: set up a simple circuit, use a multimeter and some code written for testing each of the pins can be tested in the case there is some issue that needed to be checked with the SBC where the pins are deemed suspect. Power testing is not an incredibly pressing need as it is expected that the draw of the SBC will be quite significant regardless, so sticking with manufacturer's specifications will be fine unless there is some fault discovered that needs troubleshooting. For the operability with other devices some troubleshooting needed to be done to guarantee the camera used was correctly configured for use with the Raspberry Pi. The Raspberry Pi needed to be configured for use of the webcam manually through the command line, which was figured out through a quick search online and then tested when the OpenCV python library package was configured onto the device (knocking out two birds with one stone for testing if the package was correctly configured).

8.1.3 Radio Control Transceiver and Receiver

For testing the RF transceiver and receiver the following needed to be done:

- Test the connection between the boards and the TX/RX modules

- Test connection between the TX and RX modules at various distances
- Test power considerations for operating the modules
- Test latency between two modules at demo range

For the first three items a preliminary test of whether we could get two separate boards to communicate with each other was done, with the procedure being to set up the connections for each of the boards to the communication module and uploading code for each such that one is a transceiver broadcasting a “Hello World!” string every half-second and a receiver that decodes the message and writes it to a serial monitor. During this process we could also troubleshoot any issue regarding the settings for data transmission rate and channel selection.

It was during this time that we determined that for this prototype it would be better to use the lower range nRF24L01+ module over the longer-range version as the lower range module was more reliable in establishing a connection between the two devices at the ranges we were testing than their longer-range counterparts. The long-range modules needed to be more directed towards each other at the given ranges whereas for the shorter-range modules the modules simply needed to have a line of sight with each other that was much easier to establish. Once we were able to get the modules to connect reliably at ranges longer than 3 meters, we could start on the final point. For determining if there would be any issues with latency such that the device would, at 3 meters, not be able to achieve latency below 100 milliseconds, the program used to test the prior points is edited such that the transceiver now broadcasts the “Hello World!” message on repeat continuously with no delay. On the receiving end we will have the serial monitor used prior to also display what times the messages are being displayed and use the separation of times between displayed messages to roughly determine if the latency of the two modules will be too much. From this test we were able to determine that the latency was well below the specification set, the average latency being in the 10s of seconds and the maximum latency being double that. Given these results we could determine that RF communications worked fine and the process of testing other aspects of the project that will rely on these modules can proceed.

8.2 Software Testing

Software testing was a necessary part of the project as it verified the operability of the software components and made sure that there was nothing amiss. With software testing the testing occurred throughout the design and prototyping process to make sure that each function written was functional both before and after it is uploaded to the hardware and that the code written and uploaded is compatible with the code written and uploaded for the other parts of the project.

8.2.1 Unit Testing

The initial software testing stage tested the applications developed in a simulated environment to find all the logic errors and bugs in code that existed internally by testing through all the individual parts of code that are to handle specific functions. This stage took advantage of the various debugging features available in the main development environments used to best sort out any baseline issues that arose in development that would've been detrimental to the project if not caught early. This initial stage did have its difficulties in trying to evaluate communications between devices, which required some stand-in inputs for the purposes of testing to verify how the devices would act independently based on what the expected outputs of the other device were.

8.2.2 Integration Testing

In the integration testing stage testing was done to determine how the code written and simulated in the initial unit testing stage fared when uploaded and used in the actual hardware used in the demonstration. In this stage the utilization of multimeters was necessary to verify the integrity of the connections between devices if issues regarding connection arose and utilizing LEDs for troubleshooting to verify that communication between devices was occurring even if the action that was being requested from the device wasn't. Much of the debugging that in the simulation phase in software testing was simply done through the testing environment had to be deliberately implemented in this phase of testing. This stage was meant to determine how all the parts of code developed up to this point were able to merge and become whole, integrated applications for each of the devices developed for. Once the integration testing was completed and all the software was able to work together, system testing took place to determine how the whole of the project was able to work together.

8.2.3 SBC

The SBC, being the main point of contact with the camera, needed for not only determining position and magnification of the system onto the diffused surface but for the actual object tracking as well. For the SBC to perform these functions, OpenCV was necessary, as the SBC did not have the means to properly interface with the camera natively and could only be operated through a software package such as OpenCV. Testing the configuration of the OpenCV library was performed to ensure it was properly implemented on the SBC and so

that further work could be done. With that out of the way, testing of the object detection software could be done.

8.2.4 Object Tracking

To ensure that the program could accurately identify and track the laser beam's profile, the algorithm used by the program had to undergo testing to guarantee the identification of the beam and tracking was accurate. The OpenCV library has plenty of options for how to implement this, whether it be comparing the input to common objects that the library is pre-trained to recognize or evaluating the input alone with some set of given parameters set by the programmer. For our purposes the program we used utilized the latter approach, which evaluated each of the frames from the video input and compared the HSV (Hue, Saturation, Luminance Value) color values of each of the pixels to the parameters set in the program to find objects to track. This option allowed for less time to be dedicated solely to setting up object tracking as instead of training the program to pick out an object and continuously having to fine tune it for finding some random configuration of pixels, the program can instead be tuned to filter out the correct parts of the image and track the most significant objects. For tracking the program needed to be able to find the center of the object it detected and plot on screen where the center of the detected object is in comparison to the center of the object detected in the prior frame. It also needed to be able to do this quickly enough so that the framerate of the tracking is such that it isn't too jittery or imprecise for tracking more fine movements of the laser beam profile. To alleviate any issues regarding framerate the program used had to have the number of frames per second saved and the resolution of the video whose frames were to be analyzed to be varied for determining the best way to get the best balance of image resolution and frame rate.

Initial tests of the object tracking to determine how individual components of the program to be used, such as how to save the operated video and how to get the program to filter through the appropriate HSV values, were run not on the SBC but on a desktop computer in order to get an idea of what the program is capable of on more optimal hardware that can better handle the computational needs of the program. Once the program was shown to be effective on desktop hardware the program was ported to the SBC after similar tests to determine if the OpenCV library was functional on the device. Once the base limits for the SBC's use of the program were found, stress testing began.

Once both prior parts of the training and testing were completed the computer was stress tested to determine how much variation the computer can handle in identifying and tracking. The stress testing entailed testing how well the computer could analyze an image given some amount of degradation to the image and how well the computer can correctly track a beam given other possible objects being in view, such as reflections on off parts of the mechanical components of the magnification system. The aim was to have the computer be

able to discern between the actual beam profile and any other miscellaneous objects that may enter the camera's view that would be unavoidable to keep away from the testing area. Once the computer reached acceptable levels of accuracy the computer continued to be tested on what it can track to make sure there is no strange last-minute deviation that had not been accounted for prior to demonstration.

8.2.5 Microcontrollers

For the microcontroller the main software test that needs to be done is on how to handle incoming commands from the controller device and use them to operate the 3 motors used. The tests will also need to handle how much adjustment needs to be made by the motor depending on the input of the control device. For the motor control testing the software will be tested to calibrate how the input translates into actual motor movement. This will be done by connecting the microcontroller to the motors used through the driver boards for the motors and to whatever means are used for through the controller device's interface to adjust the particular motors being adjusted. Based on what is deemed to be necessary to allow for best control over the motors, whether it be increasing the sensitivity to make the adjustments quicker or lower the sensitivity to make the adjustments more refined, the code used on the microcontroller is altered to make the needed adjustments and is tested once again to verify if the changes are to the liking of the users. This can also be used to test how the microcontroller is able to handle incoming commands from the control device and allow for determinations of what needs to be done to improve whatever variable needs to be improved, such as latency between the commands of the control device and the actions being done by the microcontroller.

9. Part List

Parts list	Part name	Manufacturer	Part number	Cost
Biconvex Lens A	N-BK7 Bi Convex Lens, Ø50.8, F=100.0 mm Uncoated	ThorLabs	LB1630	$38.00
Biconcave Lens B	N-BK7 Bi-Convex Lens, Ø25.4 mm, f = 175.0 mm, Uncoated	ThorLabs	LB2297	$35.16
Biconvex Lens C	N-SF11 Bi-Concave Lens, Ø25.4 mm, f = -25.0 mm, Uncoated	ThorLabs	LB1294	$22.92
Ø50.8 mm Cage Plate	Large 60mm Cage Plate, Metric	ThorLabs	LCP01/M	$42.15
Ø25.4 mm Cage Plate (2)	30mm to 60mm Cage Adapter	ThorLabs	LCP33	$43.26 ($86.52)
Ø25.4 mm Retaining Ring (2)	retaining Ring For stackable lens mount 0.08 thick	ThorLabs	SM1RR	$4.64 ($9.28)
Guiding Rods	Extension Rod 8 inch: Pack of 4	ThorLabs	ER8-P4	$45.79
Camera	Logitech C615 Full HD Webcam	Logitech	960-000733	49.99
Laser Source	532 nm 50 mW green laser diode	Lilly Electronics	532MD-50-1348-CAB	$20.00
Full Spectrum Light	Full Spectrum 800 Lumen Lightbulb	NorbSMILE	A19 LED	$19.99
BandPass Filter	D = 12.50 mm Cut on 527 nm Cut off 537 nm Transmission: > 50% @ 532 OD = 3 Angle of Incidence: 0	Edmunds Optics	#47-813	$160.00
CdS 5506 Light Dependent Resistor	CdS 5506	Amazon		$20.00

Parts list	Part name	Manufacturer	Part number	Cost
MCU	Arduino Nano Every	Arduino AG		$28.20/3 = $9.40
SBC	Raspberry Pi 4 Model B 8 GB	Raspberry Pi Trading LTD		$~~95~~($0, preowned
RF Transmitter/Receivers	nRF24L01+	Nordic Semiconductor ASA		$4
Stepper Motor 1	Nemas 17, 63.74 Oz.in	StepperOnline	17HS15-1504S1	$8.67
Stepper Motor 2	Nemas 17, 63.74 Oz.in	StepperOnline	17HS15-1504S1	$8.67
Stepper Motor 3	Nemas 17, 18.4 Oz.in	StepperOnline	17HS10-0704S	$8.56
Stepper Motor 4	Nemas 17, 18.4 Oz.in	StepperOnline	17HS10-0704S	$8.56
Battery	LifePO4	Eco-Worthy	Sku: L13060202004-1	$60.32
Fan 1	Fan Tubeaxial	AdaFruit Industries LLC	3368	$3.50
Fan 2	Fan Tubeaxial	AdaFruit Industries LLC	3368	$3.50

Table 21: Parts List

10. Results

The final product is a box that can detect and trace a laser off a diffused surface. The device is battery operated for portability and is weather-proof in a water resistant coated wooden casing. The device is able to be controlled by a user to zoom in and out through several specific zoom positions over 3 meters away from the device, making it remotely controlled. The transmitted data can be sent over 3 meters away and can trace where the beam has been in real time. The zoom is able to achieve 3x magnification. Our device can filter out all light other than the 532 nm laser light, optimal for outdoor use. The device can also measure in lux the amount of light collected by the system. Post processing of the images can provide an intensity profile over time.

A few goals for the project were not feasible for several reasons. The goal that the magnification would be 4x was not able to be met given our budgetary and time restraint and had to be compromised in the design. The lenses would have had to be custom made and purchased to be able to achieve 4x zoom while also keeping a large enough field of view for image processing. The compromise of a 3x zoom was chosen because of the budget-friendly options in lenses and the large enough field of view for image processing. Additionally, the goal that the device would be able to center the laser on the image track the laser beam in real time, was not feasible. The device became too heavy for easy movement of the entire box, which would have been necessary for laser centering and tracking. The cost of the parts to accommodate the weight and still have precise movement was out of budget.

The final device was able to accomplish a lot of the design goals, but there are improvements that can be made that were discovered late in the building process or were not foreseen. The device was able to filter out all of the ambient light however an ND filter needs to be added to prevent the camera from over saturating which would aid in image processing of the 533 laser light that did go through the system. Ideally the device would be able to process an intensity profile in real time but it is able to process this data in post.

11. Operation

For proper operation of the prototype devices used, the following section is included. This section covers how each of the devices used are to be operated as well as any steps that need to be followed to prevent any issues with the prototype devices.

11.1 Initialization

This section covers the set up of the devices used and what needs to be done in set up to prevent any issues later on.

To set up the SBC one must set up the power connections for the device, the video output so the user can interface with the SBC properly, and connect the needed input components, including the camera for video input and a keyboard and mouse for user commands. Once all of these are set power on the SBC and upon start-up find the laser tracking program and prepare to start when the remaining components are ready.

Setting up the LDR device is simple as it operates off its own power supply; simply turn on the power for the device and do quick measurements with no light reaching the sensor and a normal ambient light reaching the sensor to verify the device is measuring within the correct parameters.

Onto the transceiver, which also operates off its own power. As such, it simply needs to be turned on, which must occur prior to the powering on of the transceiver as having the receiver active prior can cause issues with motor operation, as the motors will move if there is no connection set between the transceiver and the receiver before the motor control is initialized. Next is to power on the receiver, which is done by connecting the 12V barrel plug connected to the battery to the barrel jack on the receiver board. When the receiver is plugged in, the transceiver and receiver should connect with each other. If they fail to connect it will be obvious as the motors will move without any user input. If they do not immediately connect, reposition the transceiver and make sure the two devices have a line of sight for their RF communication modules. Once a connection is determined to have been established, all one must do to finish the initialization is make sure the lenses are in the proper position, which to start will have the lenses such that they are at the marked “A” locations. When all of the parts are set, make sure the device is pointed at the diffused surface board, shut off any additional lights if needed, and turn on the laser.

11.2 Active Use

When the device is ready for use, start the laser tracking program on the SBC and verify the reflected beam profile is in view of the laser. At this point the user is able to use the transceiver device to change the magnification of the camera to best focus on the beam profile and track it. Once the tracking program is running, the program will run until the user stops it by pressing either the Q key or the ESC key (assuming there's no issues regarding memory constraints for the saved video). Given this, if the user has the magnification set and doesn't need to adjust it again they can turn off the receiver and transceiver in that order and simply turn them back on if adjustment is needed to be made later (following the initialization procedure as it pertains to these devices). While the device is operating the user can also go and monitor the LDR device regardless of whether they have turned off the RF devices.

11.3 Turning Off

Once the user has finished their experiment, the device can be turned off and the processes can be ended. Starting with the tracking program, end the program by pressing either Q or ESC. The program will terminate and save the video as output.avi in the same folder the program is located. If necessary the user can extract the file from the SBC by using a USB drive to copy the video onto the drive. Once all activity with the SBC is finished it can be shut off and the power to it can be cut. The remaining devices can be either disconnected from their batteries or have their switches turned off, as they are much less particular about when they can be powered off.

Appendix

References

"Ambient Light Sensor: Types, Circuit and Applications." *ElProCus*, 29 July 2019, https://www.elprocus.com/ambient-light-sensor-working-and-applications/.

(Andor, 2018, 2019; Brunner, 2017; *CMOS Cameras*, 2021; Instuments; Kingslake, 1989; Plumridge, 2018, 2019, 2020; Riyo Youngworth, 2012; Sasian, 2019)
Andor. (2018). *How to Define the Quantum Efficiency of CCD Cameras*. Oxford Instruments.
Retrieved 10/28 from
https://andor.oxinst.com/learning/view/article/ccd-spectral-response-(qe)

Andor. (2019). *Understanding Read Noise in sCMOS Cameras*. Oxford insturments. Retrieved 10/27 from https://andor.oxinst.com/learning/view/article/understanding-read-noise-in-scmos-cameras

Arduino AG. (n.d.). *Arduino Nano Every - Pack 3*. Arduino Nano Every. Retrieved November 5, 2021, from https://store-usa.arduino.cc/products/arduino-nano-every-pack?variant=40377141854415
A., Saleh Bahaa E. *Introduction to Subsurface Imaging*. Cambridge University Press, 2011.

Battery University. "BU-201: How Does the Lead Acid Battery Work?" Battery University, 27 Oct. 2021, https://batteryuniversity.com/article/bu-201-how-does-the-lead-acid-battery-work.

Brunner, D. (2017, 10/28). Frame Rate: A Beginner's Guide. https://www.techsmith.com/blog/frame-rate-beginners-guide/

Bluetooth SIG, Inc. (n.d.). *Learn About Bluetooth: Bluetooth Technology Overview*. Retrieved October 20, 2021, from https://www.bluetooth.com/learn-about-bluetooth/tech-overview/

Cass, S. (2021, July 28). *Quickly embed AI into your projects with Nvidia's Jetson Nano*. IEEE Spectrum. Retrieved November 19, 2021, from https://spectrum.ieee.org/quickly-embed-ai-into-your-projects-with-nvidias-jetson-nano#toggle-gdpr.

CMOS Cameras. (2021). OPT. Retrieved 9/25 from
Instuments, P. *Full Well Capacity*. teledyne imaging group. Retrieved 10/29 from
Karim Nice, T. V. W. G. G. (2020). *How Digital Cameras Work*. Retrieved 11/3 from https://electronics.howstuffworks.com/cameras-photography/digital/question362.htm

Demeritt, Clint. "12V Battery Types: Which One Is for You?" Battle Born Batteries, 18 May 2021, https://battlebornbatteries.com/12v-battery-types/.

Electromaker. (n.d.). *Nvidia Jetson Nano Development Kit-B01*. Nvidia Jetson Nano Development Kit-b01. Retrieved November 19, 2021, from https://www.electromaker.io/shop/product/nvidia-jetson-nano-development-kit-b01.

Hecht, Eugene. *Optics*. Pearson Education, Inc., 2016.

HuddleCamHD. (2021, September 27). *About*. Retrieved November 5, 2021, from https://huddlecamhd.com/webcam/.

isaac879. (2020, September 5). *Pan-Tilt-Mount*. Retrieved November 5, 2021, from https://github.com/isaac879/Pan-Tilt-Mount.

Juneau, John-Michael, "The Simulation, Design, and Fabrication of Optical Filters" (2017). Graduate Theses - Physics and Optical Engineering. 21. https://scholar.rose-hulman.edu/optics_grad_theses/21

Kingslake, R. (1989). *A history of the photographic lens*. Academic press.

Plumridge, J. (2018). *Backfocus in Astrophotography*. Atik cameras. Retrieved 10/29 from https://www.atik-cameras.com/news/backfocus-astrophotography-cameras/

Kumar, V. (2020, December 2). How to detect objects in real-time using opencv and python. Medium. Retrieved November 19, 2021, from https://towardsdatascience.com/how-to-detect-objects-in-real-time-using-opencv-and-python-c1ba0c2c69c0.

Last Minute Engineers. (2020, December 18). *In-depth: How NRF24L01 wireless module works & interface with Arduino*. Last Minute Engineers. Retrieved November 5, 2021, from https://lastminuteengineers.com/nrf24l01-arduino-wireless-communication/.

Microchip Technologies Inc. (2019). 48-pin Data Sheet – megaAVR® 0-series.

"Nonpolarizing Transmissive Filters." *Enhanced Optical Filter Design*, pp. 135–146., https://doi.org/10.1117/3.869055.ch12.

Nordic Semiconductor ASA. (2008, March). nRF24L01+ Single Chip 2.4GHz Transceiver Preliminary Product Specification v1.0.

NVIDIA Corporation. (2021, April 14). *Jetson Nano Developer Kit*. NVIDIA Developer. Retrieved November 19, 2021, from https://developer.nvidia.com/embedded/jetson-nano-developer-kit.

OpenCV team. (2020, November 4). About. OpenCV. Retrieved November 19, 2021, from https://opencv.org/about/.

"Optical Filters: Edmund Optics." *Edmund Optics Worldwide*, https://www.edmundoptics.com/knowledge-center/application-notes/optics/optical-filters/.

"Optical Filter Spectral Features - CWL, FWHM, Transmission, and Blocking." *Alluxa Optical Filters and Thin-Film Coatings*, 24 May 2021, https://www.alluxa.com/optical-filter-specs/spectral-features/.

"Optical Filter Spectral Features - CWL, FWHM, Transmission, and Blocking." *Alluxa Optical Filters and Thin-Film Coatings*, 24 May 2021, https://www.alluxa.com/optical-filter-specs/spectral-features/.

"Optical Filters: Edmund Optics." *Edmund Optics Worldwide*, https://www.edmundoptics.com/c/optical-filters/610/.

Plumridge, J. (2019). *What is dynamic and tonal range?* Lifewire. Retrieved 10/27 from https://www.lifewire.com/what-is-dynamic-range-493728

Plumridge, J. (2020). *Why You Should Care About Your Camera's ADC*. Lifewire. Retrieved 10/29 from https://www.lifewire.com/the-adc-of-a-digital-camera-493714

Raspberry Pi Trading LTD. (n.d.). *Raspberry pi documentation*. RP2040. Retrieved November 5, 2021, from https://www.raspberrypi.com/documentation/microcontrollers/rp2040.html#welcome-to-rp2040

Raspberry Pi Trading Ltd. (2020). RP2040 Datasheet.

Raspberry Pi Trading Ltd. (2019, June). Raspberry Pi 4 Model B Datasheet.

Raspberry Pi. (n.d.). *Raspberry pi 4 model B*. Raspberry Pi. Retrieved November 5, 2021, from https://www.raspberrypi.com/products/raspberry-pi-4-model-b/.

Riyo Youngworth, E. B. (2012). Fundamental considerations for zoom lens design (tutorial). SPIE optical engineering and applications, san diego, califorina.

Sasian, J. (2019). Zoom lenses. In *Introduction to lens design* (pp. 196-206). cambridge university press.

ssheshadri. (2019, December 17). Jetson Nano Developer Kit User Guide. NVIDIA Corporation.

Texasinstruments, director. YouTube, Texas Instruments, 10 Dec. 2018, https://www.youtube.com/watch?v=Gk4Hib99wkc. Accessed 5 Nov. 2021.

Torvalds, Linus (2005, April 7). "Re: Kernel SCM saga." linux-kernel. Retrieved November 19, 2021.

U.S. Department of Commerce National Telecommunications and Information Administration Office of Spectrum Management. (2016, January). United States Frequency Allocation Chart.

Copyright Permissions

Copyright

This software is Copyright (C) 2010-2018 Mike McCauley. Use is subject to license conditions. The main licensing options available are GPL V3 or Commercial:

Open Source Licensing GPL V3

This is the appropriate option if you want to share the source code of your application with everyone you distribute it to, and you also want to give them the right to share who uses it. If you wish to use this software under Open Source Licensing, you must contribute all your source code to the open source community in accordance with the GPL Version 23 when your application is distributed. See https://www.gnu.org/licenses/gpl-3.0.html

Commercial Licensing

This is the appropriate option if you are creating proprietary applications and you are not prepared to distribute and share the source code of your application. To purchase a commercial license, contact info@airspayce.com

```
Copyright (c) 2008 Brad Montgomery <brad@bradmontgomery.net>

Permission is hereby granted, free of charge, to any person obtaining a copy of
this software and associated documentation files (the "Software"), to deal in
the Software without restriction, including without limitation the rights to
use, copy, modify, merge, publish, distribute, sublicense, and/or sell copies
of the Software, and to permit persons to whom the Software is furnished to do
so, subject to the following conditions:

The above copyright notice and this permission notice shall be included in all
copies or substantial portions of the Software.

THE SOFTWARE IS PROVIDED "AS IS", WITHOUT WARRANTY OF ANY KIND, EXPRESS OR
IMPLIED, INCLUDING BUT NOT LIMITED TO THE WARRANTIES OF MERCHANTABILITY,
FITNESS FOR A PARTICULAR PURPOSE AND NONINFRINGEMENT. IN NO EVENT SHALL THE
AUTHORS OR COPYRIGHT HOLDERS BE LIABLE FOR ANY CLAIM, DAMAGES OR OTHER
LIABILITY, WHETHER IN AN ACTION OF CONTRACT, TORT OR OTHERWISE, ARISING FROM,
OUT OF OR IN CONNECTION WITH THE SOFTWARE OR THE USE OR OTHER DEALINGS IN THE
SOFTWARE.
```

Software

Laser Tracking Code:

```
import sys
import argparse
import cv2
import numpy

# Set up for saving tracked video
fourcc = cv2.VideoWriter_fourcc(*'XVID')
# Video will be saved as output.avi with a framerate of 15fps and
resolution of 640x480
out = cv2.VideoWriter('output.avi', fourcc, 15.0, (640,480))

class LaserTracker(object):

    # Set parameters for video input and the HSV value threshold
    # HSV Threshold: H = 0-60; S = 0-255; V = 200-255
    # default video input resolution: 640x480
          def __init__(self, cam_width=640, cam_height=480, hue_min=0,
hue_max=60,
                 sat_min=0, sat_max=255, val_min=200, val_max=255,
                 display_thresholds=False):

        self.cam_width = cam_width
        self.cam_height = cam_height
        self.hue_min = hue_min
        self.hue_max = hue_max
        self.sat_min = sat_min
        self.sat_max = sat_max
        self.val_min = val_min
        self.val_max = val_max
        self.display_thresholds = display_thresholds

        self.capture = None  # camera capture device
        self.channels = {
            'hue': None,
            'saturation': None,
```

```
            'value': None,
            'laser': None,
        }

        self.previous_position = None
        self.trail = numpy.zeros((self.cam_height, self.cam_width, 3),
                                 numpy.uint8)

    def create_and_position_window(self, name, xpos, ypos):
        # Create a window
        cv2.namedWindow(name)
        # Resize it to the size of the camera image
        cv2.resizeWindow(name, self.cam_width, self.cam_height)
        # Move to (xpos,ypos) on the screen
        cv2.moveWindow(name, xpos, ypos)

    def setup_camera_capture(self, device_num=0):
          """Perform camera setup for the device number (default device =
0).
        Returns a reference to the camera Capture object.

        """
        try:
            device = int(device_num)
            sys.stdout.write("Using Camera Device: {0}\n".format(device))
        except (IndexError, ValueError):
            # assume we want the 1st device
            device = 0
            sys.stderr.write("Invalid Device. Using default device 0\n")

        # Try to start capturing frames
        self.capture = cv2.VideoCapture(device)
        if not self.capture.isOpened():
            sys.stderr.write("Faled to Open Capture device. Quitting.\n")
            sys.exit(1)

        # set the wanted image size from the camera
        self.capture.set(
```

```
                                        cv2.cv.CV_CAP_PROP_FRAME_WIDTH    if
cv2.__version__.startswith('2') else cv2.CAP_PROP_FRAME_WIDTH,
            self.cam_width
        )
        self.capture.set(
                                       cv2.cv.CV_CAP_PROP_FRAME_HEIGHT    if
cv2.__version__.startswith('2') else cv2.CAP_PROP_FRAME_HEIGHT,
            self.cam_height
        )
        return self.capture

    def handle_quit(self, delay=10):
        """Quit the program if the user presses "Esc" or "q"."""
        key = cv2.waitKey(delay)
        c = chr(key & 255)
        if c in ['c', 'C']:
            self.trail = numpy.zeros((self.cam_height, self.cam_width, 3),
                                     numpy.uint8)
        if c in ['q', 'Q', chr(27)]:
            out.release()
            cv2.destroyAllWindows
            sys.exit(0)

    def threshold_image(self, channel):
        if channel == "hue":
            minimum = self.hue_min
            maximum = self.hue_max
        elif channel == "saturation":
            minimum = self.sat_min
            maximum = self.sat_max
        elif channel == "value":
            minimum = self.val_min
            maximum = self.val_max

        (t, tmp) = cv2.threshold(
            self.channels[channel],  # src
            maximum,  # threshold value
            0,  # we dont care because of the selected type
```

```
            cv2.THRESH_TOZERO_INV  # t type
        )

        (t, self.channels[channel]) = cv2.threshold(
            tmp,  # src
            minimum,  # threshold value
            255,  # maxvalue
            cv2.THRESH_BINARY  # type
        )

        if channel == 'hue':
             # only works for filtering red color because the range for the
hue
            # is split
            self.channels['hue'] = cv2.bitwise_not(self.channels['hue'])

    def track(self, frame, mask):
        """
        Track the position of the laser pointer.

        Code taken from
        http://www.pyimagesearch.com/2015/09/14/ball-tracking-with-opencv/
        """
        center = None

        countours = cv2.findContours(mask, cv2.RETR_EXTERNAL,
                                     cv2.CHAIN_APPROX_SIMPLE)[-2]

        # only proceed if at least one contour was found
        if len(countours) > 0:
            # find the largest contour in the mask, then use
            # it to compute the minimum enclosing circle and
            # centroid
            c = max(countours, key=cv2.contourArea)
            ((x, y), radius) = cv2.minEnclosingCircle(c)
            moments = cv2.moments(c)
            if moments["m00"] > 0:
                center = int(moments["m10"] / moments["m00"]), \
```

```
                        int(moments["m01"] / moments["m00"])
            else:
                center = int(x), int(y)

            # only proceed if the radius meets a minimum size
            if radius > 10:
                # draw the circle and centroid on the frame,
                cv2.circle(frame, (int(x), int(y)), int(radius),
                           (0, 255, 255), 2)
                cv2.circle(frame, center, 5, (0, 0, 255), -1)
                # then update the ponter trail
                if self.previous_position:
                    cv2.line(self.trail, self.previous_position, center,
                             (255, 255, 255), 2)

        cv2.add(self.trail, frame, frame)
        self.previous_position = center

    def detect(self, frame):
        hsv_img = cv2.cvtColor(frame, cv2.COLOR_BGR2HSV)

        # split the video frame into color channels
        h, s, v = cv2.split(hsv_img)
        self.channels['hue'] = h
        self.channels['saturation'] = s
        self.channels['value'] = v

        # Threshold ranges of HSV components; storing the results in place
        self.threshold_image("hue")
        self.threshold_image("saturation")
        self.threshold_image("value")

        # Perform an AND on HSV components to identify the laser!
        self.channels['laser'] = cv2.bitwise_and(
            self.channels['hue'],
            self.channels['value']
        )
        self.channels['laser'] = cv2.bitwise_and(
```

```
            self.channels['saturation'],
            self.channels['laser']
        )

        # Merge the HSV components back together.
        hsv_image = cv2.merge([
            self.channels['hue'],
            self.channels['saturation'],
            self.channels['value'],
        ])

        self.track(frame, self.channels['laser'])

        return hsv_image

    def display(self, img, frame):
        """Display the combined image and (optionally) all other image channels
        NOTE: default color space in OpenCV is BGR.
        """
        cv2.imshow('RGB_VideoFrame', frame)
        cv2.imshow('LaserPointer', self.channels['laser'])
        if self.display_thresholds:
            cv2.imshow('Thresholded_HSV_Image', img)
            cv2.imshow('Hue', self.channels['hue'])
            cv2.imshow('Saturation', self.channels['saturation'])
            cv2.imshow('Value', self.channels['value'])

    def setup_windows(self):
                            sys.stdout.write("Using OpenCV version: {0}\n".format(cv2.__version__))

        # create output windows
        self.create_and_position_window('LaserPointer', 0, 0)
        self.create_and_position_window('RGB_VideoFrame',
                                        10 + self.cam_width, 0)
        if self.display_thresholds:
```

```
            self.create_and_position_window('Thresholded_HSV_Image', 10,
10)
            self.create_and_position_window('Hue', 20, 20)
            self.create_and_position_window('Saturation', 30, 30)
            self.create_and_position_window('Value', 40, 40)

    def run(self):
        # Set up window positions
        self.setup_windows()
        # Set up the camera capture
        self.setup_camera_capture()

        while True:
            # 1. capture the current image
            success, frame = self.capture.read()
            if not success:  # no image captured... end the processing
                        sys.stderr.write("Could not read camera frame.
Quitting\n")
                sys.exit(1)

            hsv_image = self.detect(frame)
            self.display(hsv_image, frame)
            out.write(frame)
            self.handle_quit()


if __name__ == '__main__':
    parser = argparse.ArgumentParser(description='Run the Laser Tracker')
    parser.add_argument('-W', '--width',
                        default=640,
                        type=int,
                        help='Camera Width')
    parser.add_argument('-H', '--height',
                        default=480,
                        type=int,
                        help='Camera Height')
    parser.add_argument('-u', '--huemin',
                        default=40,
```

```
                    type=int,
                    help='Hue Minimum Threshold')
parser.add_argument('-U', '--huemax',
                    default=80,
                    type=int,
                    help='Hue Maximum Threshold')
parser.add_argument('-s', '--satmin',
                    default=25,
                    type=int,
                    help='Saturation Minimum Threshold')
parser.add_argument('-S', '--satmax',
                    default=255,
                    type=int,
                    help='Saturation Maximum Threshold')
parser.add_argument('-v', '--valmin',
                    default=200,
                    type=int,
                    help='Value Minimum Threshold')
parser.add_argument('-V', '--valmax',
                    default=255,
                    type=int,
                    help='Value Maximum Threshold')
parser.add_argument('-d', '--display',
                    action='store_true',
                    help='Display Threshold Windows')
params = parser.parse_args()

tracker = LaserTracker(
    cam_width=params.width,
    cam_height=params.height,
    hue_min=params.huemin,
    hue_max=params.huemax,
    sat_min=params.satmin,
    sat_max=params.satmax,
    val_min=params.valmin,
    val_max=params.valmax,
    display_thresholds=params.display
)
```

```
    tracker.run()
```

Camera Adjustment System Receiver Code:

```
// Libraries
#include <SPI.h>
#include <nRF24L01.h>
#include <RF24.h>
#include <AccelStepper.h>
RF24 radio(14, 15); // CE pin, CSN pin

// Set up data package
struct Data_Package {
  byte button1;
  byte button2;
  byte xAxis;
  byte yAxis;
};

Data_Package data;

// Set communication address
const byte address[6] = "00001";

// Stepper motor pin setup for magnification system
const int dirPin1 = 2;
const int dirPin2 = 8;

const int stepPin1 = 3;
const int stepPin2 = 9;

const int speed1 = 10;
const int speed2 = -15;

// Stepper motor driver setup
AccelStepper stepper1(1, stepPin1, dirPin1);
AccelStepper stepper2(1, stepPin2, dirPin2);

void setup()
{
  // Motor driver setup
```

```
  stepper1.setMaxSpeed(400);
  stepper2.setMaxSpeed(400);
  stepper1.setSpeed(speed1);
  stepper2.setSpeed(speed2);

  // Motor driver pin setup
  pinMode(stepPin1, OUTPUT);
  pinMode(stepPin2, OUTPUT);
  pinMode(dirPin1, OUTPUT);
  pinMode(dirPin2, OUTPUT);

  // RF radio initialization
  while(!Serial);
    Serial.begin(9600);
  radio.begin();

  // Set radio address
  radio.openReadingPipe(0, address);

  // Set device as receiver device
  radio.startListening();
}

void loop()
{
  // Read data if available
  if (radio.available())
  {
    radio.read(&data, sizeof(Data_Package));
  }
  Serial.print("button1: ");
  Serial.print(data.button1);
  Serial.print("\n");
  Serial.print("button2: ");
  Serial.print(data.button2);
  Serial.print("\n");

  // If button 1 is pressed zoom in
```

```
  if(data.button1 == 0) {
    stepper1.setSpeed(speed1);
    stepper2.setSpeed(speed2);
    stepper1.runSpeed();
    stepper2.runSpeed();
  }

  // If button 2 is pressed zoom out
  if(data.button2 == 0) {
    stepper1.setSpeed(-speed1);
    stepper2.setSpeed(-speed2);
    stepper1.runSpeed();
    stepper2.runSpeed();
  }
}
```

Camera Adjustment System Transceiver Code:

```
// Libraries
#include <SPI.h>
#include <nRF24L01.h>
#include <RF24.h>

#define but1 2 // button 1
#define but2 3 // button 2

RF24 radio( 8, 9); // CE pin, CSN pin

// Set up data package
struct Data_Package {
  byte button1;
  byte button2;
  byte xAxis;
  byte yAxis;
};

Data_Package data;

// Set communication address
const byte address[6] = "00001";

void setup()
{
  // Activate internal pullup resistors
  pinMode(but1, INPUT_PULLUP);
  pinMode(but2, INPUT_PULLUP);

  // Initialize radio
  radio.begin();

  // Set radio address
  radio.openWritingPipe(address);

  // Set device as transceiver
  radio.stopListening();
```

```
}

void loop()
{
  // Read the user input
  data.button1 = digitalRead(but1); // Zoom in button
  data.button2 = digitalRead(but2); // Zoom out button
  data.xAxis = map(analogRead(A0), 0, 1023, 0, 255); // X-axis control
  data.yAxis = map(analogRead(A1), 0, 1023, 0, 255); // Y-axis control

  // Transmit the user input
  radio.write(&data, sizeof(Data_Package));
}
```

Intensity profile Code:

```
Imga=imread('prof3.bmp');%bmp file of desired frame
Img=rgb2gray(Imga);%converts to black and white image
I=imcrop(Img); %crops image
figure(1)%shows image
imagesc(I)
colormap('gray')
J=improfile; %intensity profile
plot(J, 'black');%plots intensity profile in darkest color (newest frame)
title('Intensity profile') %Title of plot
xlabel('Distance along Profile')%x axis lable
ylabel('Pixel Intensity')%y axis lable
ylim([0,260])%0-256 pixel intensity values
```

Intensity profile over time Code:

```
% load saved figures
fig1= hgload('figone');
fig2= hgload('fig2');
fig3= hgload('fig3');
%  Prepare 'subplot'
figure
h1=subplot(1,1,1);
h2=subplot(1,1,1);
h3=subplot(1,1,1);
copyobj(allchild(get(fig1,'CurrentAxes')),h1)
hold on
copyobj(allchild(get(fig2,'CurrentAxes')),h1)
hold on
copyobj(allchild(get(fig3,'CurrentAxes')),h1)
xlabel('Distance along Profile')
ylabel('Pixel Intensity')
legend('t_1','t_2','t_3')
```